PAUL SCHERRER INSTITUT

Paul Scherrer Institut
Laboratory for Waste Management

Progress Report

September 2003 to August 2004

The Waste Management Laboratory has two tasks: (i) to carry out an R+D programme strengthening the scientific basis for nuclear waste management, and (ii) to build and then operate – together with the SLS team – a microXAS beamline.

In its first task, the Laboratory serves an important national role by supporting the Swiss Federal Government and Nagra in their tasks to safely dispose of radioactive wastes from medical, industrial and research applications as well as from nuclear power plants. The activities are in fundamental repository chemistry, chemistry and physics of radionuclides at geological interfaces and radionuclide transport and retardation in geological media and man-made repository barriers. The work performed is a balanced combination of experimental activities in dedicated laboratories for handling radioactive elements and in the field, and theoretical modelling. The work is directed towards repository projects and the results find their application in comprehensive performance assessments carried out by Nagra.

This report summarises the activities and results achieved in the reporting period. It is organised as an overview followed by individual reports on the six waste management sub-programmes and a section on the status of the microXAS beamline.

We gratefully acknowledge the help of the Institute's management and of Nagra in our work.

A personal word from J.H.:

This is the last Progress Report under my responsibility and the overview, section 1, was not written without a certain melancholy. A period of more than twenty years of defining and helping carry-through a scientific programme comes to an end. This time has been extremely rewarding. It is not the place, here, to formulate an auto-necrology. But it is my deep wish to thank all those (far too numerous to mention individually) who have made the years challenging and rewarding. These are, in the first instance, the collaborators of the Laboratory for Waste Management, present and past, the directors of PSI and their staff, and many professionals within PSI, Nagra, Switzerland and abroad. They have broadened my horizon, and friendships have evolved. The Audit of this year has shown that the Laboratory for Waste Management is on track. May it continue to flourish in the future.

Table of Contents

1 OVERVIEW

Jörg Hadermann

The progress made in the Laboratory (LES) since September 2003 is summarised in this first section. The work within LES is organised in two projects.

The first is the **Waste Management Programme**. Its sub-programme achievements are given in sections 2 to 7. These sub-programmes are not isolated units. In fact, there is a strong interaction between them, as well as between experimenters and modellers, as can be seen to some extent from the list of co-workers on page 15. The results of the XAFS sub-programme are integrated into the other activities. It is also the aim in this first section to facilitate for the reader, an appreciation of these interactions.

The second is the **microXAS beamline project**. The achievements, together with the SLS team, are presented in section 8. The aim to better understand reactions on a molecular level at solid surfaces was the incentive for beginning the planning of the beamline. X-ray absorption spectroscopy has become an important tool in the waste management programme. The project has made impressive progress, and "first light" in the optics hutch was seen on August, 31st, 2004.

1.1 General

The current situation of waste management is characterised by a number of parallel but interlocked activities in all Swiss organisations concerned with nuclear wastes.

There is the review of the reports for the **Demonstration of Disposal Feasibility (Entsorgungsnachweis)** for spent fuel, vitrified high-level waste and long-lived intermediate-level waste for the Opalinus clay in the Zürcher Weinland.

OECD/NEA convened a group of nine internationally recognised specialists to review the post-closure radiological safety assessment following a request by the Swiss Federal Office of Energy (BFE). The review team was impressed by the overall strength and quality of the safety case prepared by Nagra. It concluded that the scientific basis for the representation of processes and barrier functions is state-of-the-art. The review team took account of the fact that the Entsorgungsnachweis is only one stage in a stepwise process. They recommend, *inter alia*, that Nagra should develop a better mechanistic understanding of glass corrosion under disposal conditions, should investigate further the bentonite interaction with other components of the disposal system, should continue its efforts in the field of geochemistry (notably on nuclide retention and the validity of chemical analogy considerations) and should elaborate further the diffusion processes. The evaluation by the Swiss authorities, notably the Swiss Nuclear Safety Inspectorate (HSK) is on-going. Their official expert opinion as well as that of other gremia is expected in the spring of next year and the decision of the Federal Council in 2006.

In parallel, work has started within Nagra and the Federal Government, to develop a **long-term programme** on nuclear waste management in Switzerland. Such a formal programme report is stipulated by the new Nuclear Law, and it is foreseen for submission to the Federal Government in 2006, after the judgement on the Entsorgungsnachweis. This programme will deal with all types of radioactive wastes, that is also with low- and intermediate-level wastes of short half-life radionuclides where progress is urgently needed after the abandoning of the Wellenberg project. This strategic report will also contain a chapter on the necessary research, development and demonstration (RD-D). The consensus between the utilities and the government is to tackle the tasks ahead in a speditive manner. This would mean that a repository for spent fuel, vitrified waste and long-lived intermediate - level wastes would go into operation in the 2040s.

From an LES point of view the most important event was the **Audit of the Laboratory for Waste Management** prompted by the Director of PSI. We gave account for our work over the past six years and presented plans for the future in a comprehensive report to the audit team of internationally recognised experts. In addition, we gave answers to specific questions in written form, and orally during the Audit meeting at PSI in February 2004. The audit team came to the following broad conclusions:

- *The performance of LES is considered to be very good. The strategic working areas of LES are well chosen, they are relevant to science and highly important to the Swiss waste management programme. The work of LES and the results produced are in general recognised to be of high quality although the contributions are not in all areas equally strong and broad. The work programme of LES contains several novel elements.*

- *LES plays in many areas a leading role on an international level and maintains a very strong international co-operation. However, the links to the Swiss scientific community and universities are felt to be currently not very strong.*
- *The strengths of LES are in the area of repository chemistry and transport phenomena. LES takes full advantage of the unique infrastructure available at PSI; the radiochemical work – which forms an essential part of LES work programme – cannot be done anywhere else in Switzerland.*
- *LES profits from the Swiss programme on waste management and the co-operation with Nagra. Through this co-operation, LES has access to the results of different research facilities (especially rock laboratories in Mont Terri and Grimsel) and can provide input to the planning of large experiments in these facilities and has also access to a large range of other information.*

Besides these general conclusions the team made specific remarks and suggestions, which are being considered. LES is confirmed in its strategic planning and also notes the agreement with the recommendations of the OECD/NEA review.

The **microXAS beamline** has made impressive progress (see section 8). The front end has been completely installed. This is a system of greater complexity than is usual since two beams, for the microXAS beam as well as for the FEMTO beam, have to be guided through all components. The installation of the torroidal mirror and of the monochromator has been completed. The delivery of the monochromator was strongly delayed and its installation caused some technical problems which have been resolved. Installed are the experimental tables and the beamline termination. “First light” in the optics hutch was achieved end of August 2004, a milestone we were eagerly looking forward to. A Kirkpatrick-Baez mirror for micro-focussing is being tested at the Advanced Light Source, Berkeley. Detector systems are either ready for operation or orders have been placed. Detector portals have been designed and are now under construction. A number of diagnostic devices to control the stability and quality of the micro beam are under development.

The necessary designs for shielding of active samples, sample holder and the containment system including a transport cover have been made. Samples will be loaded in the Hot Laboratory facility and then transported to the beamline. The safety concept has been accepted by the responsible parties. After commissioning with inactive samples, first experiments with weakly active samples are foreseen in the spring of next year, and then the extension to experiments with hot samples will follow.

The rest of this year and the first half of 2005 will be devoted to beamline commissioning. During this period, pilot experiments with expert users will be performed. The opening of the beamline for general users is foreseen for the second half of 2005.

Activities in the **5th EU Framework Programme** with LES participation have come to an end (ACTAF, ECOCLAY-II, GLASTAB, RETROCK), or are ending very soon (ACTINET, FEBEX-II). We have accomplished our tasks in all of them (see sections 2 to 5).

Within the **6th EU Framework Programme** there are a few projects, only. They cover broad and comprehensive fields in waste management. As a consequence the number of participants in each project is huge, and the danger of disintegration into independent subactivities seems large. LES is involved in all projects within its fields of competence. However, it has been our policy to focus on a few Work Packages to keep the administrative effort at a minimum.

The three projects with LES participation are:

- ACTINET-6, Chemistry and Physics of Actinides in Solution and Solid State, a Network of Excellence. We plan to bring in the microXAS beamline with its possibility to experiment with active samples to be prepared in the Hot Laboratory facility, and are involved in the Executive Committee. A common LES/INE proposal on a tutorial course in thermodynamics has been favourably reviewed.
- NF-PRO, Understanding and Physical and Numerical Modelling of the Key Processes in the Near-Field and their Coupling for Different Host Rocks and Repository Strategies, an Integrated Project (see sections 4 and 7). This project has started and we are leading a Work Package.
- FUNMIG, Fundamental Processes of Radionuclide Migration, an Integrated Project. This project has been favourably evaluated by the EU and is in the negotiation phase. It is foreseen that LES/CEA jointly lead an RTDC (see section 4).

Bilateral co-operations with external institutions and scientists have continued, as before. The long-time co-operation with Nagra was close and enjoyable. Frequent meetings dealt mainly with the Demonstration of Disposal Feasibility Study, but also with low-level waste disposal. The umbrella agreement with Nagra has been renewed for a further five years. We had our yearly meetings with the Institut für Nukleare Entsorgung (INE/FZK),

Karlsruhe, the Chemical Physics Department (DPC/CEA), Saclay, and the Institut für Radiochemie (FZR), Dresden, Germany. Co-operation within a formal umbrella agreement also continued with CIEMAT, Spain. Again, we made use of the possibility to perform measurements at the ESRF, Grenoble, at ALS, Berkeley, at APS, Chicago and at NSLS, Brookhaven. The co-operation with CRIEPI, Japan, in the field of cementitious systems continues and a final report on common activities is being drafted. On a person to person basis, we have co-operations with the University of Bern, the Federal Institute of Technology ETHZ, EAWAG Dübendorf, EMPA Dübendorf, the University of Tübingen, IRSN Paris, Technocentre Kiev, SBRAS Irkutsk, the University College of London, the Nuclear Research Centre Mol, Belgium, the University of Mainz, the Japan Nuclear Cycle Development Institute (JNC), the University of Strasbourg and are participating in various gremia of the OECD/NEA. Within the latter, we mention the Thermodynamic Data Base (TDB) Project and the Sorption Forum. We value these co-operations greatly and consider them indispensable for our work.

We have increased the number of **PhD students** performing their thesis at LES. Three students are presently integrated into our work programme, and two further proposals have been submitted. We are very glad that Professors at ETH and at the Universities of Bern and Tübingen agreed to supervise their work.

On October 13 and 14, 2003, the Waste Management Program Committee met for the yearly meeting. As usual, the work performed and future plans were discussed (AN-44-03-04). The Laboratory gratefully received valuable help and input from the members, not only during this meeting but also throughout the year.

1.2 Performance assessment

It is a characteristic feature of LES, and differentiates it from many other research institutions, that we are directly involved in performance assessment by providing model concepts and direct input data. These data are presented in a transparent and traceable way in reference reports. The majority of these reports for Entsorgungsnachweis have been published in the past reporting period; the two last ones were issued this year because of some delays (see sections 4 and 7).

The main emphasis in the reporting period was the **interaction with organisations reviewing** Nagra's performance assessment within the Demonstration of Disposal Feasibility Study (Entsorgungsnachweis). We had to answer questions posed by OECD/NEA and HSK, and provide further arguments for the choice of particular model concepts and data (see sections 2, 3 and 4). It was gratifying to see that the reviewers in these organisations appreciated and highly valued our work. In a very few cases, and probably also as a consequence of their role in the waste management community, they questioned the conservatism of selected data. In any case, their comments came as no surprise to us and gave valuable input for our future research plans.

1.3 Foundations of repository chemistry

Chemistry of repository systems is one of the main foci and fields of competence of LES. Its importance was highlighted again in the performance assessment of Entsorgungsnachweis. Here, the more generic work is addressed whereas the specific system applications are dealt with in the other subsections.

Reliable **thermodynamic data** are the basis of all our work in geochemistry. Evaluation of complex formation and stability constants is thus a permanent activity which we deal with mainly in the framework of international projects (see section 2). Within the OECD/NEA Thermodynamic Data Base, Phase II, we chair the group for evaluation of complexation of U, Np, Pu, Am, Tc, Zr, Ni and Se with simple organic ligands. This work will be completed very soon. The evaluation of zirconium carbonate complexes has started with our participation. In phase III of the NEA-TDB project the aim is to develop guidelines for evaluating solid solution thermodynamic data. A first workshop was held at PSI. IUPAC has evaluated the solubilities of transitions metal carbonates; our task is to review the evaluation from a user's point of view.

On the side of computational tools, work with the **GEMS code** is on-going together with colleagues from Kiev and Irkutsk (see section 2). The code has been made more user-friendly by adding a module for solid solution end member retrieval. A module for treatment of uncertainty space in chemical speciation has been developed. The code is now available for various operating systems used at LES, and tutorials for dealing with sorption and solid solutions are provided.

Since radionuclides in repository systems are generally present at trace concentrations (with the exception of the waste matrices, of course) the description of their behaviour in terms of **solid solutions** is important. This field is still in its infancy, and we continue to contribute to its development. Within the Gibbs energy minimisation approach to chemical speciation, surface complexation has been investigated with the aim to construct simpler and better constrained models

(section 2). An application is the incorporation of Eu(III) into calcite. New data on co-precipitation in sea water were available. The modelling points to ternary solid solution formation and two distinct co-ordination environments of Eu, which is consistent with spectroscopic information on the analogue Cm(III) (see section 2).

1.4 Repository near-field

1.4.1 Clay systems

For spent fuel and vitrified high-level waste the disposal caverns will be backfilled with bentonite, a material containing large quantities of montmorillonite. Our investigations center on the chemical behaviour of montmorillonite under repository conditions and the interaction of radionuclides with this clay mineral.

A first task is the characterisation of the interlayer water. It is well known that water in the clay interlayer has different properties from bulk water. For example, we illustrated the dependence of the water activity on compaction some time ago. We have now started to investigate the interlayer water properties on a microscopic basis using **molecular modelling** methods (see sections 2 and 3). Together with the University College of London we have performed Monte Carlo simulations. In the NaCl model system they showed how ion association depends on the interlayer water content. We tested existing tools in order to derive the self-diffusion coefficient of interlayer water. On the experimental side, this self-diffusion is being studied with quasi-elastic neutron scattering at the SINQ facility at PSI. First results indicate a reduction in the diffusion coefficient compared to that of bulk water (see section 7).

Molecular dynamics and ab initio calculations have also started to consider the acid-base reactivity of edge sites. This is important when the sorption of elements is pH dependent. These three first steps towards the goal of an atomistic description of radionuclide clay interactions have also clearly shown the need for a high performance computer system, and we are participating in the corresponding project, HORIZON.

The **thermodynamic modelling** of sorption onto montmorillonite continued (see section 4). Eleven elements, rangeing from Mn(II) to U(VI), have been evaluated within the previously developed ion exchange/surface complexation model. The data allowed linear free energy relationships to be deduced between surface complexation and aqueous hydrolysis constants. This is new for clays and for 1:1, 1:2 and 1:3 aqueous hydroxy complexes. The quality of the linear relations is very promising. It enables hitherto unknown heavy metal and actinide surface complexation constants to be estimated and the calculation of sorption values for different geochemical scenarios, and presents an important step towards a thermodynamic sorption data base.

The wet chemistry investigations which provide the basis for the thermodynamic modelling, were complemented by **spectroscopic investigations** with X-ray absorption spectroscopy, and time resolved laser fluorescence spectroscopy in co-operation with INE, Karlsruhe. The following example is mentioned: Under the reasonable assumption that Cm(III) and Eu(III) are chemical analogues, we found qualitative agreement between thermodynamic speciation and the results of laser fluorescence, but also quantitative discrepancies which need further investigations.

Because of the considerable amount of knowledge accumulated, compacted montmorillonite is an ideal model system to study the dynamic **diffusion** of reactive tracers in clays. Classical through-diffusion experiments are out of question because of the time scales involved. We have started experiments with thin membranes. First results with Sr show that the effective diffusion coefficient and rock capacity factor vary as a function of the ionic strength of the saturating solution (see section 7). To evaluate such experiments a further development of our diffusion code was necessary (see section 3).

1.4.2 Cementitious systems

Our aim is to elucidate the interaction processes of radionuclides with hardened cement paste (HCP) and with the individual HCP mineral phases. Literature data for the formation of **portlandite and $CaOH^+$** have been re-evaluated with various ionic strength correction models (see section 2). The experiments to measure the kinetics of **isosaccharinic acid** (ISA) decomposition are continuing (see section 7). ISA is the main cellulose degradation product in a cementitious environment and reduces radionuclide sorption if the concentration is above millimolar levels.

The main activities focussed on **sorption** measurements of relevant elements covering the valency range from II to VI (see section 5). The experimental methods are, also in this field, wet chemistry, time resolved laser fluorescence spectroscopy, X-ray absorption spectroscopy and X-ray diffraction. Almost no reliable information is available on the sorption of Ra(II). We started a common project on Ra uptake on HCP and its mineral components with JNC, Japan, made possible through a guest scientist grant from JNC. Handling

and phase separation methods had to be developed. First results indicate higher sorption than for Sr, but similar kinetics.

Micro-spectroscopy of Ni(II) and Co(II) loaded HCP samples showed the heterogeneity of sorption on cement. Ni-Al layered double hydroxides develop as coatings on cement minerals. The sorption of Co(II) is more complex. Part of Co(II) is oxidised to Co(III). For Eu(III) sorption isotherms (linear) were measured on hardened cement paste and calcium-silicate-hydrates (CSH). The sorption on CSH turned out to be dominant. The effect of isosaccharinic acid (ISA), a cellulose degradation product, was negligible at ISA concentrations below millimolar. This is surprising since Eu-ISA complexes should form according to thermodynamic calculations. Spectroscopic investigation with Cm(III) are planned to resolve the issue.

The sorption of Th(IV) on HCP exhibited a linear isotherm, and was again dominated by the uptake on CSH phases. Previous experiments with Sn(IV) were complemented with desorption experiments and showed complete reversibility. Sorption of U(VI) on CSH phases was investigated in co-operation with CRIEPI, Japan. Both organistions used different methods to synthesize the CSH phases. X-ray spectroscopy measurements gave similar results for the CSH phases produced by both methods and were consistent with uranophane formation.

The successful synthesis of amorphous and crystalline CSH phases allowed **co-precipitation experiments** to begin. These will yield data for the solid solution models (see section 5).

This subsection is also a natural place to report on the progress in describing **coupled chemical reaction/transport processes** (see section 3). A data bridge structure for the speciation code GEMS and the transport code MCOTAC has been developed. For efficient calculations a further optimisation of the GEMS kernel is necessary. FZR Dresden, has performed column experiments with gypsum dissolution. These have been used for code benchmarking and exhibited the importance of describing the temporal evolution of reactive surfaces. In connection with field experiments, scoping calculations have been made for a long-term study at the Grimsel Test Site. Also, samples from a railway tunnel in Opalinus clay near the Mont Terri Rock Laboratory might yield information on coupled processes such as pyrite oxidation and gypsum precipitation in the excavation disturbed zone.

1.5 Repository far-field

In the past years we have focused on investigations of **Opalinus clay**. This will also be the case in the future. The methodology of our investigations is the same as for the near-field components. We consider the important rock component mineral, illite, and the complex Opalinus clay rock. We combine wet chemistry investigations with spectroscopic examinations and thermodynamic modelling. We perform diffusion experiments in the laboratory, and in the field and develop the necessary model concepts.

Mechanistic studies have been performed for sorption of Sr, Ni, Eu and U(VI) on **illite** (see section 4). As has been done previously with montmorillonite, the clay was conditioned to its Na-form and physico-chemically characterised. Sorption edges and isotherms were measured. The model previously developed for sorption on montmorillonite was used to reproduce the experimental data on illite. The parameter values are different, of course. At low $NaClO_4$ concentrations (~0.01 M) and pH<8 cation exchange is dominating and Ca as well as Al compete with the radionuclides.

For the two elements Na and Sr, and the **Opalinus clay** system a comparison was made between sorption distribution ratios from static batch experiments and from dynamic diffusion experiments and with calculated values from the sorption model (see section 4). Agreement within a factor of 2 was seen. The question now is to what extent this agreement is valid for other elements.

Opalinus clay is heterogeneous and we are following different lines of measurement approaches to analyse the **heterogeneity**. For batch sorption of Zn scoping experiments have been performed using combined micro X-ray fluorescence and micro X-ray absorption spectroscopy. The results show that Zn is not associated with iron and calcium rich phases (see section 4). The second type of experiments where heterogeneity is being investigated are in-diffusion experiments where we have analysed the migration front of sorbing tracers. In some first scoping experiments the profile of Cs migration from a field experiment at the Mont Terri Rock Laboratory has been measured by laser ablation mass spectroscopy and X-ray fluorescence on a mm scale (see section 8). The idea behind such small scale investigations is not to up-scale the results directly to the repository dimensions. But we are convinced that the mechanistic understanding at mm scale is necessary to describe diffusion at large scale.

Laboratory experiments on diffusion in Opalinus clay samples are on-going (see section 7). For Sr,

diffusion has been measured perpendicular and parallel to the bedding. Experiments with ^{134}Cs at high concentrations have started. As in the case of diffusion in montmorillonite (see subsection 1.4), only in-diffusion experiments can be done for the more strongly sorbing tracers. An analytical technique, abrasive peeling and measurement of the tracer activity, has been developed to measure tracer migration. The position of the front and the time needed for its movement beyond a disturbed zone (steming from sample preparation) is very dependent on the tracer. Therefore scoping calculations for tracer diffusion have been performed before starting the experiments (see section 3).

Field diffusion experiments are on-going at the **Mont Terri Rock Laboratory**. We have analysed new data on HTO, iodide and sodium stemming from the DI-A experiment and seen a reasonable correspondence of diffusion coefficients between the field and laboratory experiments. Also, scoping calculations have been done for the layout of the planned long-term field experiments with Cs, Ni and Eu. The influence of anion exclusion and hyperfiltration was estimated (see section 3). Furthermore, advances in analytical measurements have been made such that iodide and iodate can be discriminated in the analysis of diffusion profiles (see section 7).

The work on analysis of fracture systems at the migration site at the **Grimsel Test Site** continued. The detailed geometry of the systems has been determined based on the information from bore cores. The present picture is too detailed for flow and transport calculations, and the next step will be simplifications for this purpose (see section 3).

A series of activities related to **colloid** chemistry and their migration are continuing (see section 6). Part of the work is analytical and part is theoretical: The single particle analysis by mass spectroscopy (ICP-MS) has been further developed and applied to thorium colloids. It is a powerful tool combining size distribution analysis with mass spectroscopy. Also, a phenomenological model has been developed for the sorption of Pu on various colloids as a function of pH and redox potential.

The international Colloid and Radionuclide Retardation Experiment at the Grimsel Test Site is coming to an end. One of the main results is that the actinides Th, Am and Pu were not retarded. This is interpreted as being a consequence of slow sorption kinetics and a flow regime quite different from repository conditions. As a successor of this project, it is planned to investigate the colloid formation at the bentonite/crystalline interface. We will also participate in this project.

Waste Management Laboratory: Sub-Programme Structure

Waste Management Programme

Management 4440xx

Jörg Hadermann, OFLA/203a (2415)
Beatrice Gschwend, OFLA/203 (2417)

Geochemical Modelling 4441xx

Wolfgang Hummel, OFLA/208 (2994)
Urs Berner, OFLA/201a (2432)
Enzo Curti, OFLA/202 (2416)
Dmitrii Kulik, OFLA/201a (4742)
Wilfried Pfingsten, OFLA/204 (2418)
Tres Thoenen, OFLA/208 (2422)

Transport Mechanisms 4442xx

Andreas Jakob, OFLA/202 (2420)
Sergey Churakov, OFLA/204 (4113)
Thomas Gimmi, OFLA/206 (2901)
Georg Kosakowski, OFLA/206 (4743)
Ralph Mettier, OFLA/205 (2368)
Wilfried Pfingsten, OFLA/204 (2418)
Luc Van Loon, OHLA/131 (2275/2257)

XAFS 4443xx

Rainer Dähn, OSUA/202 (2175)
Daniel Grolimund, WLGA/221 (4782)
Messaoud Harfouche, WLGA/219 (5289)
Beat Meyer, WLGA/231 (5168)
Dominik Kunz, OSUA/203 (4182/2274
André Scheidegger, WLGA/221 (2184),
Marika Vespa, OSUA/202 (2966/4139)

Clay Systems 4444xx

Bart Baeyens, OFLA/207 (4316)
Mike Bradbury, OFLA/207 (2290)
Rainer Dähn, OSUA/202 (2175)
Wolfgang Hummel, OFLA/208 (2994)
Dmitrii Kulik, OFLA/201a (4742)
Astrid Schaible, OSUA/203 (2278/4317)
Noreen Verde, OSUA/204 (2278/4451)

Cement Systems 4445xx

Erich Wieland, OSUA/201 (2274/2291)
Urs Berner, OFLA/201a (2432)
Jean-Pierre Dobler, OSUA/204 (2274/2289)
Andreas Jakob, OFLA/202 (2420)
Dominik Kunz, OSUA/203 (2274/4182)
Jan Tits, OSUA/201 (2277/4314)

Colloid Chemistry 4446xx

Claude Degueldre, OSUA/208 (2276/4176)
Roger Rossé, OSUA/203 (2204)

Diffusion Processes 4447xx

Luc Van Loon, OHLA/131 (2275/2257)
Mike Bradbury, OFLA/207 (2290)
Martin Glaus, OHLA/131 (2275/2293)
Fatima Gonzalez, OSUA/202
Werner Müller, OSUA/204 (2275/2269)
Roger Rossé, OSUA/203 (2204)

Studies 4449xx

Jörg Hadermann, OFLA/203a (2415)

MicroXAS Beamline Project

Management 445xxx

Design and Construction 4451xx

Infrastructure 4452xx

André Scheidegger, WLGA/221 (2184),
Rainer Dähn, OSUA/202 (2175)
Daniel Grolimund, WLGA/221 (4782)
Messaoud Harfouche, WLGA/219 (5289)
Beat Meyer, WLGA/231 (5168)
Markus Willimann, WLGA/231 (3554)

September 2004

2 GEOCHEMICAL MODELLING

W. Hummel, U. Berner, E. Curti, D. Kulik, T. Thoenen

2.1 Overview

In the period September 2003 to August 2004, covered by this progress report, the activities of the geochemical modelling group concerning Nagra's project for demonstrating disposal feasibility (*Entsorgungsnachweis*) have been concluded, mainly in terms of answering specific questions of external experts.

The work on thermodynamic databases continues: In addition to the extensive review work on Selected Organic Ligands for the OECD/NEA TDB Phase II, we are also now involved in the NEA Zr review. In both cases the aim is to finish the work by end of this year. The re-evaluation of the solubility of portlandite $Ca(OH)_2(s)$, and the stability of the $CaOH^+$ complex, key compounds in cement chemistry, has continued. We were invited to participate in the NEA TDB Phase III (guidelines for evaluating thermodynamic data for solid solutions) and in the IUPAC Subcommittee on Solubility and Equilibrium Data (solubility of transition metal carbonates).

The GEM-Selektor program package has been further developed in collaboration with external experts.

Work in the context of the EU projects GLASTAB (long-term glass corrosion rates) and ACTAF (solid solutions) came to an end. In the latter case, modelling of Eu - calcite solid solutions has been successfully concluded and the results have been published now in the open literature.

A GEM surface complexation theory has been developed with the aim of deriving non-electrostatic activity coefficient terms in surface-binding/ complexation models from "classic" adsorption isotherms.

As a new activity, Monte Carlo simulations of NaCl in Na-montmorillonite interlayers have been started, as a contribution to understand the peculiarities of aqueous chemistry in compacted clay systems.

2.2 Work for demonstrating disposal feasibility (*Entsorgungsnachweis*)

Several times in the past, progress on establishing solubility limits for performance assessment was briefly reported here. In the meantime, work on this topic has been completed and was appraised by HSK, the Swiss regulatory body. LES received a very good evaluation for the proposed maximum concentrations of some 30 safety relevant elements in the case of clay systems, as well as in the case of cementitious environments.

HSK judged the reference values and their associated bandwidths (usually the "upper limit"). The proposed limits were rated "traceable in every single case" and "justified" in the vast majority of cases.

For spent fuel and vitrified high level wastes in a bentonite near-field, HSK draw conclusions different from our proposals only for the solubility limits of Pa and Ra.

For Pa nearly no useful experimental data are available. This directed HSK to favour an analogy with Pu(V) instead of selecting the analogy with tetravalent actinides, as LES did.

A difference of three orders of magnitude was recognised for the maximum solubility of Ra, because LES used a solid solution concept to establish the limit, whereas HSK favoured the solubility of pure $RaSO_4$. In particular, LES considered the barite content of the near-field to form $(Ra,Ba)SO_4$ solid solutions. A controversy on the validity of such concepts at the waste/near-field boundary was partly resolved on the basis of new data on the Ba-content of the waste itself. Such discussions revealed the necessity to reconsider the present simple concepts and clearly indicated a more rigorous coupling of chemistry and transport phenomena in the future.

In the case of intermediate level long-lived wastes in cementitious high pH environments, only the solubility of uranium was judged differently. Experimental data in this pH region are very scarce and discrepancies finally concentrated on the interpretation of one single study (MORONY & GLASSER, 1995), where HSK's point of view was more conservative than LES' opinion.

A team of international experts was charged by the NEA to review the Swiss performance assessment "Entsorgungsnachweis" (NEA, 2004). During the final phase of the review (Nov. 24-28), members of the "thermodynamic modelling" group actively participated in oral sessions at Nagra's headquarters, during which they had to give detailed answers and clarifications to reviewers' questions on specific issues (particularly concerning glass corrosion).

2.3 Thermodynamic databases and software

2.3.1 OECD/NEA TDB review project

The international project "OECD/NEA TDB Phase II: Chemical Thermodynamics of Compounds and Complexes of U, Np, Pu, Am, Tc, Zr, Ni and Se with Selected Organic Ligands" still consumed a large fraction of the time of its chairman (W. Hummel) in the period September 2003 to August 2004.

Two out of three major chapters, concerning the ligands citrate and edta (ethylenediaminetetra-acetate) and comprising about 700 reviewed references and more than 500 draft manuscript pages, went through the external peer review process and are now ready for publication.

The problems concerning the third major chapter (oxalate) are resolved now. End of July 2003 two reviewers, mainly responsible for this chapter, announced their resignation from the project, and subsequently a new expert (L. Rao, LBNL) joined the review team. With a concerted team effort the oxalate chapter is now close to completion.

E. Curti has been invited as reviewer in the NEA TDB Zr review to take over responsibility for the Zr carbonate chapter in a late stage of this review project. So far only preliminary work is completed.

D. Kulik has been invited as an expert to participate in the NEA TDB Phase III project "guidelines for evaluating thermodynamic data for solid solutions". The kick-off meeting of this new NEA TDB project was held at PSI (2nd June 2004), where he presented a draft tentative work program for the expert group.

2.3.2 IUPAC solubility data project

W. Hummel has been elected as a new member of the IUPAC Subcommittee on Solubility and Equilibrium Data (SSED).

So far, this commitment involved the participation in the 3rd Annual Meeting of SSED at the University of Aveiro, Portugal (24-25 July 2004) as the representative of the "user community" of solubility data, and the participation in the IUPAC review of solubilities of transition metal carbonates as "editorial consultant". The latter task consists of commenting on drafts of the on-going review from the viewpoint of application of solubility data.

2.3.3 Portlandite and $CaOH^+$ formation constants: A problem of ionic strength correction?

Based on the fact that portlandite and the $CaOH^+$ complex are key compounds when fundamental thermodynamic data have to be established for cementitious environments, we described a re-evaluation of the $CaOH^+$ formation constant from literature data using the SIT formalism and a multi-dimensional regression in last year's progress report. With this re-evaluated constant ($\log_{10}K°_{CaOH+}$ = 0.98 ± 0.02) and with the portlandite solubility product from DUCHESNE & REARDON (1995) which in fact had been evaluated on the basis of a "Pitzer" model, we reproduced nearly all portlandite solubilities in alkali hydroxide solutions reported over the last hundred years (black curve in Fig. 2.1, note that actually $\log_{10}K°_{Ca(OH)2}$ = -5.17 was used to model the curve).

However, we then recognised that these two constants did not reproduce the measured data any better than when a Davies- or an extended Debye-Hückel model was chosen instead of the SIT ionic strength correction model. (Note that both former models produce nearly identical results). We thus adapted the constants in two alternative ways:

1) The blue curve was obtained by assuming that the "*DUCHESNE & REARDON (1995)*" solubility product of portlandite (-5.17) is correct. To obtain a reasonable fit, we had to increase $\log_{10}K°_{CaOH+}$ to 1.42.

2) The green curve was obtained by assuming that our $\log_{10}K°_{CaOH+}$ = 0.98, evaluated from independent portlandite solubility data in different electrolyte solutions, is applicable. In this case, a sensible fit requires an increase in the $\log_{10}K°_{Ca(OH)2}$ to -4.87.

At the first glance, all three models reproduce the experimental data in an equivalent manner (Fig 2.1), but a closer look on a magnified view provided in Fig. 2.2 reveals some shortcomings:

a) The black curve (the SIT model) does not yet match with the experimental point at 0.297/0.00168, which represents the average analysis of more than 75 preparations of a "reference artificial cement pore water" between 1997 and 2003 (TITS & WIELAND, 2003). Since this data point is considered to be very reliable, the model should reproduce it.

b) The blue curve represents the Davies/extended Debye-Hückel models. It matches the experimental point at 0.297/0.00168, but as a consequence of $\log_{10}K°_{CaOH+}$ = 1.42, $CaOH^+$ dominates the solution. Unfortunately, there is no independent evidence for this dominance in the literature.

c) The green curve also represents the predictions according to Davies/extended Debye-Hückel models and matches the experimental point at 0.297/0.00168. There is no dominance of $CaOH^+$, but this model overestimates total dissolved Ca by more than 10% at low alkali concentrations.

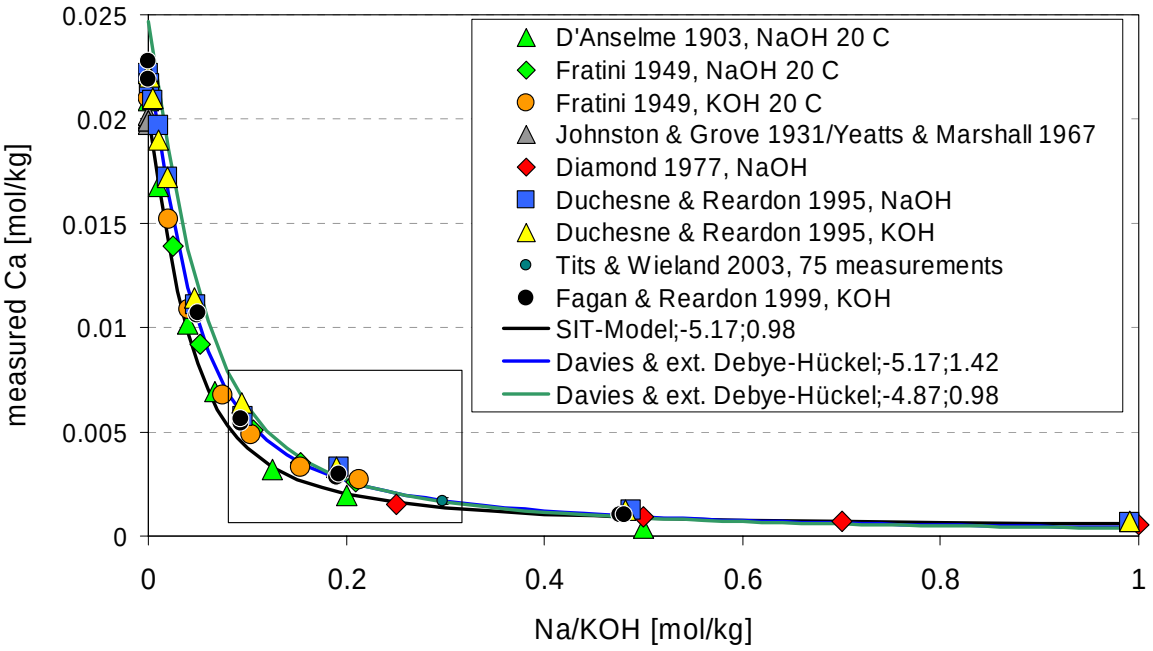

Fig. 2.1: *The solubility of portlandite ($Ca(OH)_2$) in alkali hydroxide solutions. Several ionic strength correction models, including different formation constants, seem to reproduce the experimental data from the last hundred years equally well. However, a detailed look to a magnified view (marked rectangle, see Fig. 2.2) reveals discrepancies that may have far-reaching consequences for a future "cement" thermodynamic database.*

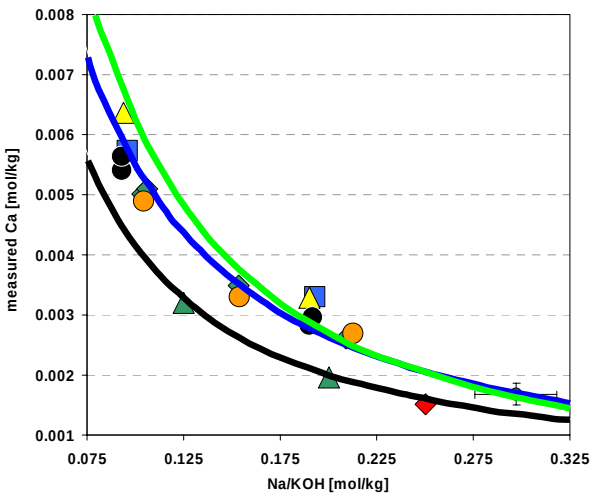

Fig. 2.2: *Magnified part of Fig 2.1. Differences are discussed in the text. Note the outstanding relevance of the experimental point at 0.297/0.0168 (95% confidence level), resulting from 75 independent preparation analyses of LES' reference artificial cement pore water. A sensible model has to reproduce this point.*

The solubility of portlandite and particularly the (weak) formation of $CaOH^+$ fall into a concentration range where the choice of the ionic strength correction model has a large impact on the relative stability associated with the two compounds. This large impact would then be carried forward to nearly all items of a future thermodynamic "cement" database (CSH-phases, Ca-aluminates, ettringites, etc.), and would have severe consequences for the quality of this database. There is thus a need to thoroughly and consistently re-investigate this simple system, to quantify the impact of the selection of an ionic strength correction model, and to propose a credible set of data based on traceable arguments.

2.3.4 The GEM-Selektor program package v.2-PSI

The GEM-Selektor v.2-PSI code developed at LES since 2000 is an implementation of the improved IPM-2 Gibbs energy minimization algorithm (CHUDNENKO et al., 2002). Taken together with the Nagra/PSI TDB 01/01 (HUMMEL et al., 2002), the GEMS code is more suitable for simultaneous modelling of aqueous speciation, surface complexation, co-precipitation and solid solution formation than the commonly available LMA speciation codes. Since 2000, the GEMS code has been used in various modelling applications related to LES research program. The GEMS-PSI program package v. 2.0.1 is currently available for Win32, Linux and Mac OS X as a release candidate 6 for download from http://les.web.psi.ch/Software/GEMS-PSI/.

To date, more than 220 downloads from all over the world were registered. Learning the code is much facilitated by the online screenshot tutorial, to which sections on adsorption- and solid-solution modelling were added. The online documentation was enhanced with PDF manuals describing thermodynamic calculations (TP corrections, activity coefficients, SCMs) performed within the GEMS-PSI code. The standard installer/uninstaller for Windows32 is provided since GEMS-PSI release candidate 4 (rc4). An overview of IT/programming needs for further development of GEMS-PSI has been presented in the form of internal communication (AN-44-04-08).

Some of these needs were covered in June-July 2004, during the programming session at PSI (with S.Dmitrieva, A.Rysin, K.Chudnenko). The work was concentrated on writing up new UnSpace and DualTh modules, as well as Linux and Mac OS X releases of GEMS have been finalized.

Preparation of an encapsulated GEM-IPM module for coupling with the fluid-mass-transport (FMT) codes had been identified as an important task. As a first step, the Data Bridge structures for data exchange between the fluid-mass-transport (FMT) and the GEM parts have been prepared (D. Kulik, W. Pfingsten, in collaboration with F. Enzmann, Gutenberg University, Mainz, Germany). As the second step, the isolated GEM-IPM "chemistry" module v. 2 (S. Dmitrieva, D. Kulik) was prepared that already uses Data Chemistry and Data Bridge structures for coupling with (FMT) codes. The "GEMIPM2K" program is presently under testing.

The prototype of UnSpace module is running and under testing for further development within a new collaboration project with Drs. K. Chudnenko, I. Karpov, and Mrs. S. Dmitrieva. The module is a GEM-Selektor implementation of innovative GEM Uncertainty Space approach for sensitivity analysis of solid-aqueous chemical equilibrium models (CHUDNENKO et al., 2004).

The DualTh module is an implementation of Dual-Thermodynamic calculations used by us in retrieval of thermodynamic properties of solid solution end-members from experimental or geochemical partitioning data (CURTI et al., 2004). The module prototype is also under testing; the goal of its development is to make this retrieval much more efficient and save our work time.

2.4 Thermodynamic modelling

2.4.1 Eu – calcite solid solution thermodynamics

As a continuation of the study carried out in the context of the EU project ACTAF (see progress report 2003), modelling work was extended by including a third data set (ZHONG & MUCCI, 1995) in addition to the two data sets considered previously (LAKSHTANOV & STIPP, 2004; TITS et al., 2003). Zhong and Mucci's data were obtained from coprecipitation experiments with synthetic seawater at pH ~ 8 and pCO_2 ~ 0.01 bar, i.e. at intermediate conditions compared to the other two investigations. The aim was to test our formerly derived binary solid solution model, which postulated $EuO_{9/8}(CO_3)_{3/8}$ as minor end-member stoichiometry, against a set of independent data.

To our surprise, the binary model failed to reproduce Zhong and Mucci's data. After testing all combinations of the seven Eu end-members under consideration, we came to the conclusion that the three datasets can be modelled simultaneously only by assuming a ternary solid solution with $EuO_{(3-x)/2}(OH)_x$ and $EuH(CO_3)_2$ as minor end-members. By means of DualTh calculations performed with the GEMS-PSI code we could fix the Gibbs free energies of these two Eu end-members to $G^*_{EuH(CO3)2}$ = -1733 ± 2 kJ mol^{-1} and $G^*_{EuO(OH)}$ = -955 ± 2 kJ mol^{-1}. Fig. 2.3 shows the overall fit of the data obtained with the ternary model.

Our results suggest that two distinct Eu coordination environments may coexist in calcite, depending on pH-pCO_2 conditions: at low pH and high pCO_2 the $EuH(CO_3)_2$ stoichiometry prevails, while at high pH and low pCO_2 the oxide end-member prevails. This model is corroborated by laser fluorescence results (STUMPF & FANGHÄNEL, 2002), which indicate the coexistence of two distinct Cm(III) species in calcite, one partially hydrated, the other completely dehydrated.

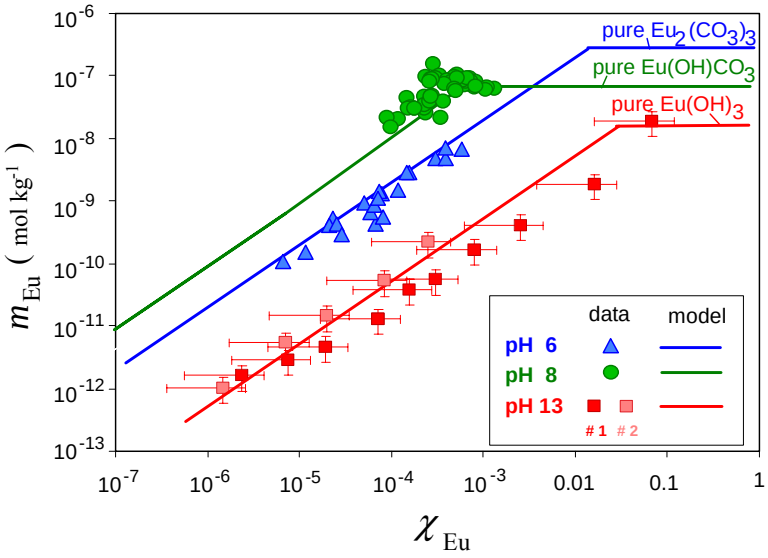

Fig. 2.3: *Ternary EuO(OH) - $EuH(CO_3)_2$ - $CaCO_3$ solid solution model (GEM-PSI calculations) compared with Eu-calcite coprecipitation and recrystallization data obtained under widely different pH and pCO_2 conditions. The horizontal lines define the solubility limits of the least soluble pure Eu solid for the relevant experimental conditions. In these regions, the solid solution coexists with the indicated pure Eu solid. The data stem from ZHONG and MUCCI (1995) (circles), LAKSHTANOV and STIPP (2004) (triangles) and TITS et al. (2003) (squares, denoting two separate series of experiments, #1 and #2).*

2.4.2 GEM surface complexation theory and modelling

Aquatic equilibria involving adsorption on mineral-water interfaces (MWI) can be computed without mole balance constraints for surface sites, similar to aqueous - solid solution equilibria (KULIK, 2002). This implies an appropriate choice of standard and reference states for surface species at MWI, although no conventions exist so far. Choices for GEM models are: a unimolal standard state at reference surface density $\Gamma_o = 2\cdot10^{-5}$ [mol·m^{-2}] and specific surface area $A_o = 5\cdot10^5$ m^2·mol^{-1} at 1 bar pressure and defined temperature; and a hypothetical "infinite surface dilution" reference state at zero surface charge and potential. It is then convenient to describe the ideal behavior of a surface species by the linear isotherm (Henry law), deviations from which can be split into an electrostatic contribution γ_E (traditional Coulombic term in EDL models), and a surface saturation / interaction contribution γ_S in any site-binding model. For non-electrostatic cases, both contributions appear to be mixed in classic equations of adsorption isotherms (Langmuir, Freundlich, BET, etc.). Recent work of D. Kulik was aimed at deriving an "activity coefficient" γ_S from the Langmuir isotherm:

$$K_L m_A = \frac{\theta}{1-\theta} \qquad (1)$$

where K_L is constant, m_A is molality of adsorbate A in solution, and $\theta = \Gamma_{SA}/\Gamma_C = m_{A.s}/m_C$ is the surface coverage fraction of adsorbed A relative to the maximum density Γ_C or molality m_C of surface sites. It is well known that at low m_A and relatively high binding energy of A to solid surface adsorption is linear, as long as the adsorbed density Γ_{SA} is small:

$$\frac{\Gamma_{SA}}{\Gamma_o} = K_{SA}\frac{m_A}{m_o}\gamma_A, \qquad (2)$$
$$\text{or} \quad a_{SA} = K_{SA}a_A, \quad a_A \to 0$$

where $m_o = 1$ [mol·kg^{-1}] is the standard molality, γ_A is the activity coefficient of A in solution, a denotes activity, and K_{SA} is the adsorption equilibrium constant that describes "ideal" behavior at "infinite surface dilution". However, at a significant surface concentration C_{SA} of adsorbed A,

$$\frac{\Gamma_{SA}}{\Gamma_o} = K_{SA}\frac{m_A}{m_o}\gamma_A(1-\theta), \qquad (3)$$
$$\text{or} \quad C_{SA}(1-\theta)^{-1} = K_{SA}a_A$$

Comparison of eqs (3) and (2) shows the term $(1-\theta)^{-1}$ staying in the place of activity coefficient:

$$\gamma_{S,L} = \frac{1}{1-\theta} = \frac{\Gamma_C}{\Gamma_C - \Gamma_{SA}} \qquad (4)$$

Behaviour of $\gamma_{S,L}$ is illustrated in Fig. 2.4. Eq (4) can be generalized to multi-dentate binding and to competitive adsorption on the same kind of surface sites, as already implemented in the GEMS-PSI code, where it should replace the provisional SAT terms suggested previously (KULIK, 2002). Using eq (4), the activity a_{SA} of adsorbed A can be expressed as

$$K_{SA}a_A = a_{SA} = C_{SA}\gamma_{S,L} = \frac{\Gamma_{SA}}{\Gamma_o}\cdot\frac{\Gamma_C}{\Gamma_C - \Gamma_{SA}} \qquad (5)$$

Comparison of eqs (5) and (2) shows that K_{SA} value depends on Γ_o but not on Γ_C. Eq (5) can be re-arranged into an adsorption isotherm where the last two terms represent the non-linear part:

$$\ln\Gamma_A = \ln(\Gamma_o K_{SA}a_A) + \ln\Gamma_C - \ln(\Gamma_o K_{SA}a_A + \Gamma_C) \qquad (6)$$

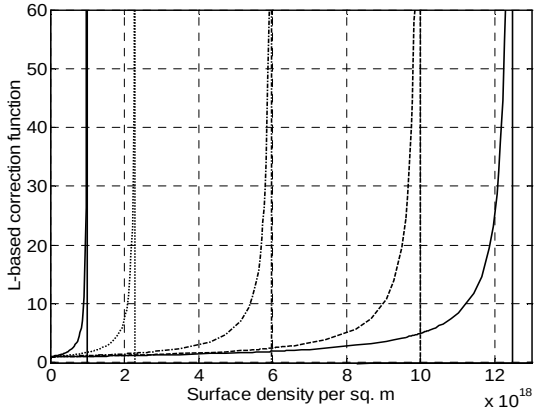

***Fig. 2.4**: Plots of $\gamma_{S,L}$ function, eq (4), at different site density parameters $\Gamma_C \cdot N_A$ (vertical lines): $1\cdot10^{18}$; $2.31\cdot10^{18}$; $6\cdot10^{18}$; $10\cdot10^{18}$; and $12.5\cdot10^{18}$ (in sites$\cdot$m^{-2}).*

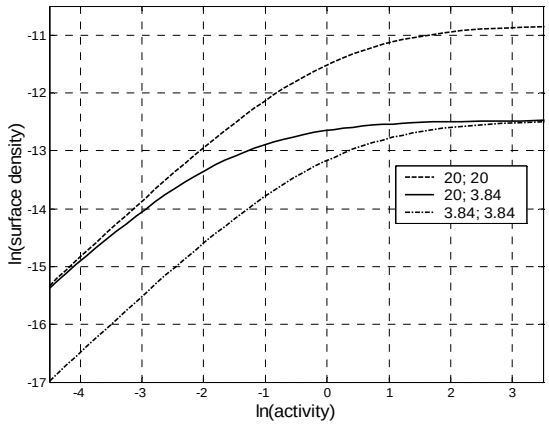

***Fig. 2.5:** Hypothetical isotherms in coordinates of activity a_A and surface density Γ_{SA} (in mol$\cdot$m^{-2}), calculated using eq (6) at K_{SA} = 1 and different combinations of Γ_o and Γ_C: (1) $\Gamma_o = \Gamma_C = 2\cdot10^{-5}$; (2) $\Gamma_o = 2\cdot10^{-5}$ and $\Gamma_C = 3.84\cdot10^{-6}$; and (3) $\Gamma_o = \Gamma_C = 3.84\cdot10^{-6}$ (in mol$\cdot$m^{-2}).*

As shown in Fig. 2.5, at fixed K_{SA}, plots of eq (6) deviate only at relatively high activities of dissolved A in response to different Γ_C parameters (curves 1 and 2). At the same Γ_C, the isotherms follow different linear parts for different $\Gamma_o \cdot K_{SA}$ values at low activities (curves 2 and 3).

By balancing the site-binding reactions like ≡S + A(bulk) = ≡SA(ads), it is easy to show that the mole balance constraint for surface sites used in traditional law of mass action surface complexation models (e.g. FITEQL code) induces the same deviation from linear "ideal" isotherm as the classic Langmuir isotherm, eq (1), does. The Langmuir isotherm can be written analogous to eq (5) as:

$$K_L m_A = \frac{\theta_A}{1-\theta_A} \quad \text{or} \quad K_L m_A = \frac{\Gamma_{SA}}{\Gamma_C}\cdot\frac{\Gamma_C}{\Gamma_C - \Gamma_{SA}}, \qquad (7)$$

where $\theta_A = \Gamma_{SA} / \Gamma_C$

Comparison of eqs (7) and (5) shows that the deviation from linear adsorption built into the Langmuir isotherm is a specific case of our eq (5) if and only if $\Gamma_o = \Gamma_C$ (curves 1 and 3 in Fig. 2.5). Therefore, the (competitive) monodentate Langmuir isotherm, eq (7), is built into the site-binding models based on the mole balance constraint for surface sites. Hence, such models cannot reproduce curves like (2) in Fig. 2.5 without a simultaneous change of $\Gamma_o = \Gamma_C$ and K_{SA}. This also explains why the law of mass action fitted adsorption constants cannot be compared without scaling to the same "standard" Γ_C (KULIK, 2002).

Thus, it should be difficult for non-electrostatic site-balance-based models to reproduce physically reasonable isotherms, e.g. BET, Frumkin, or Freundlich, especially those for the multi-layer adsorption. This problem can be solved by splitting the isotherm into "ideal" and "non-ideal" parts and representing the latter as an activity coefficient term, as shown above. A method for doing this can be deduced by comparing eqs (7) and (5). Eq (5) can easily be obtained from eq (7) by multiplying both sides by $m_o\Gamma_C / m_o\Gamma_o$, by denoting $m_A / m_o \cdot \gamma_A = a_A$, $\Gamma_{SA}/\Gamma_o = C_{SA}$, $(1-\theta_A)^{-1} = \gamma_{S,L}$,

and substituting

$$K_L \cdot m_o\Gamma_C / \gamma_A\Gamma_o = K_{SA} \qquad (8)$$

The whole conversion, in fact, consists in eq (8) that relates the concentration constant K_L to the

thermodynamic constant K_{SA}. The new method is applied here to the QCA (quasi chemical approximation) isotherm for *n*-dentate surface binding suggested by LAVIOLETTE & REDDEN (2002), written for our purposes as

$$K_L^{(n)} m_A = \theta_n \frac{(1-\theta_n)^{n-1}}{(1-n\theta_n)^n},\ 1 \le n \le 4 \qquad (9)$$

where $\theta_n = \Gamma_n / \Gamma_C$

and Γ_C is density of *n*-dentate adsorbed species (in mol·m^{-2}). Eq (9) reduces to the Langmuir isotherm eq (1) for $n = 1$.

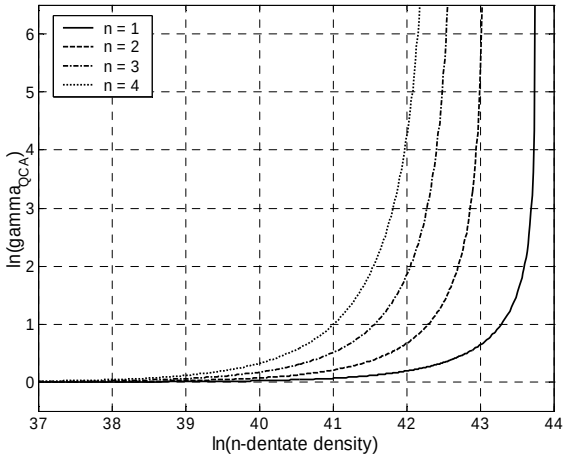

Fig. 2.6: *Behavior of* $\gamma_{S,n}$*, eq (10), as function of surface density* Γ_n *(in molecules·m*$^{-2}$*) of* n*-dentate adsorbate at* n *= 1; 2; 3 and 4 and at the complete coverage total site density* $N_A \cdot \Gamma_C = 10 \cdot 10^{18}$ *m*$^{-2}$.

To obtain the γ_S term, let us multiply both sides of eq (9) by $m_o \Gamma_C / \gamma_A \Gamma_o$ and re-arrange:

$$K_{SA}^{(n)} a_A = a_{SA}^{(n)} = \frac{\Gamma_n}{\Gamma_o} \cdot \gamma_{S,n} \qquad (10)$$

where $\gamma_{S,n} = \frac{(1-\theta_n)^{n-1}}{(1-n\theta_n)^n} = \frac{\Gamma_C(\Gamma_C - \Gamma_n)^{n-1}}{(\Gamma_C - n\Gamma_n)^n}$

The $\gamma_{S,n}$ function, eq (10), reduces to the $\gamma_{S,L}$ function, eq (4), at $n = 1$. Plots of $\gamma_{S,n}$ at different values of *n* are shown in Fig. 2.6.

In conclusion, the proposed method to derive γ_S expressions (surface activity coefficients) can and will be used for analysing other popular adsorption isotherms (BET, Frumkin, Freundlich etc.) describing effects of multi-layer adsorption, interactions between surface species, and site/surface heterogeneity, which all become more pronounced at elevated surface loadings. This opens a way to construct simpler, better constrained, and more reliable surface complexation models, both in Gibbs energy minimisation and law of mass action implementations.

2.5 Monte Carlo simulation of NaCl in Na-montmorillonite interlayers

Much of the water present in compacted clay systems, where the content of water is low, is likely to be adsorbed on the internal and external surfaces of clay minerals, so that the physical and chemical properties of water are affected by interfacial phenomena. Experiments at room temperature have shown that the dielectric constant of water, ε, is significantly lower near surfaces (ε < 10) than in bulk water (ε ≈ 80). Other experiments at room temperature have shown that ε of water in clay-water systems decreases systematically as the water content is reduced. The reduction of ε increases the electrostatic forces between cations and anions, favoring the formation of neutral or low-charge ion pairs or complexes. This results in an increase of the corresponding stability constants. Geochemical modeling of porewaters in compacted clays using stability constants determined for bulk water may therefore not be appropriate. Furthermore, a reduction of ε may also influence diffusion in compacted clays. In all 2:1 clays (apart from talcs and pyrophyllites) the substitution of Si^{4+} by Al^{3+} in tetrahedral layers and of Al^{3+} by Mg^{2+} in octahedral layers leaves the TOT layers negatively charged. This is compensated in the interlayer by diffuse double layers of charge-compensating cations close to the surfaces of the TOT layers. If a clay is sufficiently compacted, the diffuse double layers of adjacent surfaces may overlap, preventing the diffusion of anions. This effect is called „Donnan exclusion“. Consequently, the formation of neutral ion pairs or complexes, due to the reduced ε, may enhance diffusion in places where double layers overlap, since neutral species are not subject to Donnan exclusion.

In order to investigate the potential formation of neutral ion pairs in compacted clays, a series of Monte Carlo simulations of NaCl in the interlayer of Na-montmorillonite has been started, in collaboration with N.T. Skipper (University College, London). The simulation cell consists of a 31.7 x 36.6 Å^2 sheet of Na-montmorillonite, where the interlayer is sandwiched between two TOT half-layers (see Fig. 2.7). The composition of the simulation cell is $Na_{18}(Si_{186}Al_6)_{tet}(Al_{84}Mg_{12})_{okt}O_{480}(OH)_{96} \cdot aH_2O \cdot bNaCl$.

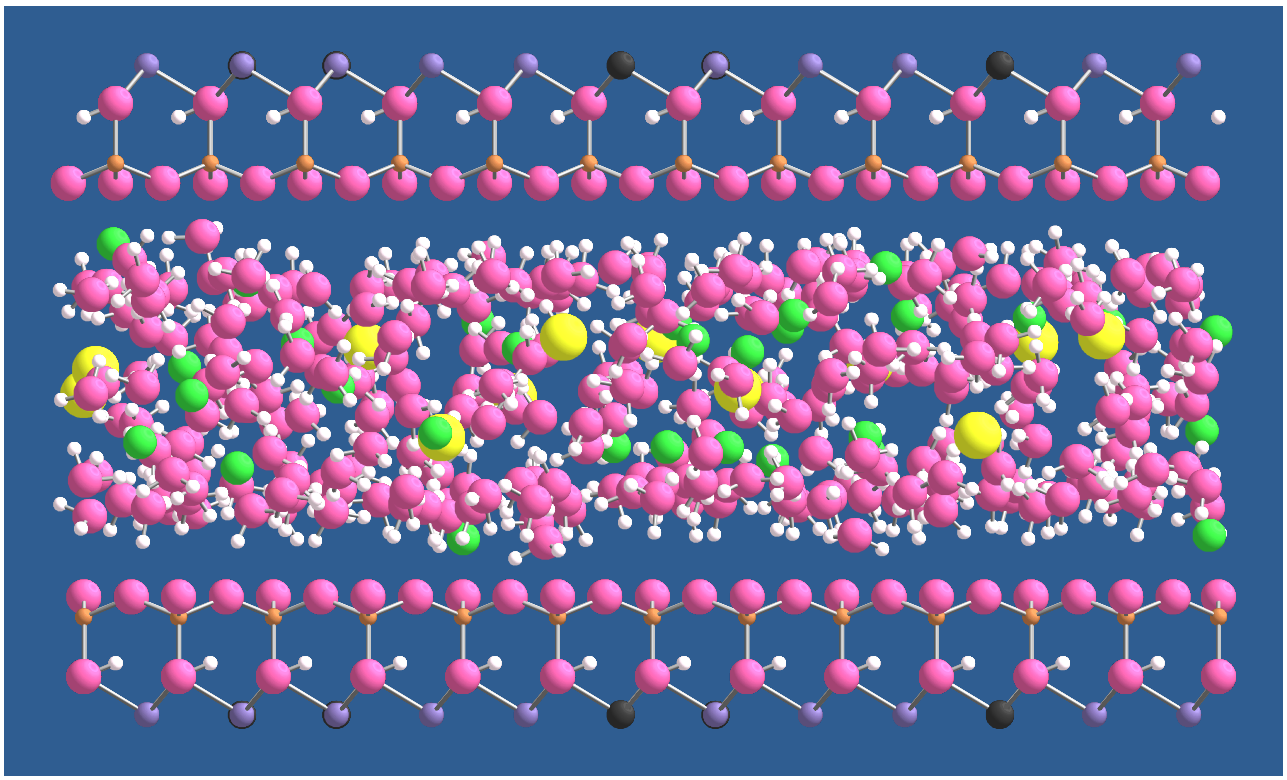

Fig. 2.7: *Na-montmorillonite simulation cell containing 312 H_2O molecules in the interlayer, as well as 18 Na^+ (for charge balance of the TOT-layer) and 13 NaCl. Green spheres are Na and yellow spheres are Cl. Projection onto the yz-plane.*

The number a of water molecules in the interlayer was systematically reduced from 1000 to 144 (resulting in a decrease of the layer thickness from about 35.7 to 14.5 Å). The number b of NaCl in the interlayer was correspondingly adjusted from 42 to 6 in order to keep the interlayer solution constant at 2.3 molal. Monte Carlo simulations in the NPT (particle number, pressure, temperature) ensemble at 10^5 Pa and 25° were done with program MONTE v. 5.4 (developed by N.T. Skipper), using periodic boundary conditions, i.e., the simulation cell was repeated infinitely in all three directions. The starting configuration was obtained by setting the TOT half-layers a certain distance apart, placing the 18 Na^+ counterions on two planes in the interlayer with a fixed distance from the TOT half-layers.

The remaining interlayer particles (a water molecules, b Na^+ cations, and b Cl^- anions) were distributed randomly. During simulations, the TOT layers were allowed to move as rigid sheets in the z-direction while the interlayer particles were allowed to move freely in all three directions.

Preliminary results indicate that the extent of ion association increases as the amount of interlayer water is reduced. This is illustrated by Fig. 2.8, where the running coordination number of Na with Cl (average number of Cl seen by Na as a function of radial distance) is shown for different water contents. The plateau starting at about 2.8 Å gives the average number of Cl atoms in the first coordination shell of Na. This coordination number changes from ~ 0.125 for 1000 interlayer waters to ~ 0.3 for 312 and to ~ 0.425 for 168 interlayer waters. Note, however, that the presence of Na^+ counterions „dilutes“ these coordination numbers. If (for 1000 waters) all of the 42 Cl particles are coordinated with Na particles, the average number of Cl in the first cordination shell of Na is 42/(42+18) = 0.70. For 312 waters this number is 13/(13+18) = 0.42 and for 168 waters it is 7/(7+18) = 0.28. It is remarkable that this last number is smaller than the corresponding coordination number obtained from the simulation. This suggests the formation of higher order NaCl complexes or clusters. The formation of such NaCl species has been predicted by BRODHOLT (1998), DRIESNER, SEWARD & TIRONI (1998), and SHERMAN & COLLINGS (2002) in molecular dynamics simulations of aqueous NaCl solutions at high temperatures, where ε of water is significantly reduced.

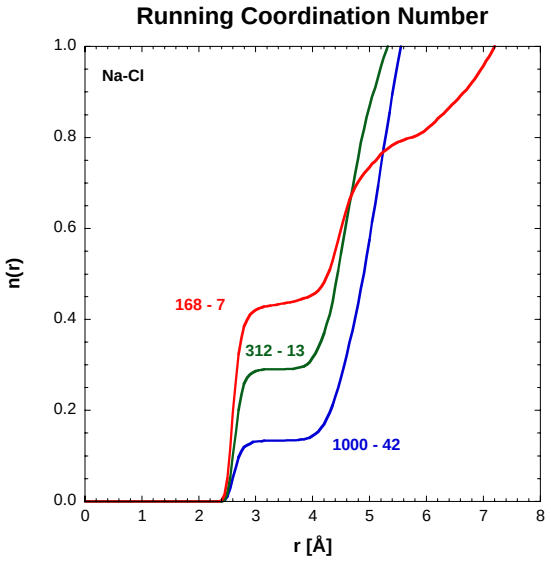

Fig. 2.8: *The running coordination numbers n(r) of Na with Cl increase as the amount of interlayer water is reduced. Results are shown for simulations with 1000 H_2O and 42 NaCl (blue), 312 H_2O and 13 NaCl (green), and 168 H_2O and 7 NaCl (red).*

2.6 EU projects

2.6.1 GLASTAB

The European project GLASTAB, dealing with the dissolution kinetics and alteration mineralogy of nuclear waste glasses, came officially to an end on October 31, 2003. A final meeting was held in Avignon on October 29-31. The documentation work required by the EU commission was completed by April, 2004. Our laboratory contributed with the evaluation of kinetic long-term experiments (work completed in the last project year) and transmission electron microscopy (TEM) of the glass alteration phases.

Final TEM measurements allowed us to throw light on the mechanisms of metal uptake by the glass alteration phases produced during the aqueous corrosion of the two Swiss reference glasses. Clay-like minerals are formed as the main alteration product from both glasses, but they have distinct compositions reflecting the chemistry of the original glasses. Aqueous corrosion of the Mg-bearing MW glass produced significant amounts of crystalline Mg-clays (saponites), whereas the Mg-free SON68 glass yielded X-ray amorphous Zn-Fe-Ni alumosilicates. It is concluded that the presence of Mg favours the clay nucleation and is partly responsible for the relatively high measured corrosion rates. The alteration of the Mg-free SON68 glass was slower, producing clays capable of incorporating significant concentrations of divalent transition metals, including Ni (^{59}Ni is a safety relevant radionuclide). Finally, a comparison of thin sections obtained from glass corroded for 5 and 12 years showed that the composition of the alteration products is stable over time.

2.6.2 ACTAF

This project terminated officially on September 30, 2003. Our modelling work on Eu incorporation in calcite was however extended as described in section 2.4.1.

2.7 Other activities

Participation of E. Curti to EXAFS-measurements at ALS (Berkeley), March 2004.

2.8 References

BRODHOLT J.P. (1998)
Molecular dynamics simulations of aqueous NaCl solutions at high pressures and temperatures. Chemical Geology 151, 11-19

CHUDNENKO K.V., KARPOV I.K., KULIK D.A. (2002)
A high-precision IPM non-linear minimization module of GEM-Selektor v.2.x PSI program code for geochemical thermodynamic modeling. PSI Technical Report TM-44-02-06

DRIESNER T., SEWARD T.M., TIRONI, I.G. (1998)
Molecular dynamics simulation study of ionic hydration and ion association in dilute and 1 molal aqueous sodium chloride solutions from ambient to supercritical conditions. Geochim. Cosmochim. Acta 62, 3095-3107

DUCHESNE J., REARDON E.J. (1995)
Measurement and prediction of portlandite solubility in alkaline solutions. Cement and Concrete Research 25, 1043-1053

HUMMEL W., BERNER U., CURTI E., PEARSON F.J., THOENEN T. (2002)
Nagra/PSI Chemical Thermodynamic Database 01/01. Universal Publishers/uPUBLISH.com, Parkland FL, 565 pp

KULIK D.A. (2002)
Sorption modelling by Gibbs energy minimisation: Towards a uniform thermodynamic database for surface complexes of radionuclides. Radiochim. Acta 90, 815-832

LAKSHTANOV L., STIPP S. (2004)
Experimental study of europium (III) coprecipitation with calcite. Geochim. Cosmochim. Acta 68, 819-827

LAVIOLETTE R.A., REDDEN G.D. (2002)
Comment on "Modeling the mass-action expression for bidentate adsorption". Environmental Science and Technology 36, 2279-2280

MORONY L.P., GLASSER F.P. (1995)
Reactions between cement components and U(VI) oxide. Waste Management 15, 243-254

NEA (2004)
Safety of Disposal of Spent Fuel, HLW and Long-lived ILW in Switzerland. An international peer review of the post-closure radiological safety assessment for disposal in the Opalinus Clay of the Zürcher Weinland. Nuclear Energy Agency, OECD, Paris

SHERMAN D.M., COLLINGS M.D. (2002)
Ion association in concentrated NaCl brines from ambient to supercritical conditions: results from classical molecular dynamics simulations. Geochemical Transactions 3, 102-107

STUMPF T., FANGHÄNEL T. (2002)
A time-resolved laser fluorescence spectroscopy (TRLFS) study of the interaction of trivalent actinides (Cm(III)) with calcite. Jour. Coll. Int. Sci. 249, 119-122

TITS J., WIELAND E. (2003)
Document journal for the preparation and analysis of artificial cement pore water 1997-2003. Personal communication

TITS J., WIELAND E., BRADBURY M.H., ECKERT P., SCHAIBLE A. (2003)
The uptake of Eu(III) and Th(IV) by calcite under hyperalkaline conditions. PSI-Bericht Nr. 02-03

ZHONG S., MUCCI, A. (2004)
Partitioning of rare earth elements (REEs) between calcite and seawater solutions at 25°C and 1 atm, and high dissolved REE concentrations. Geochim. Cosmochim. Acta 59, 443-453

2.9 Publications

2.9.1 Peer reviewed journals and reports

CURTI E., KULIK D., TITS J. (2004)
Solid solutions of trace Eu(III) in calcite: Thermodynamic evaluation of experimental data over a wide range of pH and pCO_2. Geochim. Cosmochim. Acta (in press)

HUMMEL W. (2004)
The influence of cyanide complexation on the speciation and solubility of radionuclides in a geological repository. Environmental Geology 45, 633-646

HUMMEL W. (2004)
Solubility equilibria and geochemical modelling in the field of radioactive waste disposal. Pure & Applied Chemistry (submitted)

THOENEN T., BERNER U., CURTI E., HUMMEL W., PEARSON F.J.[1] (2004)
Development and application of the Nagra/PSI Chemical Thermodynamic Data Base 01/01. In: Gieré R., Stille P. (eds.) Energy, Waste, and the Environment: A Geochemical Perspective. Geological Society, London, Special Publications, 236, 561-577
[1] Ground Water Geochemistry, New Bern, USA

WERSIN P.[1], CURTI E., APPELO C.A.J.[2] (2004)
Modelling bentonite-water interactions at high solid/liquid ratios: swelling and diffuse double layer effects. Appl. Clay Sci. (available on line)
[1] Nagra, Wettingen, Switzerland
[2] Hydrochemical Consultant, Amsterdam, The Netherlands

2.9.2 Conferences/Workshops/Presentations

BERNER U.
Status of cement modelling – future investigations in the view of cement/bentonite interactions. International Workshop on Bentonit–Cement Interaction in Repository Environments, April 14th/16th 2004, NUMO(Jp)/Posiva(Fin), Tokyo, Japan

CURTI E.
Summary of results obtained during the GLASTAB project. Final meeting of EU-project GLASTAB (5th framework programme), Avignon, 29-31 October 2003

CURTI E.
Glass corrosion: Results of GLASTAB project. Oral presentation at PSI Bereichskonferenz (BERK) 13 February, 2004

CURTI E., KULIK D.A., TITS J.
Solid solutions of trace Eu(III) in calcite: A thermodynamic study. Oral presentation, 13th Annual V.M.Goldschmidt Conference, 5-11 June 2004, Copenhagen, Denmark (Abstract: Geoch. Cosmoch. Acta 68 (11S), p.A82)

HUMMEL W.
Geochemical processes considered in radioactive waste disposal studies. Oral presentation, 227th ACS (American Chemical Society) National Meeting, 28 March - 1 April 2004, Anaheim, CA, USA

HUMMEL W.
Solubility equilibria and geochemical modelling in the field of radioactive waste disposal. Invited lecture, 11th International Symposium on Solubility Phenomena Including Related Equilibrium Processes, 25-29 June 2004, Aveiro, Portugal (Abstract IC, p. 27)

KULIK D.A.
Introducing GEM-Selektor v.2-PSI: A tool for modelling redox-sensitive partitioning equilibria in aquatic systems. Poster presentation, International Workshop on Biochemical Processes Involving Iron Minerals in Natural Waters, 16-21 November 2003, Centro Stefano Franscini, Monte Verità, Switzerland.

KULIK D.A.
Thermodynamic modeling with GEM-Selektor v.2-PSI program package. Oral presentations at the LES Waste Management Committee meeting 13 October 2003, and at the Work meeting with FZ Rossendorf delegation, 21 October 2003, Villigen, PSI

KULIK D.A.
On standard-state chemical potentials and activity coefficients of surface species on mineral-water interfaces. Oral presentation, International Workshop on Sorption Processes at Oxide and Carbonate Mineral Water Interfaces (SOPRO 2004), 25-26 March, 2004, Karlsruhe, Germany (Abstract: FZKA Bericht 6986, 80-85)

KULIK D.A., CURTI E., TITS J.
Retrieval of stoichiometry and stability of solid-solution end members by "dual-thermodynamic" calculations. Oral presentation, 13th Annual V.M.Goldschmidt Conference, 5-11 June 2004, Copenhagen, Denmark (Abstract: Geoch. Cosmoch. Acta 68 (11S), p.A82)

KULIK D.A., KARPOV I.K.[1], KERSTEN M.[2]
Dual-thermodynamic modeling of solid solution – aqueous solution equilibria. Oral presentation, 11th International Symposium on Solubility Phenomena Including Related Equilibrium Processes, 25-29 June 2004, Aveiro, Portugal (Abstract O8, p. 38)
[1] SB RAS, Irkutsk, Russia
[2] Gutenberg University, Mainz, Germany

2.9.3 Internal reports

BERNER U. (2003)
Minutes of the 16th Waste Management Program Committee Meeting, October 13th/14th 2003. PSI Internal Report AN-44-03-04

CHUDNENKO K.V.[1], KARPOV I.K.[1], KULIK D.A., BERNER U., HUMMEL W., ARTIMENKO M.V.[1] (2004)
GEM Uncertainty Space approach for sensitivity analysis of solid-aqueous chemical equilibrium models: A pilot study. PSI Technical Report TM-44-04-01
[1] SB RAS, Irkutsk, Russia

KULIK D.A., BERNER U., CURTI E. (2004)
Modelling chemical equilibrium partitioning with the GEMS-PSI code. In: PSI Scientific Report 2003 / Volume IV, Nuclear Energy and Safety (edited by B.Smith and B.Gschwend), Paul Scherrer Institute, Villigen, Switzerland, March 2004, 109-122 (ISSN 1423-7334)

KULIK D.A., BERNER U., CURTI E., HUMMEL W., PFINGSTEN W., THOENEN T. (2004)
IT/Programming needs in relation to further development of GEMS-PSI modelling package, PSI Internal Report AN-44-04-08

SCHWYN B.[1], WERSIN P.[1], BERNER U., WIELAND E., HUMMEL W., THOENEN T., NEALL F.[2], SMITH P.A.[3] (2004)
Near field chemistry of an ILW repository in Opalinus Clay, Nagra Internal Report, Wettingen, 70p
[1] Nagra, Wettingen, Switzerland
[2] Neall Consulting, UK
[3] SAM Ltd., Edinburgh, Scotland, UK

2.9.4 Others

KULIK D. (2004). Web pages for distribution and documentation of GEM-Selektor modelling code, v.2.0.1-PSI (release candidate 6):
http://les.web.psi.ch/Software/GEMS-PSI/

3 TRANSPORT MECHANISMS

A. Jakob, S. Churakov, T. Gimmi, G. Kosakowski, R. Mettier, W. Pfingsten

This section gives an overview of the work carried out in the past year within the Geosphere Transport Subprogram.

Geosphere transport modelling is one of the key activities of the Waste Management Laboratory LES and, hence, the working activities of the group - despite the very restricted man-power - cover a wide range of research areas and tackle many important scientific questions.
Our main goal is to achieve an increased understanding of the most important transport mechanisms and processes and to quantitatively estimate their effects on the mobility of migrating radionuclides. For this purpose we develop state-of-the-art models whose quality is investigated thoroughly by modelling experiments on the laboratory and field scale. Furthermore, we require the predictive quality of such models to be tested in new experiments. Such a procedure leads to refined models which are highly reliable and will be used periodically for safety assessment purposes.

Main areas of investigations in the last twelve months were:

- The analysis of **diffusion** experiments on the laboratory and field scale through pure phases such as montmorillonite and through Opalinus clay from the Benken and Mont Terri area;
- work in the frame of **molecular modelling** for investigating the mobility of radionuclides through clays and their interaction with the solid phase;
- **reactive transport modelling** applying MCOTAC;
- the derivation of **more realistic fracture geometries** from the analysis of Grimsel bore cores which can be used in transport modelling;
- work in the frame of the EU-concerted action **RETROCK**.

In April 2004 Dr. Sergey Churakov joined the group for working in the area of molecular modelling.
His background is geochemistry, geology and mathematics. He studied at the Moscow State University where he graduated in 1996 in geochemistry and 1997 in applied mathematics. Later he became a PhD student at the GeoForschungs-Zentrum in Potsdam (Germany) and after earning the PhD, he became a research scientist at the Swiss Centre of Scientific Computing in Manno in Ticino, Switzerland.
In the frame of ab-initio calculations he will investigate radionuclide transport through compacted clays and the interaction of these radionuclides with the solid phase.

3.1 Overview

3.1.1 Modelling small-scale through- and out-diffusion experiments using samples of montmorillonite and Opalinus clay

This year, again, new experimental data from small-scale diffusion experiments became available for analysis. (For details about the experiments see section 7). Two types of diffusion experiments are being performed: 1) using moderately sorbing tracers such as strontium for diffusion through Opalinus clay samples from Mont Terri and Benken; and 2) through- and out-diffusion experiments with sorbing tracers on thin samples of montmorillonite. The reason behind the second type of experiments is to investigate diffusion of highly diluted radionuclides and tracer up-take mechanisms of moderately sorbing radionuclides on pure phases, hence, on simplified systems when compared to those using Opalinus clay samples. The system under consideration consists of – at least – two different porous media, the filter plates and the clay sample. It is very common to neglect the influence of the filters in the interpretation of such experiments assuming that the resulting errors on the estimated parameter values are small or at least tolerable. Due to the very limited extent of the clay samples, the effects of the two filter plates consisting of sintered stainless steel on tracer breakthrough cannot be neglected any longer. To avoid such sources for errors, our computer code had to be extended to inversely model the experimental data adequately. In addition, due to enhanced tracer up-take onto the inner surfaces of the clay, the up-stream boundary condition, i.e. the boundary at the reservoir side with the traced solution, cannot be considered constant any longer. Hence, accounting also for a time-dependent up-stream boundary condition in the model was a prerequisite. Of course, for the requirements of performance assessment, i.e. for determining values for diffusion and sorption which can be applied in performance assessments, such effects are certainly negligible. In order to gain an increased system understanding however, such model refinements are inevitable. This can also be seen in the following table with best-fit parameter values for strontium through-diffusion through a thin montmorillonite layer with a

thickness of only 1.4 mm. Each of the filter plates had a thickness of 1.5 mm. In this table a comparison of the values obtained from different modelling approaches is made, starting with a simplified model and proceeding step-wise to a more sophisticated analysis of the experimental diffusion/sorption breakthrough data.

Table 3.1: *Preliminary best-fit parameter values for the effective diffusion coefficient, D_e, and the sorption distribution coefficient, K_d, for $^{85}Sr^{2+}$ diffusion through a 1.4 mm thick planar disc of compacted montmorillonite. Starting with a simplified system where the effects of the steel filters as well as the time-dependency of the up-stream boundary condition (b.c.) on tracer transport are entirely neglected and proceeding stepwise to more appropriate modelling results in best-fit values which are significantly different.*

System under consideration	$D_e \cdot 10^{11}$ [m^2/s]	$K_d \cdot 10^3$ [m^3/kg]
no filters, b.c. = const.	3.96 ± 0.22	19.2 ± 2.4
with filters, b.c. = const.	4.58 ± 0.24	16.9 ± 1.7
with filters, b.c. = f(t)	5.37 ± 0.34	21.4 ± 2.4

3.1.2 DI-A and DR experiment Mont Terri

For the still on-going field tracer diffusion tests in Mont Terri (DI-A) additional data about the tracer concentration for HTO, I^-, Na^+ in the borehole and, newly, in the adjacent rock were available for an in-depth analysis. A careful sensitivity study was performed with respect to various parameters such as porosity, diffusion coefficient, sorption coefficient, borehole geometry, and fraction of water that can be removed by drying. Generally there was a very good agreement between the data and the results of the model when applying the laboratory parameter values for the tracer-dependent diffusion coefficient, porosity, and sorption capacity (Fig. 3.1). These results are encouraging and support the underlying idea that laboratory data obtained from small-scale experiments can indeed be used on a larger scale regarding time and space as well.

In addition, some scoping calculations for forthcoming laboratory diffusion experiments with strongly sorbing Cs^+ were performed accounting for a time-dependent reservoir concentration, hence, boundary condition on the inlet side.

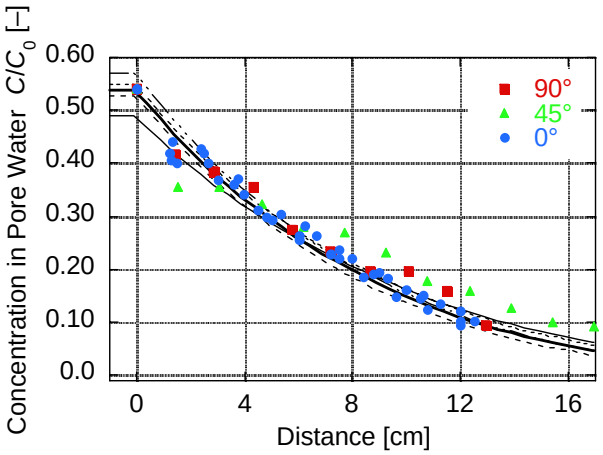

Fig. 3.1: *DI-A experiment in Mont Terri: Measured (symbols, different orientations of sub-samples with respect to layering) and simulated (lines) concentration profiles of HTO in the pore water of the rock adjacent to the borehole. The thick solid line was calculated applying transport parameter values obtained in small-scale laboratory experiment and corrected to the in-situ temperature of 14°C. The thin solid and the dashed lines were obtained for variations of the porosity and the diffusion coefficient. Note: the data for 45° and 90° had to be rescaled making these data less trustworthy for the subsequent analysis.*

For the future diffusion and retention experiment (DR) at Mont Terri a series of scoping calculations for non-sorbing HTO and strongly sorbing tracers such as Cs^+, Ni^{2+} and $Eu^{3+}$was performed. Using our own computer code different scenarios for isotropic 2D radial diffusion from a centrical borehole were investigated. Our calculations predict a fast decrease of the borehole concentrations thus, consequently, an online measurement would definitely be favourable. In order to also account for anisotropic diffusion the code "RockFlow" had to be modified. RockFlow will also be our preferential computational tool when accounting for complicated 3D geometries.

Finally, we also studied the effects of anion exclusion and hyperfiltration assuming there is a non-negligible advective-dispersive tracer transport through clay. Such effects are especially important when carefully interpreting field data using anions (e.g. chloride) as tracers.

3.1.3 Molecular modelling

In spring 2004 we started working in the area of molecular modelling. Presently, two group members are mainly active in this field and, hence, molecular

modelling has already become a major activity within the transport modelling group. One of us is performing ab-initio calculations; a second member of the group is doing work in the frame of molecular dynamics.

1) It has been understood for a long time that the edge sites of the clay minerals play a central role in controlling the pH-dependent uptake of ions by Opalinus clays (OPA). Various models have been proposed to explain edge-site reactivity based on experimental data. In those models the distribution of the reactive sites and the site capacities are the fitting parameters. Even if the empirical model describes pH-dependent transformations in OPA reasonably well the detailed understanding of the acid-base equilibria on the atomistic level is still missing due to the effects of extreme anisotropy and complexity of the phyllosilicate crystal structure.
As a starting point for our investigations the simplest example of a di-octahedral phyllosilicate, pyrophyllite ($Al_2Si_4O_{10}(OH)_2$) was used to study the acid-base reactivity of the edge sites in OPA. The structure of pyrophyllite can be thought of as hexagonally ordered planes of alumina octahedra sandwiched between two siloxane planes and commonly referred to as TOT-layer. In the idealised structure of pyrophyllite the TOT-layer does not carry any permanent electrical charge making impossible the ion retardation by exchange mechanism. The ion uptake in the pyrophyllite occurs preferentially by sorption on the edge site and it is known to be pH-dependent.
The lateral facets of pyrophyllite are formed by breaking Si-O-Si and Al-O(H)-Al bonds in the TOT-layer. Upon the bond breaking the oxygen, alumina and silicon sites localised on the surface become reactive and readily adsorb the H_2O molecules from air or aqueous solutions.
Initially, the water molecules are adsorbed by the mechanism of chemical sorption, where the H_2O dissociates and forms Si-OH bonds to the surface silica atoms. When all available Si-sites are saturated by OH groups the water uptake continues as molecular sorption because of electrostatic attraction between the surface and the water dipole. The optimised (010) surface of pyrophyllite is shown in Fig. 3.2. The chemically sorbed water can be seen as the OH groups bound to the Si and Al site. The physically adsorbed molecular water is trapped by electrostatic interaction between positively charged Al sites and the lone electron pair of the water molecules. It has to be remembered, however, that the interface between the pyrophyllite surface and the solution is a dynamical system which undergoes thermal fluctuations. Since OH groups are strongly bounded to the surface, the kinetic energy of the atomic motion at room temperature is not sufficient to break the metal-OH bonds. In contrast, the physically sorbed water molecules can leave the surface. In the presence of a solution the liberated absorption sites will be occupied by other molecules. The rate of such an exchange is controlled by the water pressure at the interface and the temperature.
The surface structure shown in Fig. 3.2 corresponds to the dynamically average atomic geometry close to the pH of zero charge. Upon change of the pH in the solution the surface atoms will participate in protonation/de-protonation reactions. Acid-base reactivity of different sites in the structure can be estimated calculating the so-called electronic Fukui functions:

$$f^+(r) = \rho_{N+1}(r) - \rho_N(r)$$
$$f^-(r) = \rho_N(r) - \rho_{N-1}(r)$$

where the $\rho_N(r)$ is the ground state electron density of the equilibrium structure with N electrons. The $\rho_{N+1}(r)$ and $\rho_{N-1}(r)$ are the electron densities of the N+1 and N-1 electron systems with the same atomic geometry as $\rho_N(r)$. The $f^+(r)$ has local maxima near the atoms and functional groups involved in the protonation reaction while $f^-(r)$ is associated with the sites participating in the de-protonation. In the figure $f^-(r)$ and $f^+(r)$ are shown on two separate plots as a set of coloured iso-surfaces. The visualised Fukui functions clearly indicate that both de-protonation and protonation occur more easily on the edge sites and not on the basal oxygen atoms. Although some green areas appear near the internal oxygen sites, the amplitude is much smaller compared to that of the edge sites. The protonation reaction on the (010) surface of pyrophyllite (see also Fig. 3.2 - upper part) occurs by addition of protons to the Al-OH sites and results in the formation of the surface alumina atom coordinated by two water molecules. As mentioned, the weakly bound water molecules can escape the surface leaving a positively charged cation-phobic interface. This conclusion is in good agreement with generally observed cation de-sorption in low pH aqueous solutions. According to the lower part of Fig. 3.2 the de-protonation occurs on superficial Si-OH and HO-Al-OH_2 sites. Thus, the high pH protons will be desorbed in solution leaving Si-O and O-Al-OH sites exposed on the (010)-surface of pyrophyllite. Those sites contribute to the overall negative surface charge favouring strong cation sorption at high pH.

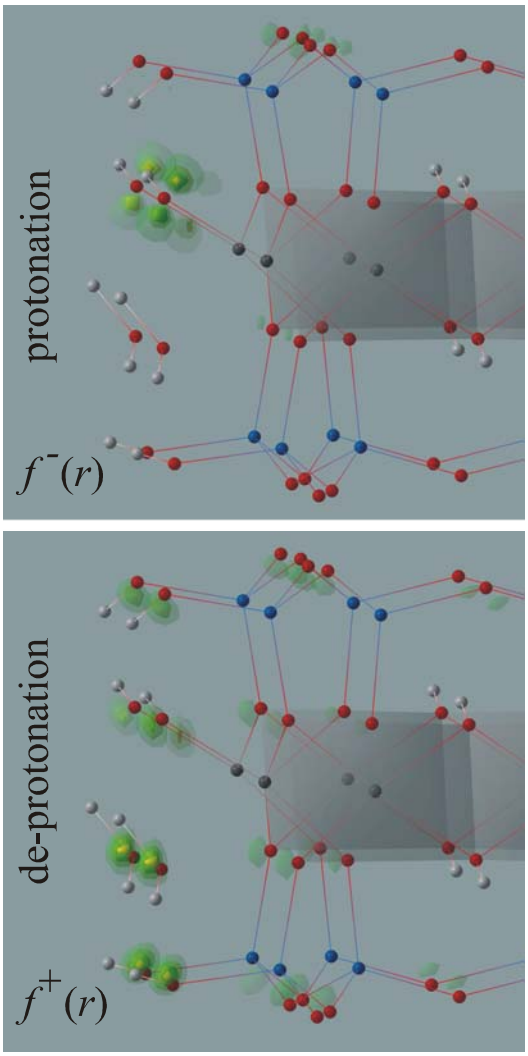

Fig. 3.2: *Fragment of the optimised (010) surface of pyrophyllite. Blue spheres represent the silicon atoms, dark-grey show the alumina, red mean oxygen atoms and light grey denote the hydrogen atoms. The grey shadowed area emphasises [AlO_6] octahedra of the TOT-layer. Chemically (strongly) adsorbed water builds Si-OH groups at the surface. The strongly bound Al-OH sites are formed at the costs of intra-crystalline water of pyrophyllite. The weakly bound H_2O molecules are attached to the surface Al sites by electrostatic interaction between positively charged aluminum atoms and lone electron pairs of the water molecules. The Fukui functions are shown by coloured iso-surfaces, using a green to yellow colour scheme where yellow corresponds to the higher values. The local maxima of $f^-(r)$ and $f^+(r)$ are localised near the oxygen sites preferentially participating in the protonation and de-protonation reactions respectively. Yellowish colours indicate higher site reactivity.*

2) Molecular modelling techniques, such as Monte Carlo (MC) and classical molecular dynamics (MD) simulations are well established for modelling processes related to the transport of radionuclides in compacted clay systems and for assessing their extent and importance. The MC-calculations provide the equilibrated system as starting point for the subsequent MD-calculations.

Activities in the field of molecular modelling so far have concentrated on the testing of the numerical tools and on setting up the necessary working environment. It was found that porting the software packages "Monte" (MC-code) and DL_POLY (general purpose MD-code) to our computing platforms was a non-trivial task. Especially "Monte" had to be debugged intensively in close co-operation with the computer code's author Neal Skipper from the University College London. In addition, based on many tests performed on the local Merlin cluster it turned out that the available computer resources at PSI are insufficient for our purposes. We therefore submitted a proposal with a detailed specification of our future computer requirements to the leader of the upcoming high-performance computing project called "HORIZON" (Adelmann, 2004).

First MC and MD calculations are currently under way. They concentrate on the state and dynamics of water and ions in the interlayers of Na-montmorillonite. A snapshot of such a system is shown in the figure below.

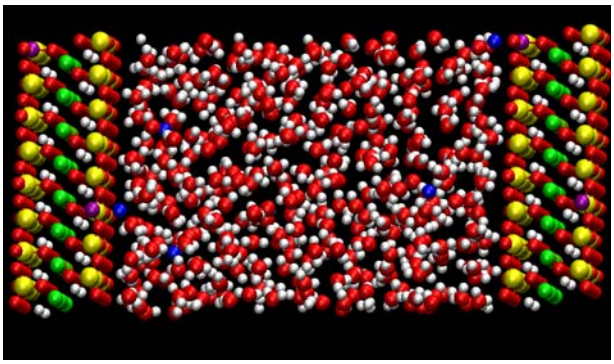

Fig. 3.3: *Snapshot of a molecular dynamics simulation of a single charged montmorillonite clay sheet surrounded by 384 water molecules and 6 Na^+ counter-ions (blue) in the interlayer. Oxygen atoms are red, H atoms are white, the tetrahedral Si atoms are yellow, octahedrally coordinated Al is green, Al atoms replacing Si are purple and Mg atoms replacing Al in the octaeder layer are orange. The thickness of the water layer, i.e. the interlayer spacing, is about 3.3 nm.*

From such calculations it is possible to extract values for the self-diffusion coefficient of the interlayer water. Data for the system shown are close to those values for bulk water ($D_w \approx 2 \cdot 10^{-9}$ m^2/s).
The motion of the sodium counterions is strongly influenced by the clay surface because they are predominantly present as outer-sphere hydrated complexes.
In the near future we will proceed with our investigations along two mayor lines: (1) the dynamics and state of ions (radionuclides) in the interlayer of compacted clays and (2) the dynamics and state of the interlayer water under the influence of external forces.

3.1.4 Reactive transport: GEMS-MCOTAC coupling

For the planned coupling of the geochemical code GEMS and the reactive transport code MCOTAC, a first step was taken by defining a data-bridge structure allowing exchange of transport-relevant data between the GEMS-kernel and MCOTAC, which initially will be via data files. For this purpose, the GEMS-kernel program was isolated from its graphical user interface environment to run in a batch-type mode reading structured input files, calculating equilibrium conditions and writing the result to files which can be used for further transport calculations. With this rudimentary procedure the incorporation of the Gibbs-Free-Energy minimisation concept for equilibrium speciation calculations into MCOTAC can be tested. Later on, all other GEMS options should be included in the reactive mass transport calculations, i.e. taking into account solid solutions, etc. Generally, GEMS equilibrium computations are slightly slower than those for comparable law-of-mass-action computation-based geochemical codes (e.g. PHREEQC). Therefore, a further optimisation of the kernel is on-going to improve the GEMS applicability within the framework of multi-component mass transport calculations, which require a much higher computational performance than single geochemical speciation calculations. The incorporation of the GEMS chemical module will also allow the direct use of the PSI/Nagra thermodynamic database for reactive transport calculations; future reactive transport calculations take advantage of further GEMS developments, e.g. trace-element chemistry, solid solutions, uncertainty space etc.

3.1.5 Benchmarking: Gypsum dissolution depending on accessible reactive mineral surface area

In order to understand reactive transport processes and to model them in a sophisticated way, laboratory column experiments were performed in the Institute of Radiochemistry in Rossendorf (Germany) investigating especially the available reactive mineral surface. Regarding performance assessments, coupled processes become important when mineral reactions are involved, especially in the near-field of a cementitious repository where the high-pH leachate induces primary mineral dissolution and secondary mineral precipitation in the host rock. Both processes affect the reactive mineral surface areas for diverse sorption processes. In a laboratory column experiment the dissolution of gypsum mixed with quartz sand by distilled water was investigated. The measured calcium breakthrough could be modelled only by assuming a kinetic dissolution process for gypsum including a variable reactive mineral surface area. As gypsum grains dissolve, their reactive surface area becomes smaller, reducing the gypsum dissolution rate and resulting in a more pronounced tailing for the leached calcium concentration. A series of calculations for benchmarking purposes was performed for this column experiment. Fig. 3.4 shows the results of three competitive models – MCOTAC, a model by Kuechler (2002) and HYDROBIO-GEOCHEM (Yeh, 1998).

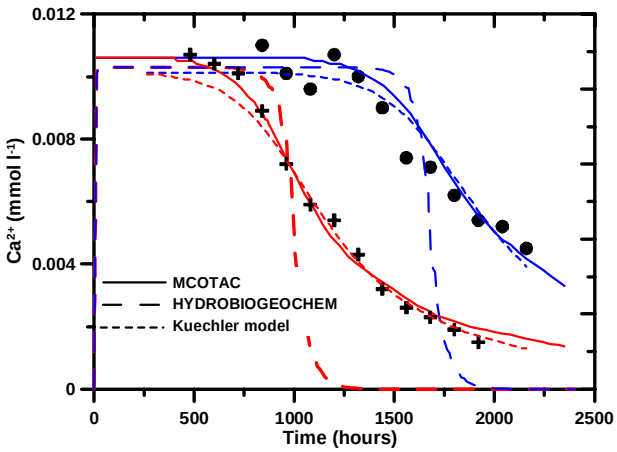

***Fig. 3.4**: Application of three different reactive transport codes describing the gypsum leaching by distilled water in a column where the free Ca^{2+} concentration was measured at 0.3 m (✚) and 0.5 m (●). MCOTAC (solid lines) and a model by Kuechler (broken lines) include both a kinetic model with variable reactive surface area of gypsum (decreasing surface with increasing gypsum dissolution). While MCOTAC accounts for the gypsum grain surfaces in terms of spheres, the Kuechler model uses an empirical equation instead relating the gypsum mass at time t to the initial gypsum mass. For the HYDROBIOGEOCHEM code, (dashed lines) a constant mineral surface area was assumed, and hence, the fitting was clearly less accurate.*

As can be seen, accounting for variable mineral surface areas is inevitable; otherwise the fits are very poor.
New experiments including mineral and sorption reactions and a subsequent inverse modelling are foreseen. They will result in an improved understanding of sorption processes in combination with changing mineral surfaces due to, e.g., alteration processes.

3.1.6 Grimsel high pH-plume experiment (HPF) and the long term cement study (LCS)

Further modelling applying MCOTAC was performed in the framework of the HPF / LCS project. Of special interest were the observed shorter breakthrough times measured for identical dye tracer experiments with evolving time of the injection of the high-pH solution. Such experiments with dyes were performed every three months during the long-term injection of the high-pH solution. The induced mineral reactions continuously change the porosity and hydraulic conductivity in the heterogeneous shear zone. Such effects were taken into account by an appropriate fit-parameter set; also series of calculations for Cs, Co and Eu migration were performed regarding different evolution scenarios for the shear zone heterogeneity and possible effects of mineral reactions induced by the injected high-pH solution.
Further estimations for the plume extensions and for the tracer recoveries had to be made in order to get – finally – the licence permission from the authority (HSK) for the final tracer injection.

3.1.7 Complex 3D fracture network data as a basis for advanced flow and transport modelling

The extraction of realistic fracture geometries from bore core observations on Grimsel crystalline rock permits investigating the effects of structure and characteristics of fracture networks on flow and transport, especially those associated with shear zones, at a level of detail otherwise rarely available.
Once this geometric information has been extracted and digitalised, the obvious next step is to compare the obtained actual geometry with that of former studies. Such a comparison is achieved on two levels: First, the statistical analyses of the size, strike and dip of the elements used in building up the extracted geometric model give us information about the number and position of main fractures, their connectivity among each other and their continuity throughout the rock volume under investigation.
The following figure shows an example of such a statistical analysis, implying three almost parallel main structures. This agrees well with the ‘three to four interconnected parallel planes’ geometry used in earlier models of the shear zone (Hadermann and Heer, 1996).

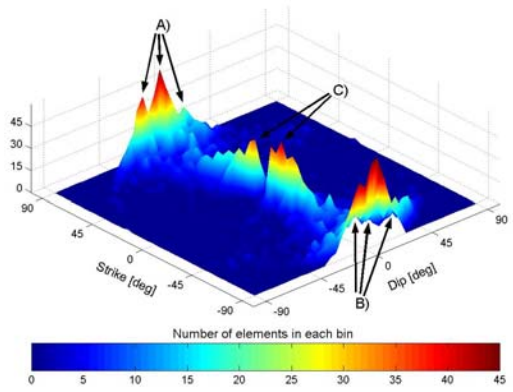

Fig. 3.5: *2D histogram of strike and dip of the fracture system. Strike and dip of all 5022 triangular elements are binned into 40 bins each. The content value of each bin is then used as a point in this surface plot, depicted in vertical direction and by colour. The two peaks at the top left (A) and bottom right (B) are actually two parts of the same peak, caused by the co-linearity of the elements’ normal-vectors facing in diametrically opposed directions. In each of these peaks, three sub-peaks can be identified, which are interpreted as three nearly parallel and mainly planar fractures. The central peak (C) signifies a large number of peaks at high angles to the main fractures, representing the interconnections of the main features.*

Secondly, in the long run, the more important approach is to set up and run a flow and transport model of the fracture network using the obtained geometric information in order to reproduce the breakthrough data from former field experiments and to critically test the results obtained by earlier transport models. However, due to partial inadequacies in the dataset and also due to the extreme complexity of such geometries, the resulting digital geometry is not suited to be directly used as a geometric basis for flow and transport calculations. Therefore, among the most critical tasks necessary to obtain a useful geometric basis is the filling of gaps in the dataset either through statistical reproduction of equivalent networks or through careful interpolation. Another important task is the simplification of the geometry, from initially more than 8000 elements towards a more reasonable approximation of the true geometry. A large portion of such a simplification can be achieved by replacing subsets of elements which appear to be nearly co-planar with truly planar structures. Often, the two processes of filling gaps and

simplifying the geometry can be combined, when co-planar elements of an apparently planar structure are visible above and below the gap. Obviously, such a specialised manipulation of geometric elements required the development of certain tools and routines, mostly created by using Matlab.
Further work will include modelling migration experiments conducted prior to the extraction of the studied rock volume as well as comparisons of results obtained from applying the geometric information to different modelling approaches.

Complementary to the above PhD project, tracer transport in complex 3D fracture networks is investigated in co-operation with Gennady Margolin (University of Notre Dame, USA) and Brian Berkowitz (Weizmann Institute, Israel). A final publication with details of our study and their results is currently in preparation.

3.1.8 Work performed in the frame of the EU-concerted action RETROCK

RETROCK examines how the retention processes are and should be recognised in performance assessment models for deep geological repositories hosted by crystalline rocks. The overall objective of the project is to develop a common basis for incorporating geosphere retention phenomena in the performance assessments. The main focus is in examining whether the simplifications adopted in the performance assessments can be defended with results of more complex process models, with facts from experimental investigations and other results from observations on natural systems.
After three years, RETROCK will come to an end in November 2004.

In RETROCK our main focus this year was on work package 2 (from a total of 3) entitled “Examination of concepts”. Our contribution to work package 2 was a comprehensive article concerning matrix diffusion; the in-depth examination of the current understanding and approaches of different sub-processes associated to matrix diffusion, such as, e.g., channelling, anion exclusion or pore plugging - reactive transport. Other important aspects like the consequences of a possible limited extension of the porous rock accessible for matrix diffusion, or the question how to deal with possible time-dependencies in transport modelling, etc. were discussed in detail, too. In addition, eight different performance assessments from Sweden, Finland and Switzerland were examined with the aim of finding out, how matrix diffusion was addressed, and whether a consistent picture emerges regarding the varying methodology of the different radioactive waste organisations.
Finally, due to its comprehensiveness it was decided to publish our contribution as an independent PSI report and a Nagra technical report.

3.1.9 PhD research proposal, time-of-flight (TOF) neutron scattering

A proposal for allocation of beam time at FOCUS (SINQ – the PSI neutron source) for the next two years was submitted and approved in February 2004. (Further details can also be found in section 7.) Following the assessment of the applicants, Fatima Gonzàlez from Spain was appointed for the project. She started her work in January 2004. The PhD project aims at characterising diffusive transport of solutes through compacted clays at various scales. She started to run a series of laboratory diffusion experiments of HTO through compacted clay samples of 1-cm thickness using Na- and Ca-Montmorillonite, Na- and Ca-Illite, Kaolinite, Pyrophyllite and for two different ionic strengths of the external solution. In the near future she will compare the values for the macroscopic diffusion coefficients with those on the nm scale deduced from quasi elastic neutron scattering. In order to successfully link the observations at the two different scales, it is also necessary to characterise, by various methods, the texture of the clay samples, especially particle sizes, particle orientation, etc.

3.1.10 Radionuclide transport in the excavation disturbed zone

To investigate radionuclide transport and geochemical reactions within the excavation-disturbed zone (EDZ) in argillaceous shale, foreseen as a host rock for a nuclear waste repository, samples from a three meter long, horizontal drill core have been collected during a drilling campaign in a 130 year old railway tunnel. The samples vary from highly fractured, air- and groundwater-altered, near-tunnel sections to undisturbed clay sections further away. Samples from this bore core can be used for reactive transport experiments, e.g. cement–clay interactions and for radionuclide through- and out-diffusion experiments in order to investigate transport and geochemical processes in the EDZ. Such an open-tunnel scenario resembles repository conditions during construction, filling and monitoring phase, where for some period oxidizing conditions cause pyrite oxidation accompanied by gypsum precipitation. The changed mineralogical composition and additional structural changes in the EDZ may have a pronounced effect on the radionuclide transport properties in the EDZ, which have to be investigated experimentally, and analysed by reactive transport modelling. Its results should also be compared with results from experiments and subsequent modelling of radio-

nuclide transport in undisturbed, unaltered samples from Benken and Mont Terri.

3.1.11 Work performed for the colloid and radio-nuclide retardation experiment (CRR)

The work on the project „Colloid and Radionuclide Retardation experiment (CRR)“ has come to an end. The necessary project reports were externally reviewed and they will be printed by the end of 2004 (GUIMERA et al., 2004; KOSAKOWSKI AND SMITH, 2004).

3.1.12 Work for the Opalinus clay performance assessment (Entsorgungsnachweis)

Linked to the safety analysis for Opalinus Clay there was a lengthy discussion with the NEA and KNE reviewers about specific details of the performance assessment. Their additional questions had to be answered in written form.

The FRAC3DVS calculations for the safety assessment of the planned Swiss repository for high-level radioactive waste in the Opalinus clay formation were published in the final project report.

Furthermore, a report concerning the pore structure of Opalinus clay was completed.

3.1.13 References

ADELMANN A. (2004)
A science-based case for large-scale computation at PSI. PSI Report 04-04, Paul Scherrer Institut, Villigen, Switzerland

GUIMERA J., KOSAKOWSKI G., IIJIMA K., PUDEWILLS A., SMITH P. (2004)
The CRR final project report series: 3 - results of the supporting modelling programme, Nagra Technical Report NTB 02-04, Wettingen, Switzerland (in print)

HADERMANN J., HEER W. (1996)
The Grimsel (Switzerland) migration experiment: integrating field experiments, laboratory investigations and modelling, Journal of Contaminant Hydrology, Vol. 21, 87 – 100

KOSAKOWSKI G., SMITH P. (2004)
Modelling the transport of solutes and colloids in a water-conducting shear zone in the Grimsel Test Site. PSI Bericht Nr. xx, Nagra NTB 04-01, (in print)

KUECHLER R., NOACK K. (2002)
Transport of reacting solutes through the unsaturated zone. Transport in Porous Media, Vol. 49, 361 - 375

YEH G.-T., SALVAGE K.M., GWO J.P., ZACHARA J.M., SZECSODY J.E. (1998)
HYDROBIOGEOCHEM: A Coupled Model of HYDROlogic Transport and Mixed BIOGEO-CHEMical Kinetic/Equilibrium Reactions in Saturated-Unsaturated Media, ORNL/TM-13668, Oak Ridge National Laboratory, Center for Computational Sciences, Oak Ridge, TN 37831, USA

3.2 Publications

3.2.1 Peer reviewed journals and reports

JAKOB A. (2004)
Matrix diffusion for performance assessment – experimental evidence, modelling assumptions and open questions. PSI-Bericht Nr. 04-08, Nagra NTB 04-07

KOSAKOWSKI G. (2004)
Anomalous transport of colloids and solutes in a shear zone. Journal of Contaminant Hydrology, Vol. 72, 23 - 46

KOSAKOWSKI G. (2004)
Time-dependent flow and transport calculations for Project Opalinus Clay (Entsorgungsnachweis). PSI-Bericht Nr. 04-10, Nagra NTB 03-10

PFINGSTEN W., PARIS B.[1], SOLER J.M.[2], MÄDER U.K.[3] (2004)
Tracer and reactive transport modelling of interactions between high-pH fluids and fractured rock: Field and laboratory experiments. Journal of Geochemical Exploration (in print)
[1] ITASCA-Consulting, Lyon, France
[2] CSIC-IJA, Barcelona, Spain
[3] Rock-Water Interaction (RWI), University of Bern, Switzerland

URSINO N.[1], GIMMI T. (2004)
Combined effect of heterogeneity, anisotropy and saturation on steady state flow and transport. Structure recognition and numerical simulation. Water Resources Research, Vol. 40, W01514, doi: 10.1029/2003WR002180
[1] University of Padova, Italy

VAN LOON L.R., JAKOB A. (2004)
Evidence for a second transport porosity for the diffusion of HTO in a sedimentary rock (Opalinus clay): Application of through- and out-diffusion techniques. Transport in Porous Media (submitted)

WERSIN P.[1], VAN LOON L.R., SOLER J.M.[2], YLLERA A.[3], EIKENBERG J., GIMMI T., HERNAN P.[4], BOISSON J.-Y.[5] (2004)
Long-term diffusion experiment at Mont Terri: first results from field and laboratory data. Applied Clay Science (in print)
[1] Nagra, Wettingen, Switzerland
[2] CSIC-IJA, Barcelona, Spain
[3] CIEMAT, Madrid, Spain
[4] ENRESA, Madrid, Spain
[5] IRSN, Fontenay-aux-Roses, France

3.2.2 Conferences/Workshops/Presentations

CHURAKOV S.V. (2004)
Dehydration-carbonation reaction on brucite surface and proton dynamics in the topaz-OH. Theoretical chemistry group seminar, University of Zürich, Zürich, Switzerland (oral presentation)

GAUTSCHI A.[1], BAEYENS B., BRADBURY M.H., GIMMI T., MAZUREK M.[2], MARSCHALL P.[1], SCHWYN B.[1], VAN LOON L.R., WABER N.H.[2], WERSIN P.[1] (2004)
Geoscientific basis for making the safety case for a SF/HLW/ILW repository in Opalinus Clay in NE Switzerland (Project Entsorgungsnachweis) – II: The geosphere as a transport barrier: Hydraulic, diffusion, and sorption properties. In: Geological Disposal: Building Confidence using Multiple Lines of Evidence, Proceedings of the first AMIGO workshop, Yverdon-les Bains, Switzerland, 3 - 5 June 2003, OECD/NEA, Paris, France, 63 – 70. (oral presentation)
[1] Nagra, Wettingen, Switzerland
[2] Rock-Water Interaction (RWI), University of Bern, Switzerland

KOSAKOWSKI G. (2003)
Modelling tracer tests at the Grimsel test site – selected results from the Colloid Radionuclide Retardation (CRR) experiment. Research Seminar Applied Geology, 12 November 2003, University of Tübingen, Germany (oral presentation)

KOSAKOWSKI G. (2003)
Numerical Investigations about the Influence of Glacial Loading on the Transport of Radionuclides in the Opalinus Clay Formation. NEA-IGSC workshop on "Stability and buffering Capacity of the Geosphere for Long-term Isolation of Radioactive Waste: Application to Argillaceous Media", 9 - 11 December 2003, Braunschweig, Germany (poster)

MARSCHALL P.[1], HORSEMAN S.[2], GIMMI T. (2004)
Characterisation of gas transport properties of Opalinus Clay, a potential host rock for radioactive waste disposal. Proceedings of the IFP research conference Gas-Water-Rock Interactions Induced by Reservoir Exploitation, CO_2 Sequestration, and other Geological Storage, November 2003
[1] Nagra, Wettingen, Switzerland
[1] British Geoloigcal Survey, Keyworth, Nottingham, UK

MAZUREK M.[1], GAUTSCHI A.[2], GIMMI T., LEU W.[3], MARSCHALL P.[2], MÜLLER W.H.[2], NAEF H[4]., WABER N.H.[1] (2004)
Geoscientific basis for making the safety case for a SF/HLW/ILW repository in Opalinus Clay in NE Switzerland (Project Entsorgungsnachweis) – VI: Geosphere stability: Learning from the past to predict future long-term evolution. In: Geological Disposal: Building Confidence using Multiple Lines of Evidence, Proceedings of the first AMIGO workshop, Yverdon-les Bains, Switzerland, 3 - 5 June 2003, OECD/NEA, Paris, France, 79 – 86 (oral presentation)
[1] Rock-Water Interaction (RWI), University of Bern, Switzerland
[2] Nagra, Wettingen, Switzerland
[3] Geoform AG, Minusio, Switzerland
[4] Büro für angewandte Geologie und Kartographie, St. Gallen, Switzerland

METTIER R., KOSAKOWSKI G., KOLDITZ O.[1] (2004)
Extracting realistic fracture network geometry from borecore data. Gordon Research Conference on Flow and Transport in Porous Media, 11 – 16 July 2004 Queens College, Oxford, United Kingdom (poster)
[1] University of Tübingen, Germany

PFINGSTEN W. (2003)
Modelling dye, Cs, Co and Eu spreading for best-fit-run#10 parameters. 11. HPF - Project Meeting, 27 - 28 November 2003, Wettingen, Switzerland (oral presentation)

PFINGSTEN W. (2004)
Modelling of Cs, Co and Eu transport within a dipole flow field in a high-pH altered, heterogeneous shear zone. EGU General Assembly 2004, 25 - 30 April 2004, EGU, Nice, France (oral presentation)

PFINGSTEN W. (2004)
Influence of porosity distribution and available surface area on Cs, Co and Eu breakthrough - Assumption to "generate" an early breakthrough. 12. HPF - Project Meeting, 28 - 29 May 2004, Meiringen, Switzerland (oral presentation)

SOLER J.M.[1], PARIS B.[2], PFINGSTEN W., MÄDER U.K.[3] (2004)
Flow and reactive transport modeling in the framework of GTS-HPF. International Symposium on Water-Rock Interaction WRI-11, 27 June - 2 July 2004, Saratoga Springs, New York, USA. Proceedings Vol. 2, 983 - 987. A.A. Balkema Publishers (oral presentation)

[1] CSIC-IJA, Barcelona, Spain
[2] ITASCA-Consulting, Lyon, France
[3] Rock-Water Interaction (RWI), University of Bern, Switzerland

3.2.3 Internal reports

GIMMI T. (2003)
Porosity, pore structure, and energy state of pore water of Opalinus Clay from Benken. Nagra Interner Bericht, Nagra, Wettingen, Switzerland

JAKOB A. (2004)
The author's response to the reviewer of the RETROCK work package 2 contribution entitled – The scientific basis of matrix diffusion. PSI Internal Report AN-44-04-05

KOSAKOWSKI G., THOENEN T., CHURAKOW S. (2004)
Investigation of Radionuclide Migration in Clays using Molecular Modelling Techniques. PSI Internal Report, AN-44-04-03

KOSAKOWSKI G. (2004)
Author's response to a review by P. Robinson of "Time-dependent flow and transport calculations for Project Opalinus Clay (Entsorgungsnachweis)". PSI Internal Report, AN-44-04-06

PFINGSTEN W., KULIK D. (2004)
Coupled flow, transport and geochemical processes in a heterogeneous repository near-field using high performance computers. PSI Internal Report AN-44-04-04

PFINGSTEN W. (2004)
Minutes of a meeting on high performance computing of NES groups interested in the HORIZON high performance computing application. PSI Internal Report AN-44-04-07

PFINGSTEN W. (2004)
Estimations of Cs, Co and Eu migration in a heterogeneous, high-pH altered shear zone at Grimsel test site compared to that of a non-sorbing dye-tracer (uranine). PSI Internal Report AN-44-04-10

3.3 Teaching

KOSAKOWSKI G. (2003)
Geostatistics II. Lecture series for the course "Masters in Applied Environmental Geoscience", University of Tübingen, Germany, WS 2003/2004

KOSAKOWSKI G. (2004)
Geostatistics I. Lecture series for the course "Masters in Applied Environmental Geoscience", University of Tübingen, Germany, SS 2004

3.4 Review work for scientific journals

Applied Geochemistry,
Journal of Contaminant Hydrology,
Water Resources Research.

4 CLAY SYSTEMS

B. Baeyens, M. Bradbury, R. Dähn, M. Mantovani, A. Schaible

4.1 Introduction

The sorption data base (SDB) reports for Opalinus clay and MX-80 bentonite, used in the safety assessment of a waste repository for spent fuel, high-level and long-lived intermediate-level waste (Entsorgungsnachweis), have been evaluated by the HSK. A further report considering the influence of the interaction between a high pH plume and the Opalinus clay host rock on sorption has been completed.

Mechanistic sorption studies of key radionuclides are continuing on illite and montmorillonite clay minerals. The sorption of Sr(II), Ni(II), Eu(III) and U(VI) on illite (du Puy) could be successfully modelled with a combined cation exchange and surface complexation model. Part of this work was carried out within the 5th EU framework project ACTAF.

A milestone in the mechanistic sorption investigations of metals on montmorillonite was achieved with the establishment of a linear free energy relationship (LFER) for 11 elements between the strong site surface binding constants and the corresponding aqueous hydrolysis constants. This LFER was than subsequently used to estimate surface complexation constants for heavy metals and actinides for which only poor or no sorption data is available.

A further important study was on the sorption of Eu(III) and Cm(III) on illite and montmorillonite and the linkage between wet chemistry results combined with modelling, and time resolved laser fluorescence spectroscopy (TRLFS) investigations. These studies were performed within the framework of a bilateral co-operation between LES/PSI and INE/FZK.

Measurement campaigns at the Rossendorf beamline (ROBL) and the Advanced Light Source (ALS) on U(VI)/illite and Zn/Opalinus clay respectively were successful. The latter showed the importance of performing combined XRF and XAS measurements on a micro-scale to determine the fate of heavy metals in heterogeneous systems.

The 5th EU framework project FEBEX II is coming to an end. The bentonite porewater investigations and the sorption studies of Cs(I), Sr(II) and U(VI) on montmorillonite have been completed. The results from a joint CIEMAT/PSI investigation on Febex bentonite porewater chemistry have been published.

Studies on the influence of the presence of inorganic carbonate on the uptake of radionuclides on montmorillonite and illite are one of the main subjects in the 6th EU framework integrated projects NF-PRO and FUNMIG respectively. The former project started in January 2004 whereas the latter will start at the beginning of next year.

M. Mantovani retired in May 2004. Noreen Verde joined the *Clay Systems* sub-programme in August 2004.

4.2 Performance assessment

The two sorption data bases (SDBs) for the near- and far-fields (BRADBURY & BAEYENS, 2003a,b) used in the safety assessment of a waste repository for spent fuel, high-level and long-lived intermediate-level waste (Entsorgungsnachweis) have been critically reviewed by the Swiss Federal Nuclear Safety Inspectorate (HSK). The work was positively evaluated and judged to have a high quality. The large body of "in house" sorption data sets measured and used in the development of the SDB was especially praised. An overview of the procedures used to derive sorption values for the different elements is illustrated in Fig. 4.1 where the selected distribution ratios (R_d) and estimated uncertainties are summarised for the Opalinus clay SDB.

Fig. 4.1 illustrates that for some elements (red bars) a full mechanistic model was used to derive R_d values. For the majority of elements (blue bars) "in-house" sorption edges and isotherms were available and a semi mechanistic approach was adopted to derive sorption data. For the remaining elements single point measurements or expert judgement was the only means of compiling sorption values. In some cases the choice and validity of chemical analogues and the potential influence of inorganic carbon were questioned by HSK, and these uncertainties need to be resolved in the future.

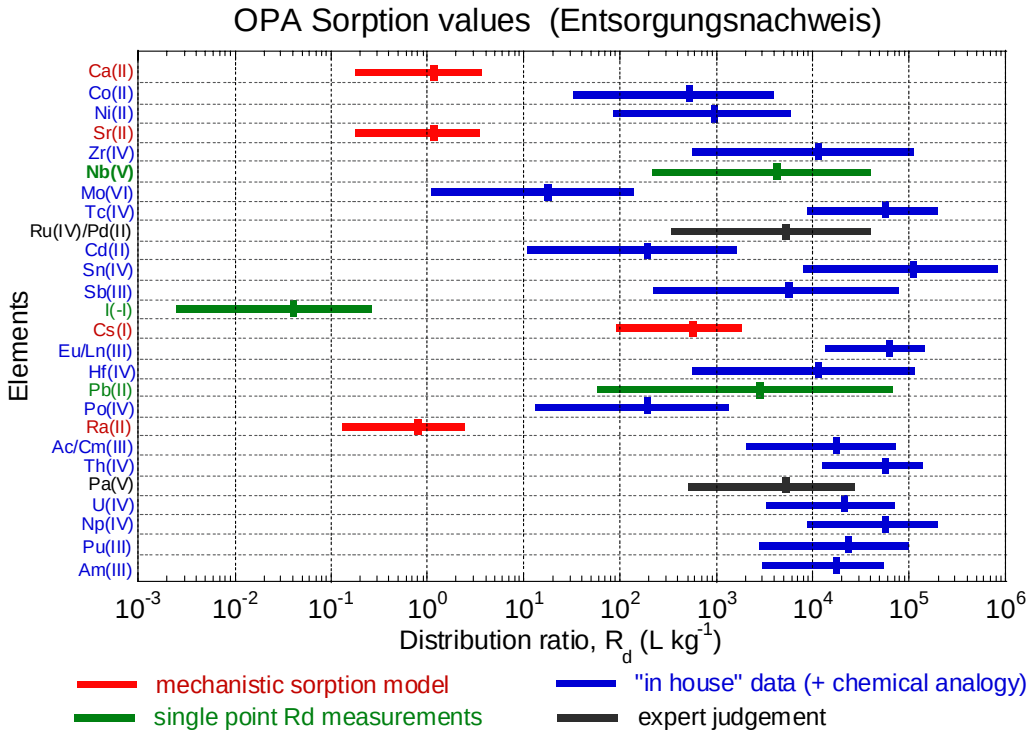

Fig. 4.1: *Sorption values and uncertainty ranges selected for the Opalinus clay SDB.*

The interaction of groundwater with the large quantities of cement/concrete used in the construction and backfilling of caverns containing long-lived intermediate level radioactive waste may give rise to the release of a pulse of hyperalkaline fluid (pH plume) into the surrounding rock. Since the pH of this plume could remain in excess of 12.5 for tens of thousands of years many minerals in a sedimentary host rock would be unstable leading to dissolution reactions, secondary mineral precipitation and changes in groundwater chemistry. The effects of the interactions between a pH plume and Opalinus clay on the sorption properties of the formation has been assessed and appropriate sorption data bases have been compiled. A report on this work has been published (BRADBURY & BAEYENS, 2004a).

4.3 Mechanistic sorption studies

Illite and montmorillonite are important clay mineral components in many argillaceous rocks and bentonites under consideration throughout Europe as host formations and backfill materials for the deep disposal of radioactive waste. A good understanding of the sorption characteristics of such rock types over a wide range of conditions is particularly important in this context. The mechanistic studies continue the "bottom-up" approach to sorption which began with the investigations on montmorillonite and bentonite. The idea is that by understanding the sorption processes on single mineral phases and developing models to describe them, this knowledge can be applied to understand and quantitatively predict the uptake of elements in complex mineral/ groundwater systems. The aim of this work is to provide a basis for this approach.

4.3.1 Illite

In an extensive study the physico-chemical, protolysis and sorption characteristics of Sr(II), Ni(II), Eu(III) and U(VI) have been measured on illite and modelled over a wide range of pH, sorbate and $NaClO_4$ concentrations. The majority of this work was carried out within the 5th EU framework project ACTAF.

Samples of illite (du Puy) were carefully conditioned to the Na-form and physico-chemically characterised. Potentiometric titrations on suspensions of the Na-illite were carried out using a batch back titration technique in 0.01, 0.1 and 0.5 M $NaClO_4$ background electrolytes from pH ~2 to ~12 in an inert atmosphere glove box. The supernatant solutions from each titration experiment in each series were analysed for K, Mg, Ca, Sr, Si, Al, Fe and Mn.

Sorption edges (R_d versus pH at trace sorbate concentrations and constant ionic strength) were determined for Sr(II), Ni(II), Eu(III) and U(VI) on Na-illite as a function of $NaClO_4$ concentration under anoxic conditions ($CO_2 \leq 2$ ppm, $O_2 \leq 2$ ppm.). Sorption isotherms for the same set of radionuclides

under similar conditions were measured for Na-illite suspensions in 0.1 M $NaClO_4$ at fixed pH values.

The titration data were modelled in terms of the protolysis of two amphoteric edge sites ($\equiv S^{W1}OH$ and $\equiv S^{W2}OH$) without an electrostatic term. The protonation/deprotonation constants and site capacities obtained from the titration measurements were then fixed. The sorption edge and isotherm data were modelled with strong ($\equiv S^{S}OH$) and weak ($\equiv S^{W1}OH$) surface complexation sites, assumed to have the same protolysis constants, again without electrostatic terms. Uptake by cation exchange was included in all of the calculations. This sorption model, the 2 site protolysis non-electrostatic surface complexation and cation exchange (2SPNE SC/CE) model, had been developed previously for montmorillonite and was used to describe the sorption characteristics of Sr(II), Ni(II), Eu(III) and U(VI) on Na-illite over a wide range of conditions.

At 0.01 M $NaClO_4$ and pH < 8 the sorption of Sr(II), Ni(II), Eu(III) and U(VI) was dominated by a cation exchange mechanism. The strong dependency of sorption on pH observed under these conditions arose from the competitive effects of Ca and Al on the uptake of the sorbate. Selectivity coefficients for Ca and Al with respect to Na were deduced from these measurements.

A report on this work has been written (BRADBURY & BAEYENS, 2004b)

4.3.2 Montmorillonite

Literature and "in house" sorption edge measurements on montmorillonite for eleven elements: Mn(II), Co(II), Ni(II), Zn(II), Cd(II), Eu(III), Am(III), Sn(IV), Th(IV), Np(V) and U(VI), have been modelled using the 2SPNE SC/CE model in terms of their uptake on strong ($\equiv S^{S}OH$) sites. In this modelling exercise the protolysis constants and site capacities derived from previous work (BRADBURY & BAEYENS, 1997) were considered to be non-adjustable parameters and were fixed in all of the calculations. In this manner a set of surface complexation constants for the strong sites on montmorillonite was established. Cation exchange was always included in the modelling and wherever the measured data allowed, selectivity coefficient values were extracted.

In the field of aqueous phase thermodynamics it is well established that relationships can be found between the free energies of formation of metal complexes and thermodynamic (or non thermo-dynamic) properties of the metal ions or ligands. Such systematic dependencies are commonly termed linear free energy relationships (LFERs).

By analogy with aqueous phase coordination chemistry, seeking LFERs would seem to be an obvious step to test the consistency of the data and to interpret trends. The LFERs so far presented in the literature generally only involve surface complexation constants on (synthetic) oxides and the first hydrolysis constant for relatively limited data sets (e.g. DUGGER et al., 1964; SCHINDLER et al., 1976; DZOMBAK & MOREL, 1990).

In the case of montmorillonite up to four surface complexation reactions involving the metal cation and 1:1, 1:2, 1:3 aqueous hydroxy complexes were required to reproduce the sorption edge data. The whole of this data was included, and the results are shown in Fig. 4.2 on a single plot. The linear correlation between the surface complexation constants and the corresponding aqueous hydroxy species was found to be very good.

A similar exercise was carried out for the weak ($\equiv S^{W1}OH$) sites by modelling sorption isotherms. Despite the fact that relevant data are sparse, and weak site complexation constants could only be calculated for Ni(II), Zn(II), Eu(III) and U(VI), a very acceptable correlation between the site binding constants and aqueous hydrolysis constants was found. This particular exercise highlighted the lack of data on montmorillonite suitable for modelling in terms of weak site types.

Surface complexation constants cannot be calculated from theoretical considerations. In radioactive waste disposal for example, sorption data for Pd(II), Pb(II), Pu(III), Zr(IV), U(IV), Np(IV), Pu(IV) and Pa(V) are either very poor or not available at all. The LFER approach, based on the above, was used to estimate surface complexation constants on strong sites for these heavy metals and actinides on montmorillonite.

The surface protolysis constants, site capacity values, selectivity coefficients and surface complexation constants derived in this and previous studies, coupled with the LFERs established for the strong and weak sites on montmorillonite, is viewed as forming the basis for a thermodynamic sorption data base. Instead of the usual distribution ratio approach used in performance assessment, the way begins to open up to methods capable of calculating sorption values specific to different geochemical scenarios. A paper on these investigations has been accepted for publication (BRADBURY & BAEYENS, 2004).

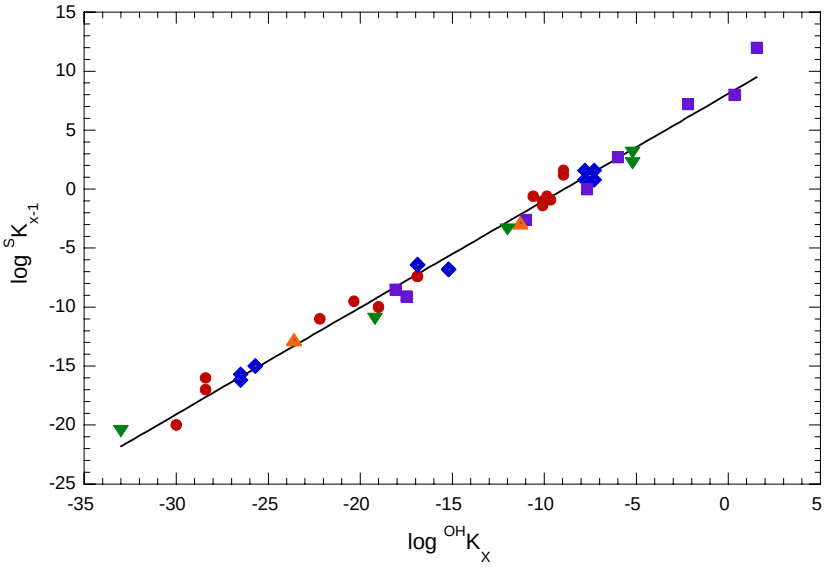

Fig. 4.2: *Correlation of surface complexation constants ($^{S}K_{x-1}$) of species sorbing on the strong sites of montmorillonite with the corresponding hydrolysis constants ($^{OH}K_{x}$). (●) Mn(II), Co(II), Cd(II), Ni(II), Zn(II), (♦) Eu(III), Am(III), (■) (Sn(IV), Th(IV), (▲) Np(V), (▼) U(VI).*

4.3.3 Cation exchange capacity of illite

The isotope dilution technique using Na and Cs as index-cations was used to determine the cation exchange capacity (CEC) of illite du Puy as a function of background electrolyte composition. The work showed, in accord with previous studies, that the CEC values were in the order Cs-CEC > Na-CEC. Sodium is commonly chosen as index-cation in CEC determinations using the isotope dilution method. The experimentally measured Na-CEC values for Na-illite increased from ~75 to ~200 meq kg^{-1} for $NaClO_4$ concentrations in the range 5.6 x 10^{-4} to 1.25 x 10^{-2} M. Cesium CEC determinations showed a much less pronounced trend over a $CsNO_3$ concentration range from 10^{-3} to 10^{-2} M. A reference Cs-CEC value of 225 meq kg^{-1} was chosen. Careful chemical analyses of the supernatant solutions revealed that Ca and Mg at the (sub) µmolar level were present in all the determinations, despite the extensive conditioning procedures used. Competition between (Ca + Mg) and Na for the exchange sites was put forward as an explanation for the variation of Na-CEC values. This hypothesis was confirmed in a series of single (^{45}Ca) and double (^{45}Ca plus ^{22}Na) labeling experiments. A two site cation exchange model was developed with site capacities and $^{Ca}_{Na}K_c$ values for each site: planar site capacity =180 meq kg^{-1}, $^{Ca}_{Na}K_c^{PS}$ = 2; type II site capacity = 45 meq kg^{-1}, $^{Ca}_{Na}K_c^{II}$ = 80. The model was able to predict the Na and Ca occupancies in the Na-CEC experiments for $NaClO_4$ concentrations from 5.6 x 10^{-4} to 0.1 M. A recommendation arising out of this work was that Cs should be used instead of Na as the index-cation for determining the CEC of illite (BAEYENS & BRADBURY, 2004).

4.3.4 Bentonite porewater model testing

In almost all high-level waste repository concepts highly compacted bentonite in one form or another is the preferred material for backfilling and sealing the emplacement tunnels. During re-saturation with groundwater the bentonite swells and seals against the emplacement tunnels. The nature and distribution of the water in highly compacted re-saturated bentonite (interlayer-water, double layer water, "free"porewater) and the composition of the porewater component is still a matter under discussion. The ability to give a chemically well founded porewater composition is essential since such knowledge is a pre-requisite for predicting near-field solubilities, developing sorption data bases, understanding diffusion processes and also for assessing the influence of long term groundwater-bentonite interactions.

The aim of this study was to test the BRADBURY & BAEYENS (2002) model in terms of its ability to predict one of the most important parameters for any porewater, namely the pH. The bentonite porewater model is capable of making clear and definite predictions regarding pH based on the (fixed) site capacities of the amphotheric ≡SOH sites, their

(fixed) protolysis characteristics, and the hypothesis that the bentonite powder is initially in equilibrium with air. Also, provided the solid to liquid (S:L) ratio is sufficiently high, the montmorillonite will have a buffering effect on the pH of any solution with which it is placed in contact. The concept behind the test is to take a powdered bentonite and an electrolyte containing known quantities of acid or base, and mix them together at a high S:L ratio in a sealed container and allow them to react in the absence of air. If the model concepts and parameter values are valid then the model should be able to predict the pH measured in such experiments.

4.3.5 Retention in Opalinus clay

The dominant transport mechanism in argillaceous rocks is diffusion and the key parameter in transport calculations is the apparent diffusion coefficient (D_a). D_a values can be either directly determined from "in-diffusion" type experiments (laboratory or field), or they can be calculated from separately determined parameters such as the effective diffusion coefficient, D_e, and the distribution ratio, R_d. The former are obtained from "through-diffusion" tests whereas the latter comes from batch sorption measurements. An important key question invariably arises as to whether it is justifiable to use sorption values determined on dispersed systems to calculate D_a values for highly compacted ones.

A study has been conducted in which a contribution to this question has been made. Table 1 summarises R_d values obtained from some careful "through-diffusion" tests (see sub-programme diffusion), batch sorption measurements and geochemical modelling calculations for Na and Sr in the Mont Terri Opalinus clay system.

***Table 4.1**: Comparison of R_d values (m^3 kg^{-1}) obtained from different approaches for Na and Sr in the Opalinus clay system.*

Element	Diffusion	Batch sorption	Modelling
Na	0.9×10^{-4}	1.5×10^{-4}	
	1.0×10^{-4}	to	2.5×10^{-4}
	1.9×10^{-4}	2×10^{-4}	
	1.3×10^{-4}		
Sr	7.4×10^{-4}	1.3×10^{-3}	6×10^{-4}
	7.1×10^{-4}		

The results in Table 1 clearly indicate that within a factor of 2 the three independent approaches yield the same R_d values for Na and Sr in the Opalinus clay system. This result is very promising but certainly needs further investigations on metals with more complex chemistries and sorption characteristics in order to increase the confidence in up-scaling to the Opalinus clay host rock.

4.4 Surface analysis studies

The further development of the sorption models (see sections 4.3.1 and 4.3.2) and their credibility will depend on verifying (or not) the major assumptions contained in them. In this endeavour high resolution surface analytical techniques such as X-ray adsorption spectroscopy (XAS) and time resolved laser fluorescence spectroscopy (TRLFS) will undoubtedly make important contributions. Already distinctions made in the model between cation exchange (outer sphere complex formation) and surface complexation (inner sphere complex formation) under a variety of different conditions have been confirmed by spectroscopic measurements. It is essential to make much closer links between wet chemistry measurements, modelling and spectroscopic techniques in terms of the identity and structure of surface species for real progress to be made.

4.4.1 TRLFS

Because of its high fluorescence spectroscopic sensitivity, sorbed species of Cm(III) on clay minerals can be studied on a molecular level at very low concentrations by TRLFS. Cm(III) is a good chemical analogue for trivalent actinides and lanthanides and allows comparisons to be made with sorption measurements and modelling studies of for example Eu(III) in a concentration region important in radioactive waste disposal and not readily accessible by other surface spectroscopic techniques. The ability to make measurements in the sub-micromol region is particularly attractive because the sorption behaviour and modelling of Eu(III) on two of the most abundant and important clay minerals in nature i.e. montmorillonite and illite, is well established.

The aims of this work are clear cut: To model the sorption edge data for Eu on conditioned and purified Ca-montmorillonite and Na-illite carried out under well defined conditions using the 2SPNE SC/CE model to predict the surface complexes and their pH regions of stability. The predictions based on wet chemistry and modelling can then be compared with TRLFS measurements of Cm carried out on Ca-montmorillonite and Na-illite in the same background electrolytes as a function of pH. The TRLFS measurements are able to distinguish between different surface species and yield information on the hydration sphere about the Cm species sorbed on the surface. The idea is to compare and contrast the results from the two sources and to see whether a

consistent picture for the sorption of Cm/Eu on montmorillonite and illite can be found. In the following the results obtained for Eu/Cm sorption on Ca-montmorillonite are given. (This work is part of a bilateral co-operation between LES/PSI and INE/FZK.)

The uptake of Eu at trace concentation as a function of pH on montmorillonite has been measured in 0.066 M $Ca(NO_3)_2$. The sorption edge was subsequently modelled using the 2SPNE SC/CE model (see section 4.3.2). The modelling results are shown in Fig. 4.3 where aqueous and sorbed Eu species distributions are presented as % of total Eu concentration as a function of pH.

TRLFS spectra were taken on Cm sorbed onto Ca-montmorillonite as a function of pH in the range 3 to 12. At increasing pH there was a clear red-shift of the Cm emission band which was accompanied by an increase of the fluorescence lifetime. Peak deconvolution of the spectra suggested the existence of three Cm surface species. This is illustrated in Fig. 4.4.

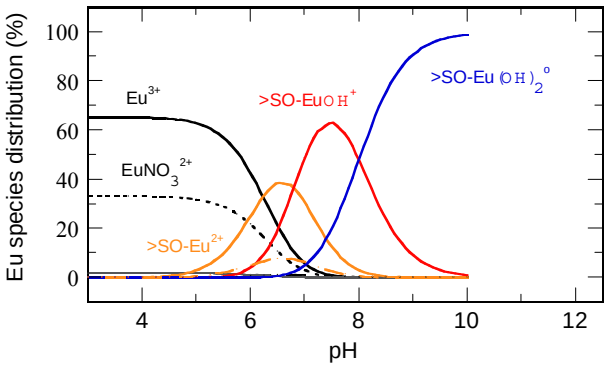

Fig. 4.3: *pH dependent aqueous and surface species distribution of Eu(III) on Ca-SWy-1 obtained from the 2SPNE SC/CE model.*

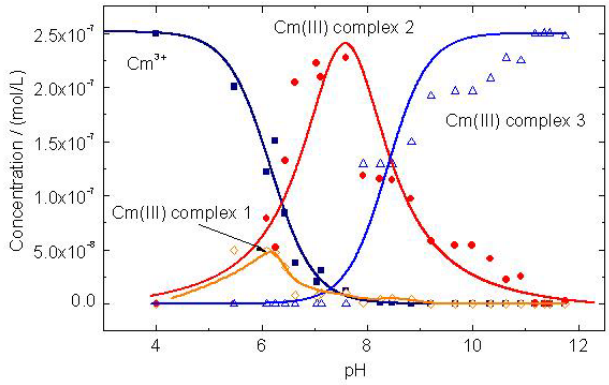

Fig. 4.4: *pH dependent aqueous and surface species distribution of Cm(III) on Ca-SWy-1 obtained from TRLFS.*

A comparison of Figs 4.3 and 4.4 indicate that three inner-sphere surface complexes are identified. However, differences appear in the peak broadness and heights of the individual inner-sphere complexes, and the pH at which the peak height maxima occur. The source of this discrepancy remains unresolved at the moment. The important conclusion drawn from this study is that a qualitative agreement exist on Cm(III)/ Eu(III) uptake mechanism obtained from TRLF and an independent prediction from the 2SPNE SC/CE model.

4.4.2 EXAFS

EXAFS investigations on the Eu/montmorillonite system at the Eu K-edge suffered from technical problems, and an energy dispersive detector which would have allowed measurements at the Eu L_{III}-edge on montmorillonite which contains Fe, was not available. Instead a study on the uptake of Nd onto montmorillonite as a chemical analogue for Eu was initiated. Nd has the advantage that the Nd-L_{III}-edge is below the Fe-K-edge, therefore no Fe-fluorescence is excited hampering the EXAFS measurements.

A Nd treated P-EXAFS montmorillonite (SWy-1) sample with a loading of 45 µmol/g was prepared at pH 7.0 in an 0.3 M $NaClO_4$ background electrolyte. Nd L_{III}-edge XAFS spectra were recorded at the Dutch-Belgium-Beamline (DUBBLE) at the European Synchrotron Radiation Facility (ESRF), Grenoble, France. P-EXAFS spectra were recorded with the electric field vector at $\alpha = 10°$ and 80° with respect to the plane of the self-supporting clay film. $k^3\chi(k)$ P-EXAFS spectra of a Nd treated self-supporting montmorillonite film are shown in Fig. 4.5 indicating an angular dependence. With increasing α the intensity of the shoulder at 5.0 $Å^{-1}$ increases and the wave frequency at 5.0 $Å^{-1}$ shifts slightly. The changes in spectral shape and frequency indicate that the coordination chemistry of Nd is anisotropic, i.e. that its coordination environment is oriented with respect to clay layers. A comparable anisotropic angular dependence was observed by SCHLEGEL et al. (2003) investigating the uptake of Nd onto hectorite. The observed anisotropy in the P-EXAFS spectra suggests that Nd is directly bond to the clay structure. Further data analysis of the P-EXAFS spectra using theoretical approaches such as FEFF calculations (REHR et al., 1991) are in progress.

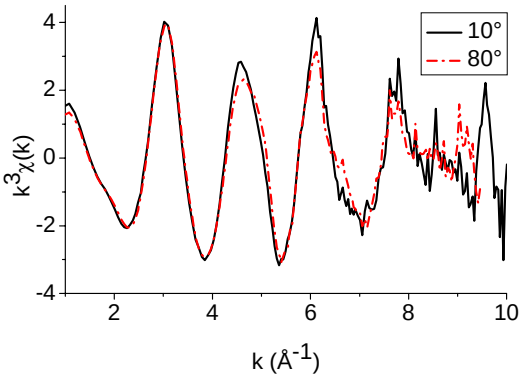

Fig. 4.5: *k3-weighted Nd LIII-edge P-EXAFS spectra of a Nd treated montmorillonite film (pH 7.0) at α angles of 10° and 80°.*

Zn/Opalinus Clay – First scoping experiments have been carried out with the aim of testing combined micro X-ray-fluorescence (micro-XRF) and micro X-ray absorption spectroscopy (micro-XAS) approach for metals sorbed on heterogeneous samples. Thin sections of OPA samples were prepared from a core from a deep bore hole and were saturated for 1 h with synthetic OPA porewater. In an uptake experiment, these thin sections were allowed to react for 24 h with 10^{-4} M Zn dissolved in the porewater. Using micro-XRF and micro-XAS at the 10.3.2 beamline at the ALS (Berkeley) the influence of the different mineral phases on the uptake of Zn onto OPA was investigated. Different locations were analysed with an X-ray beam size down to 5 x 5 µm and a first result is shown in Fig. 4.6.

Fig. 4.6 reveals that Zn is heterogeneously distributed in the sample. No association with Fe rich (e.g. pyrite) and Ca rich phases (e.g. calcite) could be observed. These scoping measurements showed the importance of performing XRF experiments on the micro-scale followed by XAS measurements on selected spots to determine the fate of heavy metals in heterogeneous clay systems and are crucial to the future microXAS measurements at the SLS.

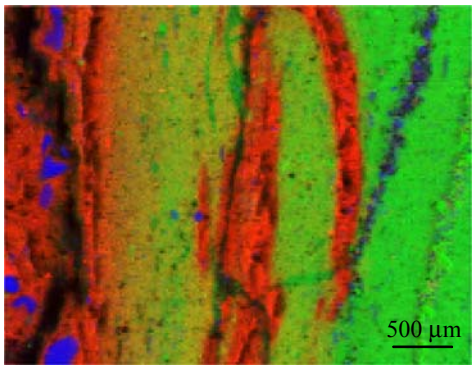

Fig. 4.6*: XRF fine maps of a Zn treated OPA sample (red: Zn, green: Fe, blue: Ca).*

4.5 EU framework projects

4.5.1 ACTAF

The activities within the ACTAF project have been completed and the main achievements are discussed in sections 4.3.1 (sorption on illite) and 4.4.2 (U(VI) XAS results). Contributions to the final technical report have been made.

4.5.2 FEBEX II

The main focus within the FEBEX II project in the past year was the study of the sorption of Sr(II) and U(VI) on montmorillonite. The porewater chemistry studies of Febex bentonite have been completed and a paper on this subject has been published (FERNADEZ et al., 2004). The sorption results are briefly summarised below.

Strontium – Sorption edges (0.01 and 0.1 M $NaClO_4$ on Na-SWy-1) and isotherms (0.1 M $NaClO_4$ on Na-SWy-1 at pH 7.2, and 0.005 M $Ca(NO_3)_2$ on Ca-SWy-1 at pH 7.6) have been determined. At pH < 9, the data could be interpreted by a simple cation exchange mechanism. The edges and the isotherm on Na-SWy-1, and the isotherm on Ca-SWy-1, could be modelled with ${}^{Sr}_{Na}K_c$ = 4.5 and ${}^{Sr}_{Ca}K_c$ = 1.0 respectively. At pH above 9 a clear increase in sorption occurred for the 0.1 M Na-SWy-1 edge data, which is due to surface complexation.

Uranium - Sorption edges (0.01 and 0.1 M $NaClO_4$ on Na-SWy-1) and isotherms (0.1 M $NaClO_4$ on Na-SWy-1 at pH 5.0 and pH 6.8) have been measured and could be successfully modelled using the 2SPNE SC/CE model. The results of these investigations have been included in the LFER study discussed in section 4.3.2.

4.5.3 6th EU framework projects

The objectives for the *Clay Systems* sub-programme are to extend the existing 2SPNE SC/CE model for montmorillonite (NF-PRO) and illite (FUNMIG) to include the influence of aqueous phase carbonate species. The aim is then to test the model predictions against sorption isotherms measured on bentonite and argillaceous rocks under chemically realistic conditions.

4.6 High lights, low lights

The SDB reports for Opalinus clay and MX-80 bentonite were positively evaluated by HSK.

Liner free energy relatioships could be established between strong site surface complexation binding constants for 11 metals on montmorillonite and the corresponding aqueous hydrolysis constants. A

similar LFER was also found for the weak sites on montmorillonite but included only 4 metals.

The preliminary results of MX-80 interaction with solutions at a range of pH values are tending to validate the pH predicted from the model calculations.

Distribution ratios for Na and Sr on Opalinus clay obtained independently from (i) through diffusion tests, (ii) batch sorption measurements and (iii) geochemical modelling studies yielded consistent values. These results contribute to the important key question as to whether it is justifiable to use R_d values determined on dispersed systems to calculate D_a values for highly compacted ones.

The sorption studies of Cm(III) and Eu(III) on clay minerals linking wet chemistry/modelling and surface analysis (TRLFS) within the bilateral collaboration between PSI and FZK made good progress, and joint publications are in preparation.

At the beginning of 2004 collaboration with the HASYLAB (Hamburger Synchrotron Strahlungs-labor) was established to investigate the uptake of Eu onto montmorillonite at the W1 beamline using a Johann type spectrometer. This type of spectrometer allows the detection of Eu(III) fluorescence at the Eu-L3 edge in the presence of a matrix containing relatively high levels of Fe, which would normally gives rise to strong interference. Unfortunately, due to a miss-cut of the Si(110) analyzer crystal of the spectrometer, first experiments foreseen for the spring of 2004, were delayed.

4.7 References

BRADBURY M.H., BAEYENS B. (1997)
A mechanistic description of Ni and Zn sorption on Na-montmorillonite. Part II: Modelling. J. Cont. Hydrol. 27, 223-248

BRADBURY M.H., BAEYENS B. (2002)
Sorption of Eu on Na- and Ca-montmorillonites: Experimental investigations and modelling with cation exchange and surface complexation. Geochim. Cosmochim. Acta 66, 2325-2334

BRADBURY M.H., BAEYENS, B. (2003a)
Near-field sorption data bases for compacted MX-80 bentonite for performance assessment of a high level radioactive waste repository in Opalinus Clay host rock. PSI Bericht Nr. 03-05, Nagra NTB 02-18

BRADBURY M.H., BAEYENS B. (2003b)
Far-field sorption data bases for performance assessment of a HLW repository in an undisturbed Opalinus Clay host rock. PSI Bericht Nr. 03-06, Nagra NTB 02-19

BRADBURY M.H., BAEYENS B. (2004a)
Sorption data bases for safety assessment of a waste repository for spent fuel, high-level and long-lived intermediate-level waste: Influence of the interaction between a high pH plume and the opalinus clay host rock on sorption. PSI Bericht Nr. 04-07, Nagra NTB 03-12 (in press)

BRADBURY M.H., BAEYENS, B. (2004b)
Modelling the sorption of Mn(II), Co(II), Ni(II), Zn(II), Cd(II), Eu(III), Am(III), Sn(IV), Th(IV), Np(V) and U(VI) on montmorillonite: Linear free energy relationships and estimates of surface binding constants for some selected heavy metals and actinides. Geochim. Cosmochim. Acta (accepted for publication)

DUGGER D.L., STANTON J.H., IRBY B.N., MCCONNELL B.L., CUMMINGS W.W., MAATMAN R.W. (1964)
The exchange of twenty metal ions with the weakly acidic silanol group of silica gel. J. Phys. Chem. 68, 757-760

DZOMBAK D.A., MOREL F.M.M. (1990)
Surface Complexation Modeling: Hydrous Ferric Oxide. Wiley-Interscience, New York.

MUNOZ M., ARGOUL P., FARGES F. (2003)
Continuous Cauchy wavelet transform analyses of EXAFS spectra: A qualitative approach. Am. Mineralogist 88, 694-700

REHR J.J., MUSTRE DE LEON J., ZABINSKY S., ALBERS R.C. (1991)
Theoretical X-ray absorption fine structure standards. J. Am. Chem. Soc. 113**,** 5135-5140

SCHINDLER P.W., FURST B., DICK R., WOLF P.U. (1976)
Ligand properties of surface silanol groups. I Surface complex formation with Fe^{3+}, Cu^{2+}, Cd^{2+} and Pb^{2+}. J. Colloid Interface Sci. 55**,** 469-475

SCHLEGEL M.L., POINTEAU I. (2003)
ESRF User Report 25930, CEA de Saclay. Mechanism of Nd, and Lu sorption on silicates and layered silicates by EXAFS spectroscopy

4.8 Publications

4.8.1 Peer reviewed journals and reports

BAEYENS B., BRADBURY M.H. (2004)
Cation exchange capacity measurements on illite using the sodium and cesium isotope dilution technique: effects of the index cation, electrolyte concentration and competition: modelling. Clays Clay Minerals 52, 422-432

BRADBURY M.H., BAEYENS B. (2004)
Sorption data bases for safety assessment of a waste repository for spent fuel, high-level and long-lived intermediate-level waste: Influence of the interaction between a high pH plume and the opalinus clay host rock on sorption. PSI Bericht Nr. 04-07, Nagra NTB 03-12 (in press)

BRADBURY M.H., BAEYENS B. (2004)
Modelling titration data and the sorption of Sr(II), Ni(II), Eu(III) and U(VI) on Na-illite. PSI Bericht Nr. 04-xx and Nagra NTB 04-02 (in press)

BRADBURY M.H., BAEYENS B. (2004b)
Modelling the sorption of Mn(II), Co(II), Ni(II), Zn(II), Cd(II), Eu(III), Am(III), Sn(IV), Th(IV), Np(V) and U(VI) on montmorillonite: Linear free energy relationships and estimates of surface binding constants for some selected heavy metals and actinides. Geochim. Cosmochim. Acta (in press)

FERNANDEZ A.M.[1], BAEYENS B., BRADBURY M.H., RIVAS P.[1] (2004)
Analysis of the porewater chemical composition of a Spanish compacted bentonite used in an engineered barrier. Phys. Chem. Earth 29, 105-118
[1] CIEMAT, Madrid, Spain

4.8.2 Conferences/Workshops/Presentations

DÄHN R., SCHEIDEGGER A.M., MANCEAU A.[1], BAEYENS B., BRADBURY M.H. (2004)
Uptake mechanisms of Ni(II) on montmorillonite as determined by X-ray absorption spectroscopy. Geochim. Cosmochim. Acta. 68, A164 Suppl. 1
[1] University Joseph Fourier, Grenoble, France

4.8.3 Internal reports

BRADBURY M.H., BAEYENS B. (2003)
Diffusion concepts for compacted bentonite PSI Technical Report. TM 44-03-05

4.9 Others, Teaching

SOPRO 2004.
International Workshop on Sorption Processes at Oxide and Carbonate Mineral Water Interfaces. Karlsruhe, March 25-26, 2004. Book of extended abstracts. (lützenkirchen[1], J., Stumpf[1], T., Brendler[2], V., Baeyens, B. & Grolimund, D. (eds.). Wiss. Berichte FZKA 6986, Forschungszentrum Karlsruhe, Karlsruhe, Germany
[1] Forschungszentrum Karlsruhe, Karlsruhe, Germany
[2] Forschungszentrum Rossendorf, Rossendorf, Germany

5 CEMENT SYSTEMS

E. Wieland, J. Tits, M. Vespa, J.P. Dobler, D. Kunz, M. Harfouche

with supporting contributions from M.H. Bradbury, R. Dähn, D. Grolimund, A.M. Scheidegger

5.1 Overview

In the Swiss disposal concepts cement is used to condition low-and intermediate-level (SMA in Swiss terminology) and long-lived intermediate level (LMA in Swiss terminology) radioactive wastes. Furthermore, cementitious materials will be used to surround the waste matrix in the planned LMA repository and to construct the engineered barrier system (components of lining, backfill materials). As a consequence, the near field of the planned LMA repository consists to approximately 90 weight percentage of cementitious materials. From this, approximately 20 weight percentage is hardened cement paste (HCP).

The retardation of safety-relevant radionuclides by HCP is taken into account in performance assessment studies because the source term for radionuclide migration into the host rock is determined by a combination of solubility and sorption constraints in the cementitious near field. Thus, the uptake of radionuclides by HCP and cement minerals plays a decisive role in limiting and retarding the release from the near field.

The long-term aim of the sub-programme "Cement Systems" is to develop mechanistic models of the interaction of safety-relevant radionuclides with HCP under conditions prevailing in the cementitious near field of a repository for radioactive waste. The studies are directed towards improving the quantification of the source terms and strengthening the credibility of sorption values used in performance assessment.

HCP is a complex mixture of mainly calcium (aluminium) silicate hydrates, portlandite and calcium aluminates. Macroscopic and spectroscopic studies have been performed on a sulphate-resisting Portland cement, which is used for the conditioning of radioactive waste in Switzerland, and single cement minerals, namely calcium silicate hydrates (CSH). In the period between September 2003 and August 2004 the main emphasis in the work was placed on macroscopic and spectroscopic studies with Ra(II)/Sr(II), Co(II)/Ni(II), Eu(III)/Cm(III), Th(IV)/Sn(IV) and U(VI), which are either safety-relevant radionuclides or their appropriate analogues. The investigations carried out in the last year and the results from these activities can be summarised as follows:

Uptake studies of Eu(III), Th(IV) and Sn(IV) on HCP are being performed to critically assess the sorption values determined in earlier studies. The studies are on-going.

The wet chemistry studies of the sorption and co-precipitation processes on CSH phases using Sr(II), Eu(III), Th(IV) and U(VI) as tracers have been successfully completed. The studies with Sr(II)/Eu(III) and Th(IV)/U(VI) were carried out within the frameworks of the ECOCLAY II project (5th EU framework programme) and a joint research project with CRIEPI, Japan, respectively. The reports on these topics are in preparation.

Data from extended X-ray absorption fine structure (EXAFS) investigations on U(VI) loaded CSH phases have been analysed and interpreted. This work is part of the joint project with CRIEPI.

An experimental study of the interaction of Ra(II) with HCP and CSH phases was started. The work is carried out within the framework of a joint research project with JNC, Japan.

The Ph.D. project on the influence of the inherent micron-scale spatial heterogeneity of HCP on the immobilization mechanisms of Ni(II) and Co(II) was successfully started, and the first series of micro-spectroscopic investigations has been completed. This project is based on a close co-operation between the sub-programme "Cement Systems" and the "XAS beamline" group of the LES.

The time-resolved laser fluorescence spectroscopy (TRLFS) study on Cm(III) uptake by HCP has been published (STUMPF et al., 2004). The X-ray absorption spectroscopy (XAS) study on Se(IV/VI) immobilization in HCP was resubmitted (BONHOURE et al., 2004).

A Ph.D. project proposal on "A combined macroscopic and spectroscopic study of actinide and lanthanide binding mechanisms in cementitous waste repository materials" was prepared and submitted to the NES Department for approval.

5.2 Sorption studies on HCP

In this project mechanistic studies of the radionuclide immobilization by cementitious materials are based on the combined use of batch sorption (wet chemistry) and spectroscopic techniques. TRLFS and XAS have been successfully employed in the past

years to gain a detailed knowledge of uptake processes in cementitious systems on the molecular scale (SCHEIDEGGER et al., 2000; SCHEIDEGGER et al., 2001; BONHOURE et al., 2002; BONHOURE et al., 2003; TITS et al., 2003). TRLFS studies have been performed in collaboration with Dr. T. Stumpf of the Institut für Nukleare Entsorgung, Forschungszentrum Karlsruhe, Germany, whereas in-house expertise is available for the XAS studies. The use of spectroscopic techniques enables the uptake-controlling cement mineral in the complex cement matrix to be identified. Further, such measurements are vital to the development of a mechanistic picture of the uptake processes. This level of understanding is required for detailed assessments of the long-term behaviour of radionuclides in a cementitious repository.

5.2.1 Uptake of Eu(III) and Cm(III)

Eu(III) and Cm(III) are regarded as being chemical analogues and representatives of the trivalent actinides and lanthanides. In the last year wet chemistry experiments have been performed to obtain a consistent and comprehensive set of sorption data for Eu(III). The uptake of Eu(III) by HCP was investigated using powdered HCP in contact with an artificial cement pore water (ACW). ACW is a (Na,K)OH solution (pH = 13.3) saturated with respect to portlandite and calcite.

The strong uptake of Eu(III) by HCP indicated from previous studies (WIELAND & VAN LOON, 2002) was confirmed for cement suspensions ≤ 0.1 g L^{-1}. The distribution ratios (R_d value) were found to be ≥ 100 m^3 kg^{-1}. Measurements on cement suspensions with higher solid to liquid (S/L) ratios are on-going.

Uptake of Eu(III) by HCP was found to be linear over a large concentration range, indicating that a sorption-type uptake mechanism may be involved (Fig. 5.1). Fig. 5.1 further shows that the sorption isotherms determined on HCP and a CSH phase with a calcium-to-silicium ratio (C:S) = 1.09 agree. Precipitation of a Eu(III) solid phase is indicated at solution concentrations above about 10^{-6} M. Speciation calculations suggest a concentration limit of about $2 \cdot 10^{-8}$ M at pH = 13.3 using the crystalline hydroxide, $Eu(OH)_3$(cr), as the limiting solid. $Eu(OH)_3$(cr) is expected to be the most stable solid in the cement system (BERNER, 2002). Considering the amorphous hydroxide, $Eu(OH)_3$(am), as the limiting solid, however, increases the solubility limit to about 10^{-5} M at pH = 13.3. It is to be noted that the above solubility limits are based on the assumption that the $Eu(OH)_4^-$ species exists. Neglecting $Eu(OH)_4^-$ formation and assuming $Eu(OH)_3$(aq) as the dominating species at pH = 13.3 reduces the concentration limits to about $2 \cdot 10^{-9}$ M and 10^{-6} M, respectively. The latter is in good agreement with the experimental data, indicating that $Eu(OH)_3$(am) is most probably the solubility-limiting solid phase in the cement system.

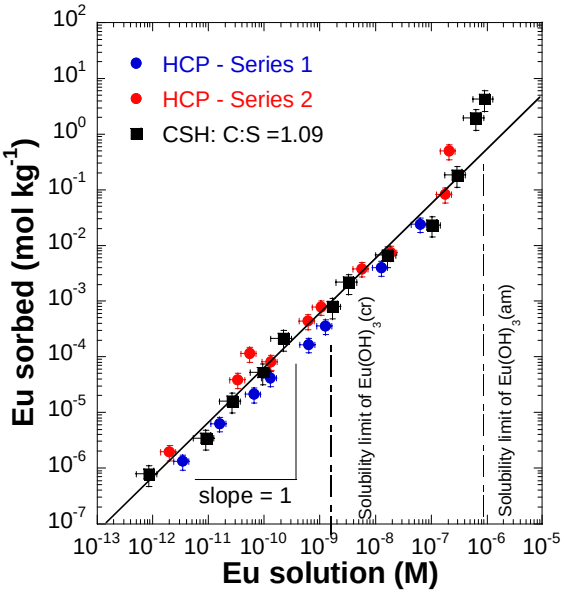

Fig. 5.1: *Sorption isotherms of Eu(III) on HCP and CSH in ACW (pH = 13.3). Experimental conditions: HCP: S/L = 0.1 g L^{-1}, equilibration time = 14 d; CSH: S/L = 0.5 g L^{-1}, equilibration time = 30 d.*

The effect of isosaccharinic acid (ISA) on the Eu(III) uptake by HCP was studied in the ISA concentration range between 10^{-5} M and $5 \cdot 10^{-2}$ M. No significant effect was observed at aqueous ISA concentrations below about 10^{-3} M. Above this concentration limit, however, the uptake of Eu(III) was reduced with increasing ISA concentration. It is to be noted that the formation of aqueous Ca(II)-ISA complexes is a possible side reaction in the HCP system under these conditions (VERCAMMEN et al., 1999). The complexation of Ca(II) by ISA increases the Ca(II) solubility in the HCP system at high ISA concentrations, which is expected to promote the dissolution of the cement matrix (WIELAND et al., 2002). For this reason, we cannot exclude that the sorption reduction observed at ISA concentrations above 10^{-3} M is caused by changes in the composition of the cement matrix, which makes a detailed interpretation of the sorption reduction in terms of complexation reactions very difficult.

In an earlier study we showed that ISA strongly influences Eu(III) uptake by calcite in the ISA concentration range between 10^{-5} M and 10^{-3} M (TITS et al., 2002). Uptake of Eu(III) was reduced by ISA due to the formation of an aqueous Eu(III)-ISA complex. Based on these results and model

calculations for the Eu(III)/ISA/HCP system it was expected that sorption reduction occurs in the given concentration range. Nevertheless, no measurable effect of ISA was observed in the experiments. To explain the discrepancy between predicted and experimental findings it is necessary to consider the formation of Eu(III)-ISA complexes on HCP (ternary complexes). Although the wet chemistry data strongly suggest the formation of these surface complexes, complementary investigations using spectroscopic techniques are needed to further corroborate the finding.

A mechanistic view of the uptake processes of trivalent actinides in cement systems was obtained from a TRLFS study of Cm(III) uptake by HCP (STUMPF et al., 2004). In the early stage of the uptake experiments (t < 10 d), Cm(III) preferentially sorbs to the portlandite component of the cement matrix or forms a non-fluorescing species, which was attributed to the formation of $Cm(OH)_3$ colloids. With time (t > 10 d), however, the formation of Cm(III) species sorbed to CSH phases of the complex cement matrix dominates. Based on lifetime analyses it was proposed that Cm(III) occupies two different position in the CSH structure.

An extension of the above studies is planned within the framework of a Ph.D. project (WIELAND et al., 2004). In the proposed study macroscopic and spectroscopic techniques (TRLFS and XAS) will be combined to further elucidate uptake processes of the trivalent actinides and lanthanides in cement systems on the molecular level. Besides Eu(III) and Cm(III), studies with Am(III) are foreseen to specifically address chemical analogy in the sorption behaviour of the above elements in these systems.

5.2.2 Uptake of Th(IV) and Sn(IV)

In this work Th(IV) and Sn(IV) are regarded as being representatives of the tetravalent actinides. Batch-type sorption studies with Th(IV) and Sn(IV) have been performed on HCP in contact with ACW.

In the case of Th(IV) the strong uptake of Th(IV) by HCP reported in WIELAND et al. (2002) and WIELAND & VAN LOON (2002) was confirmed for cement contents ≤ 0.1 g L^{-1} ($R_d \geq 100$ m^3 kg^{-1}). Measurements on cement suspensions with higher S/L ratios are on-going.

As in the case of Eu(III), the uptake of Th(IV) on HCP is linear in the concentration range between about $4 \cdot 10^{-13}$ M and $2 \cdot 10^{-9}$ M (Fig. 5.2). Fig. 5.2 also shows that the sorption isotherms on HCP and CSH (C:S = 1.09) agree, indicating that CSH could be the uptake-controlling cement mineral in HCP. Precipitation of a Th(IV) solid phase was not observed in the given concentration range. Speciation calculations indicate that ThO_2(am) would be the most stable solid phase at pH = 13.3, limiting the Th(IV) concentration at about $3 \cdot 10^{-9}$ M. Measurements at higher Th(IV) concentrations are on-going to check the solubility limits in the HCP system.

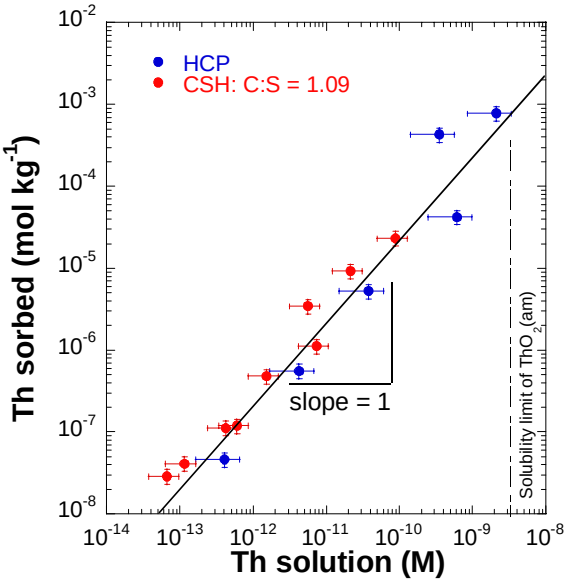

Fig. 5.2: *Sorption isotherms of Th(IV) on HCP and CSH in ACW (pH = 13.3). Experimental conditions: HCP: S/L = 0.1 g L^{-1}, equilibration time = 14 d. CSH: S/L = 0.5 g L^{-1}, equilibration time = 7 d.*

Sorption studies with Sn(IV) on HCP were performed to complete the data sets from preliminary experiments carried out during an earlier reporting period (Progress report 1999/2000). In the previous study it was found that the sorption isotherm of Sn(IV) is linear up to a concentration limit of about 10^{-6} M (BONHOURE et al., 2003). EXAFS investigations showed that Ca-stannate is the solubility-limiting phase at higher Sn(IV) concentrations. During 2003/2004 sorption-desorption experiments were carried out to test the reversibility of the uptake process at low Sn(IV) loadings (linear range of the isotherm). Desorption of ^{113}Sn was investigated by sequential replacement of ACW in HCP suspensions, i.e., centrifugation of the suspensions and replacement of the supernatant by fresh, ^{113}Sn free ACW. The R_d values were determined after each replacement of the supernatant. Changes in the R_d values were found to be small, indicating reversible binding of Sn(IV) onto HCP.

Further, sorption experiments with Sn(IV) were carried out to complement previous measurements on the influence of ISA on Sn(IV) uptake by HCP (Fig. 5.3). In Fig. 5.3 the ratio R_d/R_d^0 (= the

distribution ratio in the presence of ISA divided by the distribution ratio in the absence of ISA) is plotted as function of the ISA concentration in solution. The figure shows that ISA reduces the uptake of Sn(IV) by HCP at ISA concentrations above about 10^{-3} M. Furthermore, ISA was found to reduce Sn(IV) sorption onto an ion exchange resin (Dowex 50 XW-4) in the same ISA concentration range. Nevertheless, uptake of Sn(IV) by the resin is significantly weaker than on HCP, giving rise to large uncertainties on the data. For both systems sorption reduction can be interpreted in terms of the formation of a Sn(IV)-ISA complex in solution. The observed decrease in the Sn(IV) uptake with increasing ISA concentration can be described on the assumption that a 1:1 Sn(IV)-ISA complex forms in solution. This interpretation holds for linear and reversible sorption, which has been confirmed in the case of Sn(IV) uptake by HCP. Note that the formation of aqueous Ca(II)-ISA complexes causes the dissolution of the cement matrix at ISA concentrations above about $2 \cdot 10^{-2}$ M (broken vertical line). Data analysis is on-going with a view to deduce the stability constant of the Sn(IV)-ISA complex.

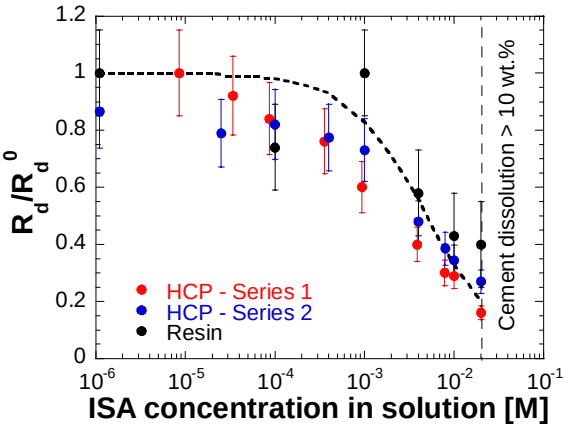

Fig. 5.3: *Influence of ISA on the uptake of Sn(IV) by HCP and Dowex 50 XW-4 resin in ACW (pH = 13.3). Experimental conditions: HCP: S/L = 1 g L^{-1}, equilibration time = 30 d; Resin: S/L= 2 g L^{-1}, equilibration time = 18 d. The dissolution of cement is > 10 wt.% at ISA concentrations ≥ $2 \cdot 10^{-2}$ M.*

5.3 Co-precipitation studies with CSH

Co-precipitation processes with amorphous or crystalline CSH phases are considered to be additional and potentially important retention mechanisms in HCP. In particular, these processes may be relevant during the solidification of radioactive waste by hydrating cement clinker material. The aim of this project is to gain a better understanding of the adsorption and co-precipitation processes of safety-relevant radionuclides with calcium silicate hydrates (CSH phases). Adsorption and co-precipitation studies on the CSH phases have been performed in the pH range between 11.5 and 13.3 to simulate the chemical conditions in the first and second stage of the cement degradation. The project currently includes studies on the adsorption and co-precipitation mechanisms of Sr(II), Ra(II), Eu(III), Th(IV) and U(VI).

Adsorption and co-precipitation studies with Sr(II) and Eu(III) were performed in the framework of and partially financed through the 5th framework project ECOCLAY II. First results from the Sr(II) and Eu(III) studies have been published in the open literature (TITS et al., 2003; TITS et al., 2004a). A detailed PSI Bericht on this work is in preparation.

Adsorption and co-precipitation studies with Th(IV) and U(VI) have been carried out within the framework of a joint research project with CRIEPI (Central Institute of the Electric Power Industry), Japan, with partial financial support by CRIEPI. The experimental tasks have been successfully completed in the last year. The results from U(VI) sorption experiments are presented below together with EXAFS measurements. A detailed report on the joint project is in preparation.

In 2004 a new short-term collaboration (6 months) was started with the Japanese Nuclear Fuel Cycle Development Institute (JNC) focussing on the uptake of Ra(II) by CSH phases and HCP with a view to comparing the sorption behaviour of Sr(II) and Ra(II) in these systems. Results from a first series of experiments are presented below.

5.3.1 CSH synthesis and characterisation

During 2003/2004 CSH phases with C:S ratios ≤ 0.7 have been synthesized and characterized in terms of solid and equilibrium liquid phase compositions to complement existing data sets of CSH phases with C:S > 0.8. These data are required for the development of a sorption model for Sr(II), and possibly Eu(III), on CSH phases based on the solid solution approach. CSH phases with very low C:S ratios of 0.5, 0.6 and 0.7 were synthesized in ACW to complete the in-house data set (Progress report 2002/2003). A second series of CSH phases with C:S ratios of 0.4, 0.6, 0.8, 1.0, 1.2, and 1.4 were synthesized in 0.01 M KOH. To date, no thermodynamic data for CSH in KOH solution are available. In contrast, ATKINS et al. (1991) have reported the corresponding data for CSH phases prepared in NaOH.

The synthesis of the CSH phases and the analysis of the equilibrium solution composition are finished.

The characterisation of the solid phases (chemical and quantitative X-ray diffraction analysis, scanning electron microscopy coupled with energy dispersive spectrometry) is on-going. From this work the basic experimental data needed for extending existing solid solution models (KULIK & KERSTEN, 2001) to Na-CSH and K-CSH phases, which are the dominating CSH phases in fresh HCP, are available, and therefore, emphasis will be placed on model development in the future.

5.3.2 Adsorption and co-precipitation processes of U(VI)

In the last year a detailed analysis of the U(VI) speciation for the conditions used in the experiments and measurements of sorption isotherms were performed. These studies were started because the large scattering in the experimental data obtained from kinetic studies of U(VI) sorption and co-precipitation processes indicated that the formation of a solubility limiting phase might control U(VI) retention in these systems.

Detailed speciation calculations were carried out in the pH range between 11.7 and 13.3 for the relevant solution compositions to identify possible solubility limiting phases. The results were compared with experimental data from in-house stability tests of U(VI) solutions. In these tests it was observed that U(VI) solutions are stable up to a U(VI) concentration of about $7 \cdot 10^{-6}$ M (pH = 13.3) and about $2 \cdot 10^{-6}$ M (pH = 12.5), respectively. Above these concentration limits, however, the U(VI) solution concentrations were found to be lower after centrifugation (1 h at 95000 g) compared to the initial U(VI) solution concentrations. This indicates the formation of a U(VI) solid phase which sedimented during centrifugation. Comparison of the calculated solubility limits for the different U(VI) solid phases reported in the literature with the experimental data revealed that U(VI) precipitation can be best described on the assumption that Ca-uranate, $CaUO_4(s)$, is formed ($\log_{10} K^0_{s,0} = (23.1 \pm 0.9)$; GUILLAUMONT et al., 2003). It is to be noted that the formation of this Ca-uranate compound in cementitious systems was already reported in the study of MORONI & GLASSER (1995).

Sorption isotherms of U(VI) were determined in pore waters of pH = 13.3 (ACW) and 12.1 ($Ca(OH)_2$ solution) in the concentration range between 10^{-10} M and 10^{-3} M on two types of CSH phases: CSH phases synthesised using the PSI method (mixing CaO suspensions with SiO_2 suspensions at different weight ratios to give target C:S ratios of 0.75 and 1.07) and CSH phases synthesised following the CRIEPI method (mixing a $Na_2SiO_3 \cdot 9H_2O$ solution with a 0.015 M $Ca(OH)_2$ solution at different volume ratios to give target C:S ratios of 0.83 and 1.0). The concentration of U(VI) sorbed onto the CSH phases ranged between about 10^{-5} mol kg^{-1} and about 0.1 mol kg^{-1}. In general, the data from the sorption isotherm measurements are consistent with the kinetic data, i.e., R_d values were found to be higher at pH = 12.1 than at pH = 13.3. The U(VI) sorption isotherms are nearly linear at pH = 12.1 (slopes = 0.81 - 0.96) for all CSH phases. At pH = 13.3, however, the shape of the sorption isotherms seems to be influenced by the method used for CSH synthesis. The isotherms of the CSH phases prepared using the PSI method were found to be approximately linear (slope = 0.80 – 0.87). The isotherms of the CRIEPI-type CSH phases, however, are clearly non-linear (slope < 0.5). Additional experiments are presently being performed to further examine whether the observed strong non-linearity was caused by sample preparation.

5.3.3 EXAFS study of U(VI) uptake by CSH

EXAFS studies were carried out to determine the structural coordination environment of U(VI) bound to CSH phases. For this, CSH phases with C:S ratios ranging between 0.65 and 1.1 were prepared using the two methods for CSH synthesis described in the previous section. The U(VI) loadings of the sorption and co-precipitation samples ranged between about $4 \cdot 10^{-3}$ mol kg^{-1} and $1.5 \cdot 10^{-2}$ mol kg^{-1}. Hence, the U(VI) surface concentrations correspond to the medium concentration range of the sorption isotherms. Uranium L_{III}-edge (17166 eV) EXAFS spectra of the samples were recorded at the Rossendorf Beamline at the European Synchrotron Radiation Facility (ESRF), Grenoble, France.

A multi-shell approach was employed for data fitting. Non-linear least square curve fitting was performed on the Fourier transforms (FTs). All single-scattering and multiple-scattering paths modelled in the fits were based on the model compound uranophane and derived from FEFF8.0. In the fitting the coordination number (N) for the first shell (= axial oxygens) was fixed ($N_{Oax} = 2$) in order to reduce the number of free parameters.

The results show that both experimental procedures for synthesising CSH solid phases provide similar structural environments for UO_2^{2+} adsorption and co-precipitation processes. Due to the higher loadings, and consequently better data quality, detailed fitting was performed on those samples prepared using the PSI method for CSH synthesis. The fit approach was then applied to analyse the EXAFS spectra of the CRIEPI samples.

The best fit to the data of all samples was obtained with a structural model consisting of three oxygen coordination shells. Low frequency oscillation arising form the backscattering of axial oxygen atoms in the low-k region are responsible for the main peak at ~1.5 Å in the FTs (Fig. 5.4). The main feature of the equatorial plane could be reproduced by two oxygen coordination shells, which are separated by approximately ~0.17 Å. At an interatomic distance, $R_{U\text{-}O}$, of ~2.24 Å (range: 2.23 - 2.27 Å) the uranium atom is surrounded by a coordination sphere consisting of 3 - 5 equatorial oxygen atoms. The third shell of oxygen atoms at an interatomic distance of ~2.41 Å ($R_{U\text{-}O}$: 2.36 - 2.45 Å) has a low coordination number (N = 0.5 - 1.5).

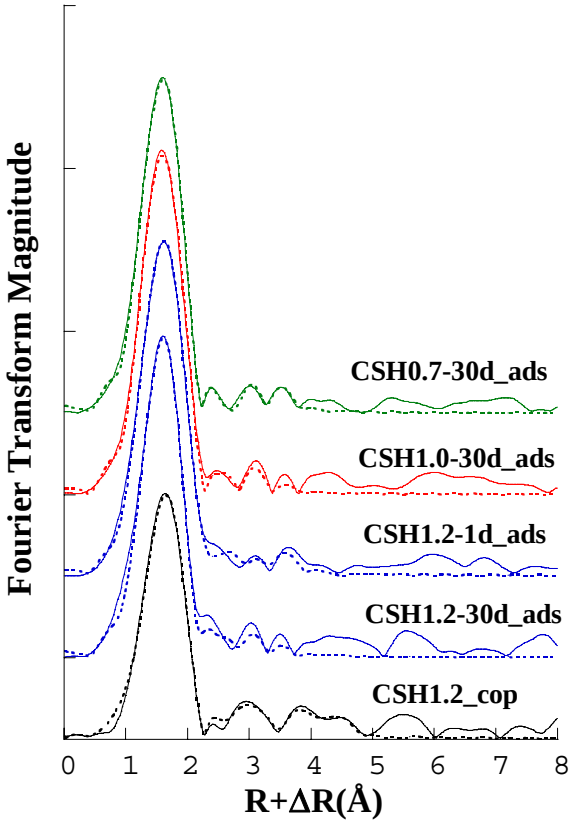

Fig. 5.4: *Fourier Transforms (FTs) of k^3-weighted EXAFS spectra for U(VI) bound to CSH phases. The lines correspond to the experimental (solid) and fitted (dashed) U-L_{III} EXAFS. FT peak positions are not corrected for phase shift. Legend: CSH0.7-30d_ads indicates the CSH sample with C:S = 0.7, where U(VI) was adsorbed and the sample equilibrated for 30 days. CSH samples were prepared using the PSI method for CSH synthesis. Notation of the other samples corresponds to the respective C:S ratios and equilibration times. For the CSH1.2_cop sample, U(VI) was added during formation of the CSH phase (co-precipitation).*

Additional backscattering contributions are attributed to Si atoms located at longer distance. At maximum, one silicon atom appears at ~3.08 Å ($R_{U\text{-}Si}$: 3.07 - 3.11 Å), and 2 to 3 Si atoms are located at a distance of ~3.75 Å ($R_{U\text{-}Si}$: 3.71 - 3.77 Å). The EXAFS data further suggest that about 2 to 3 Ca atoms are located at the distance of ~3.83 Å ($R_{U\text{-}Ca}$: 3.77 - 3.83 Å). The structural parameters deduced for the U(VI)/CSH systems were found to be similar to those reported for uranophane, $Ca(UO_2)_2(SiO_3OH)_2{\cdot}5H_2O$ (GINDEROW, 1988). Thus, a structural model for U(VI) binding in CSH phases was developed based on the coordination environment of U(VI) in uranophane.

5.3.4 Adsorption and co-precipitation processes of Ra(II)

Very few sorption data for Ra(II) on cementitious materials exist, and the few existing studies mainly report single point measurements of R_d values. Thus, our present knowledge of the uptake mechanism of Ra(II) in cementitious system is still poor. This situation can only be improved if the uptake of Ra(II) by CSH (and eventually HCP) is investigated under various experimental conditions, e.g., by varying pore water compositions, the Ra(II) concentrations, the S/L ratio etc.

The objectives of the joint project with JNC, which started in May of this year, are to determine robust sets of sorption data for Ra(II) on CSH and HCP in order to fill gaps existing in the PSI/Nagra cement sorption databases, to test whether or not CSH phases are the main sink for Ra(II) in HCP and to assess the sorption behaviour of Ra(II) in comparison with Sr(II). Thus, this study of the uptake of Ra(II) by cementitious materials is an extension of earlier in-house mechanistic sorption studies with Sr(II) on HCP and CSH phases (TITS et al., 1998; WIELAND et al., 2000; TITS et al., 2004a).

The basic experimental techniques (e.g., handling of the Ra(II) samples, phase separation etc.) have been developed. In particular, the applicability of alpha spectroscopy as a method to quantitatively measure ultra low ^{226}Ra activities (<10^{-2} Bq per sample) has been tested. The first sorption experiments (kinetics and studies of the effect of the C:S ratio on sorption) were started using initial ^{226}Ra concentrations ranging between $1.3{\cdot}10^{-8}$ M and $2.8{\cdot}10^{-8}$ M. Preliminary results show that the uptake of Ra(II) by CSH phases is very fast and comparable to the sorption kinetics of Sr(II). Furthermore, the effect of the C:S ratio on the uptake process seems to be similar for both radionuclides (Fig. 5.5). Note, however, that the R_d values obtained for Ra(II) are significantly higher than those determined for Sr(II). The work is continuing, and experiments on the reversibility of

the uptake process as well as sorption experiments on fresh and degraded HCP are planned.

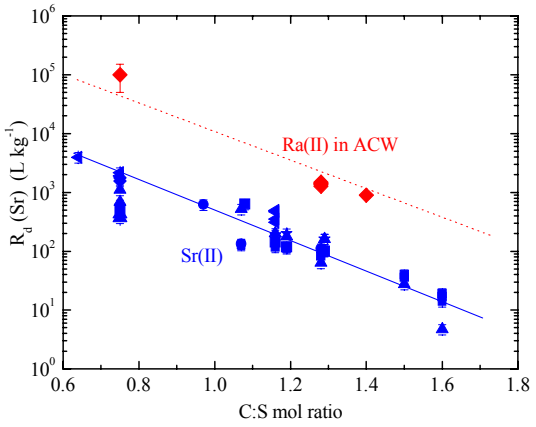

Fig. 5.5: *Comparison of R_d values for Ra(II) and Sr(II) on CSH phases with different C:S ratios.*

5.4 Micro-spectroscopic studies on the immobilization of Ni and Co in HCP

The objective of the project is to combine micro X-ray absorption spectroscopy (XAS) with micro X-ray fluorescence (XRF) and micro X-ray diffraction (XRD) to gain spatially-resolved molecular-level information on the speciation and structural coordination environment of Co(II) and Ni(II) in HCP. Using the micro-focusing techniques enables us to study the reactivity of Ni(II) and Co(II), in terms of redox processes, surface complexation reactions or the formation of new mineral phases, in connection with the inherent mineralogical heterogeneity of the complex cement matrix. Note that compact HCP is highly heterogeneous with respect to particle sizes (size range between few to a few hundred micrometers) and particle composition. The micro-spectroscopic studies are to be complemented with bulk XAS experiments to assess the relevance of the results obtained from the micro-scale studies for the overall cement system.

In the first year of the project Ni(II) and Co(II) doped HCP samples have been prepared. The experimental parameters varied were: the cement hydration time (3, 30 and 150 days), the metal loading (500 and 5000 ppm) and the counter ions (NO_3^{2-}, SO_4^{2-}, Cl^-) of the added Ni(II) and Co(II) salts. MicroXRF and microXAS experiments were conducted at the micro-focusing ALS beamline 10.3.2 and bulk-XAS experiments on beamline BM01 at the ESRF.

The micro-spectroscopic investigations showed a distinct heterogeneity of the Ni distribution in the cement matrix (Fig. 5.6a). Fig. 5.6a further reveals that Ni enriched "hot" spots formed locally as coatings on cement minerals. The Ni K-edge (8333 eV) EXAFS spectra and the corresponding FTs determined at the two different spots are shown in Fig. 5.6 b/c together with the corresponding data of reference compounds (α-$Ni(OH)_2$, β-$Ni(OH)_2$, Ni-phyllosilicate, Ni-containing layered double hydroxides (Ni-Al LDH)) and a powdered Ni-doped HCP material. The cement samples had a Ni loading of 5000 ppm. They were prepared by hydrating cement with a $Ni(NO_3)_2$ solution for 30 days. The reference compounds represent the Ni-containing cement minerals, which were expected to be formed during cement hydration.

Data analysis indicates that Ni preferentially forms a LDH-type solid phase. For example, the distinctive beat pattern at ~8 Å^{-1}, which is indicative of Ni-Al LDH (e.g., SCHEIDEGGER et al., 2000), clearly appears in the EXAFS spectrum of the bulk sample (30 days hydration). Data analysis further showed similar interatomic distances and coordination numbers for all Ni-doped HCP samples, indicating that the same Ni phase dominates in all samples irrespective of the Ni loading or anions added. The first peak of the radial structural function shown in Fig. 5.6c corresponds to a Ni-O octahedral coordination with interatomic distances of 2.03-2.06 Å. The second radial structural function peak was fitted with Ni alone, because the discrimination of Ni-Ni and Ni-Al/Si backscattering pairs in Ni-Al LDH and Ni-phyllosilicates is problematic (SCHEIDEGGER et al., 2000). The fits reveal that Ni-Ni distances (R_{Ni-Ni}= 3.09-3.11 Å) of the HCP samples are longer than in Ni-Al LDH (3.06 Å). This finding suggests that not a pure Ni-Al LDH phase was formed during cement hydration, and furthermore, that the longer Ni-Ni distances of the cement samples may be caused by the presence of β-$Ni(OH)_2$ impurities (R_{Ni-Ni} = 3.12 Å).

To further test whether this hypothesis is consistent with the observed fit results, linear least-square fitting of the experimental EXAFS spectra with linear combinations of the reference spectra was performed. Best fit results were obtained using a combination of Ni-Al LDH and β-$Ni(OH)_2$. The weight percentage of Ni-Al LDH in the Ni-doped cement samples was found to slightly increase with increasing hydration time whereas β-$Ni(OH)_2$ decreased accordingly. This finding suggests that Ni-Al LDH is the dominating Ni phase in the cement samples as previously suggested from Ni sorption experiments on HCP (SCHEIDEGGER et al., 2000).

In future studies complementary techniques, such as micro XRD and diffuse reflectance spectroscopy will be used to further substantiate the above findings. Furthermore, emphasis will be placed on the detailed

analysis of the Co data. The first results from the micro-spectroscopic investigations show a highly heterogeneous Co distribution in the cement matrix and the existence of different Co species. At some Co-rich spots, Co(II) was found to be oxidized to Co(III) during the hydration process. Further, it also appeared that the Co(III)/Co(II) ratio increased with increasing hydration time in some HCP samples. Certainly, these results are extremely important for our understanding of the immobilization of Co in cement systems and the interpretation of sorption measurements on HCP samples, and therefore, require further clarification.

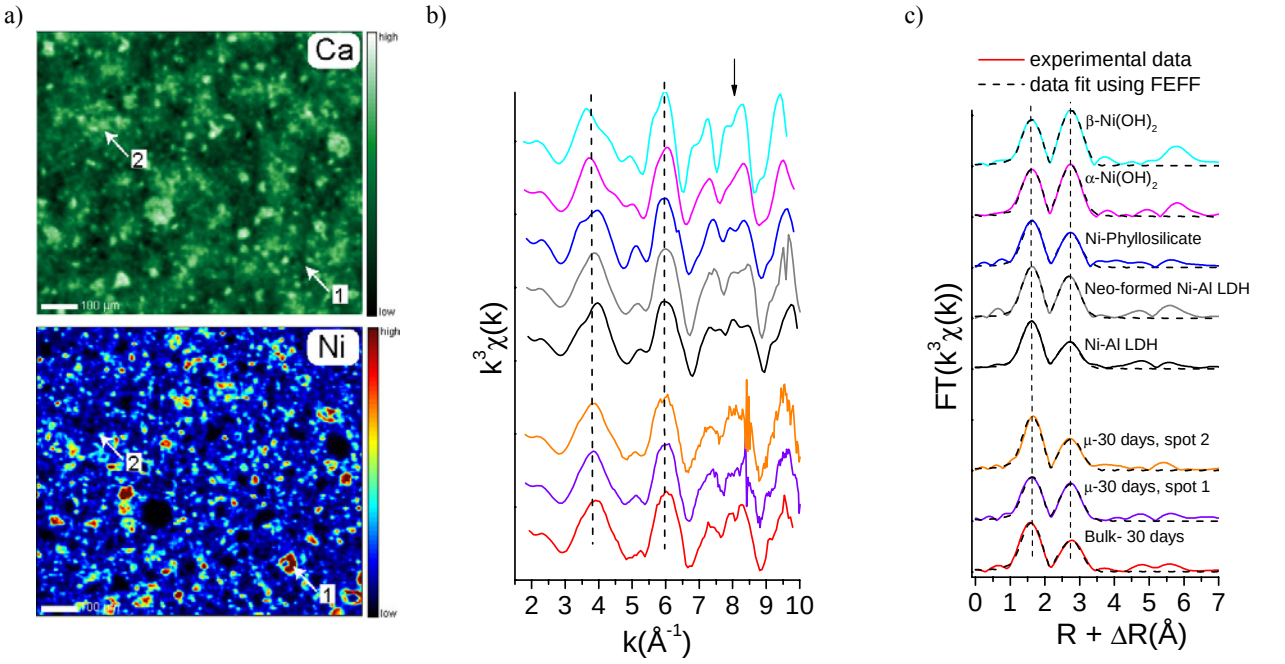

Fig. 5.6: *a) Ni and Ca element distribution in Ni-doped HCP samples. EXAFS spectra were recorded on the Ni-rich spots 1 and 2; b) k^3-weighted, normalized, background-subtracted EXAFS spectra of the Ni-doped HCP samples and reference compounds. The arrow localizes the region at ~8Å^{-1} characteristic for Ni-Al LDH; c) FT spectra of the Ni-doped HCP samples and reference compounds.*

5.5 References

ATKINS M., BENNETT D., DAWES A., GLASSER F., KINDNESS A., READ D. (1991)
A thermodynamic model for blended cement. UK DoE Report DoE/HMIP/PR/92/005

BERNER U. (2002)
Project Opalinus Clay: Radionuclide concentration limits in the cementitious near-field of an ILW repository. PSI Bericht Nr. 02-26

BONHOURE I., SCHEIDEGGER A.M., WIELAND E., DÄHN R. (2002)
Iodine species uptake by cement and CSH studied by I K-edge X-ray absorption spectroscopy. Radiochim. Acta 90, 647-651

BONHOURE I., WIELAND E., SCHEIDEGGER A.M., OCHS M., KUNZ D. (2003)
EXAFS study of Sn(IV) immobilization by hardened cement paste and calcium silicate hydrates. Environ. Sci. Technol. 37, 2184-2191

GINDEROW P.A. (1988)
Structure of l'uranophane alpha, $Ca(UO_2)_2(SiO_3OH)_2{\cdot}5H_2O$.
Acta Crystallogr. C44, 421-424

GUILLAUMONT R., FANGHÄNEL T., FUGER J., GRENTHE I., NECK V., PALMER D.A., RAND M.H. (2003)
Update on the chemical thermodynamics of uranium, neptunium, plutonium, americium and technetium. Chemical Thermodynamics Vol. 5, Elsevier, Amsterdam, The Netherlands

KULIK D.A., KERSTEN M. (2001)
Aqueous solubility diagrams for cementitious waste stabilization systems: II. End-member stoichiometries of ideal calcium silicate hydrate solid solutions. J. Am. Ceram. Soc. 3017-3026

MORONI L.P., GLASSER F.P. (1995)
Reactions between cement components and U(VI) oxide. Waste Management, 15, 243 – 254

SCHEIDEGGER A.M., WIELAND E., SCHEINOST A.C., DÄHN R., SPIELER P. (2000)
Spectroscopic evidence for the formation of layered Ni-Al double hydroxides in cement. Environ. Sci. Technol. 34, 4545 - 4548

SCHEIDEGGER A.M., WIELAND E., SCHEINOST A.C., DÄHN R., TITS J., SPIELER P. (2001)
Ni phases formed in cement and cement systems under highly alkaline conditions: An XAFS study. J. Synchrotron Radiation 8, 916 - 918

TITS J., BRADBURY M.H., WIELAND E. (1998)
The uptake of Cs, Sr, Ni, Eu, and Th by CSH phases under high cement pore water conditions. PSI Technical Report, TM-44-98-01

TITS J., WIELAND E., BRADBURY M.H., ECKERT, P., SCHAIBLE, A. (2002)
The uptake of Eu(III) and Th(IV) by calcite under hyperalkaline conditions. PSI Bericht Nr. 02-03, Nagra NTB 02-08

TITS J., STUMPF T., RABUNG T., WIELAND E., FANGHÄNEL T. (2003)
Uptake of Cm(III) and Eu(III) by calcium silicate hydrates: A solution chemistry and time-resolved laser fluorescence spectroscopy (TRLFS) study. Environ. Sci. Techn., 37, 3568 - 3573

VERCAMMEN K., GLAUS M.A., VAN LOON L.R. (1999)
Complexation of calcium by α-isosaccharinic acid under alkaline conditions. Acta. Chem. Scan. 53, 241-246

WIELAND E., TITS J., SPIELER P., DOBLER J.P., SCHEIDEGGER, A.M. (2000)
Uptake of nickel and strontium by a sulphate-resisting Portland cement. In: Applied Mineralogy in Research, Economy, Technology, Ecology and Culture, Göttingen, Germany (D. Rammlmair, J. Mederer, T. Oberthür, R. B. Heimann, and H. Pentinghaus (eds.)), Vol. 2, 705-708, Balkema, Rotterdam, The Netherlands

WIELAND E., VAN LOON L. (2002)
Cementitious near-field sorption data base for performance assessment of an ILW repository in Opalinus clay, PSI Bericht Nr. 03-06, Nagra NTB 02-20

WIELAND E., TITS J., DOBLER J.P., SPIELER P. (2002)
The effect of α-isosaccharinic acid on the stability of and Th(IV) uptake by hardened cement paste. Radiochim. Acta 90, 683-688

5.6 Publications

5.6.1 Peer reviewed journals and reports

BONHOURE I., BAUR I.[1], WIELAND E., JOHNSON C.A.[1], SCHEIDEGGER, A.M. (2004)
Se(IV/VI) oxyanion immobilization by cementitious systems: An X-ray absorption spectroscopy study. Cem. Concr. Res. (submitted)
[1] EAWAG, Switzerland

STUMPF T.[1], TITS J., WALTHER C.[1], WIELAND E., FANGHÄNEL T. (2004)
Uptake of trivalent actinides (Cm(III)) by hardened cement paste: A time-resolved laser fluorescence spectroscopy (TRLFS) study. J. Coll. Int. Sci. 276, 118-124
[1] Forschungszentrum Karlsruhe, Karlsruhe, Germany.

TITS J., WIELAND E., DOBLER J.-P., KUNZ D. (2004a)
Uptake of strontium by calcium silicate hydrates under high pH conditions: An experimental approach to distinguish adsorption from co-precipitation processes. Mater. Res. Soc. Symp. Proc. 807, 689-694

TITS J., WIELAND E., BRADBURY M.H. (2004b)
The effect of isosaccharinic acid and gluconic acid on the retention of Eu(III), Am(III) and Th(IV) by calcite. Appl. Geochem. (submitted)

WIELAND E., TITS J., BRADBURY M.H. (2004)
The potential effect of cement-derived colloids on radionuclide mobilisation in a repository for radioactive waste. Appl. Geochem. 19, 119-135

5.6.2 Conferences/Workshops/Presentations

CURTI E., KULIK D.A., TITS J. (2004)
Solid solutions of trace Eu(III) in calcite: A thermodynamic study. 14th Goldschmidt Conference, Geochim. Cosmochim. Acta 68 (11 Suppl.1), A82

FUJITA T.[1], TITS J., HARFOUCHE M., SUGIYAMA D.[1], TSUKAMOTO M.[1], WIELAND E. (2004)
U(VI) uptake by co-precipitation and adsorption processes in cementitious systems, 14th Goldschmidt Conference, Geochim. Cosmochim. Acta 68 (11 Suppl.1), A112
[1] CRIEPI, Tokyo, Japan

TITS J., STUMPF T.[1], WIELAND E., FANGHÄNEL T.[1] (2003)
The immobilisation of Eu(III) and Cm(III) by calcium silicate hydrates, 13th Goldschmidt Conference, Geochim. Cosmochim. Acta 67 (18 Suppl.1), A482
[1] Forschungszentrum Karlsruhe, Karlsruhe, Germany.

TITS J., IIJIMA K.[1], TOMURA T.[1], WIELAND E., KAMEI G.[1] (2004)
The role of CSH phases in the immobilization of strontium and radium by cementitious materials. Summer Seminar of the Division of the Nuclear Fuel Cycle and Environment of the Atomic Energy Society of Japan, 29 - 30 July 2004, Himeji, Japan
[1] JNC, Tokai, Japan

TITS J., WIELAND E. (2004)
The Role of CSH phases in the immobilization of radionuclides by cementitious materials. JAERI, Japan, 21 May, 2004

VESPA M., WIELAND E., DÄHN R., GROLIMUND D., SCHEIDEGGER A.M. (2004)
EXAFS study of Ni uptake by hardened cement paste, 14th Goldschmidt Conference, Geochim. Cosmochim. Acta 68 (11 Suppl.1), A166

WIELAND E., BONHOURE I., FUJITA T.[1], TITS J., SCHEIDEGGER A.M. (2003)
Combined wet chemistry and EXAFS studies on the radionuclide immobilisation by cement and calcium silicate hydrates, 13th Goldschmidt Conference, Geochim. Cosmochim. Acta 67 (18 Suppl.1), A532
[1] CRIEPI, Tokyo, Japan

WIELAND E., STUMPF T.[1], TITS J., FANGHÄNEL T.[1] (2004)
Wet chemistry and TRLFS studies of Eu(III) and Cm(III) uptake by cementitious materials, 14th Goldschmidt Conference, Geochim. Cosmochim. Acta 68 (11 Suppl.1), A169
[1] Forschungszentrum Karlsruhe, Karlsruhe, Germany

5.6.3 Internal reports

WIELAND E., TITS J., DÄHN R., SCHEIDEGGER A.M., STUMPF T.[1], WEHRLI B.[2] (2004)
A combined macroscopic and spectroscopic study of actinide and lanthanide binding mechanisms in cementitious waste repository materials. Ph.D. proposal
[1] Forschungszentrum Karlsruhe, Karlsruhe, Germany
[2] ETHZ, Zürich, Switzerland

6 COLLOID CHEMISTRY

C. Degueldre, R. Rosse, A.J. Kline (Trainee from University Missouri)

6.1 Introduction

The colloid sub-programme is progressing on the understanding of the potential role of groundwater colloids in the frame of the migration of radionuclides in the geosphere. The groundwater colloid properties are studied with emphasis on their properties (concentration, size distribution, nature) in the investigated aquifers.

This report summarises the cooperation work in the frame of the Grimsel Colloid Projects. Activities also included colloid studies such as the analytical tests on single particle analysis by ICP-MS and the results of a case study on Pu association on colloids and the impact redox.

6.2 Activities for the Grimsel Colloid Projects

The Colloid and Radionuclide Retardation (CRR) experiment was dedicated to the study of the in situ migration behaviour of selected actinides and fission products in the absence and presence of **bentonite colloids** in a water-conducting feature (shear zone) at the Grimsel Test Site (GTS). The main project team is the INE/FZK and a very constructive cooperation is carried out with this group. The scenario considers processes at the bentonite backfill / host rock interface as a potential source for colloids e.g. Moeri et al., 2003.

The influence of smectite colloids on the migration behaviour of U(VI), Th(IV), Pu(IV), Am(III), Np(V), Sr(II) and Cs(I) was investigated (see Fig. 6.1). Radionuclide retardation observed in the field studies increases in the sequence Np(V)~U(VI)<Sr(II)<Cs(I). For Cs, a small fraction of colloid borne breakthrough is only observed in presence of bentonite colloids. Am(III) and Th/Pu(IV) mainly migrate as colloids without retardation in the presence and absence of smectitic colloids. The radionuclide migration behaviour is discussed on the basis of results obtained in laboratory batch sorption experiments and spectroscopic studies. Consistent with the field observation, laboratory derived K_d values increase in the order Np(V)~U(VI)<Sr(II)<Cs(I). Significant kinetic hindrance for the sorption to fault gauge minerals is observed for Sr(II) and Cs(I), but also notably for Am(III) and Pu(IV). The slow sorption reaction of tri- and tetravalent actinide ions is explained by their kinetically hindered dissociation from colloidal species. In order to explain the colloidal behaviour of tri- and tetravalent actinides, even in the absence of bentonite colloids, ultracentrifugation and spectroscopic experiments are performed. It is found that up to 60 % of Pu(IV) and Am(III) species can be centrifuged off. Adding Cm(III) (5.10^{-8} mol L^{-1}) into the injection solutions instead of Am(III) allows for a spectroscopic study by using the time resolved laser fluorescence spectroscopy (TRLFS). Peak position and fluorescence lifetimes (λ = 604 nm, τ = 110-114 µs) together with the fact that Cm(III) can be widely separated by ultracentrifugation, suggest the existence of inner-sphere surface complexes on groundwater and bentonite colloids. Carbon K-edge XANES analysis of the bentonite colloids reveal the presence of considerable amounts of natural organic constituents. They are mainly of aliphatic nature containing high fractions of carboxylate groups. A contribution of these organic species towards the bentonite colloid stability and sorption of actinides is assumed to be likely. A paper on this study is ready for publication in Radiochim. Acta.

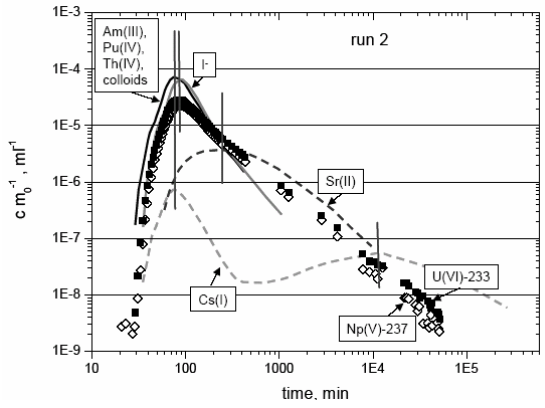

Fig. 6.1: *Breakthrough curves for ^{131}I, ^{85}Sr, ^{137}Cs, $^{241}Am/^{238}Pu$, ^{244}Pu, ^{237}Np, ^{233}U (20 mg L^{-1} bentonite colloids), radionuclide concentrations are normalised to the injected mass or activity of the respective radionuclides.*

6.3 Other colloid activities

6.3.1 Colloid analytics

Single particle analysis of **thoria colloids** in water has been tested by inductively coupled plasma - mass spectroscopy (ICP-MS). The transient signal induced by the flash of ions due to the ionisation of a thoria colloidal particle in the plasma torch can be detected and measured for the $^{232}Th+$ or $^{248}[ThO]^+$ ion masses by the mass spectrometer. The intensity of the MS signal is recorded in time scan (see Fig. 6.2.a and c).

The peaks recorded are analysed for their frequency as a function of the particle size (Figs. 6.2.b and d). The frequency of the flashes is directly proportional to the concentration of particles in the colloidal suspension (see DEGUELDRE & FAVARGER, 2003). The detection limit in colloid size is around 80 nm. This work is a continuation of the developments and the measurements of zirconia colloids presented in the progress report of last year. A paper was published in Talanta.

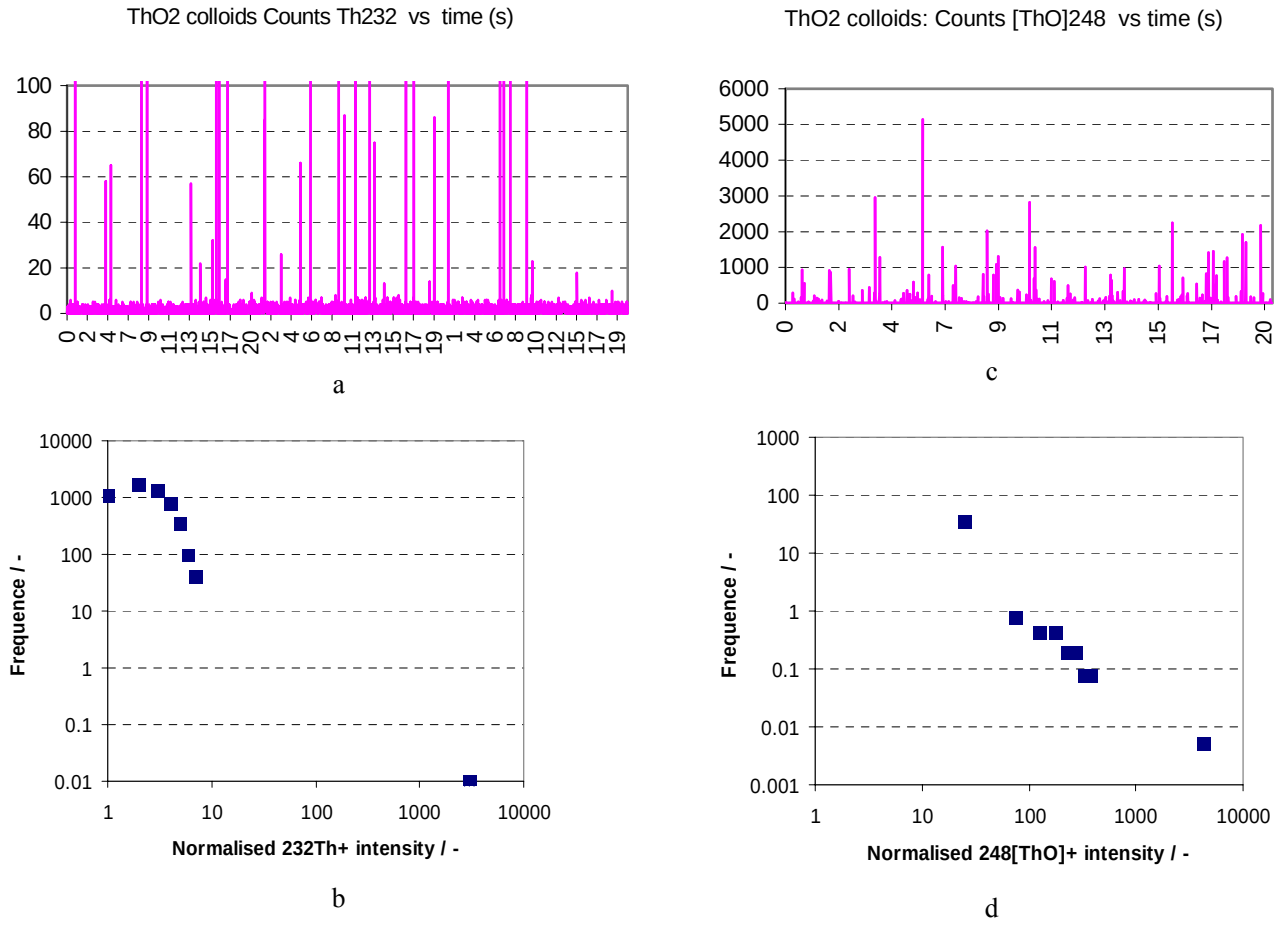

Fig. 6.2: *Analysis of thoria colloids by ICP-MS in a single particle mode*
a and c: *Signal for $^{232}Th^+$ and $^{248}[ThO]^+$ recorded in time scan, particle sample recorded during 20 seconds*
b and d: *ICP-MS signal distribution for $^{232}Th^+$ and $^{248}[ThO]^+$.*
Conditions: colloidal suspension of ThO_2 colloids, 10 ms detection time for $^{232}Th^+$ or $^{248}[ThO]^+$ ion detection, colloidal solution injection rate $2x10^{-5}$ cm^3 s^{-1} within the pure water at injection rate $5x10^{-3}$ cm^3 s^{-1} for nebulising in argon flow 19 cm^3 s^{-1} through plasma torch prior to mass analysis.

6.3.2 Pu association on colloids, effect of redox

An analytical expression that evaluates the effect of pH and the redox potential (E) was used to study plutonium sorption on colloids. It includes surface complexation with one type of surface sites and its formulation leads to a distribution coefficient (K_d) as a function of the pH (hydrolysis) and E (redox sensitive species). The formulation also considers the values of the stability and hydrolysis constants for all species present in solution and associated at the surface. Semi-empirical correlations between hydrolysis and surface complexation constants reported in literature have been applied for each colloid system. The presence of complexing ligands in solution (such as carbonates) was also taken into account. The model was applied to study the association of plutonium onto Al_2O_3, FeOOH and SiO_2 colloids, in the presence and in the absence of carbonates in solution. The tests performed with the model suggest that the oxidation of Pu(III) to Pu(IV) has the potential to increase the sorption, as demonstrated by the increased K_d values. Under natural conditions Pu may be present at oxidation states of (III), (IV), (V) and (VI), and the effect of redox potential is significant because of the differences in the sorption of each oxidation state (see

Fig. 6.3). When carbonates are present in the solution, the calculated values of distribution coefficient were lower than those calculated in the absence of carbonates, particularly in case of Pu(VI). The distribution coefficient (K_d) values obtained with the developed model are in agreement with experimental values reported for the sorption of plutonium onto colloids in the CRR program. This model can equally be applied to study the sorption of other redox sensitive elements. The work was synthesised in a TM and is now upgraded in a publication foreseen in the proceedings of the NRC6 conference.

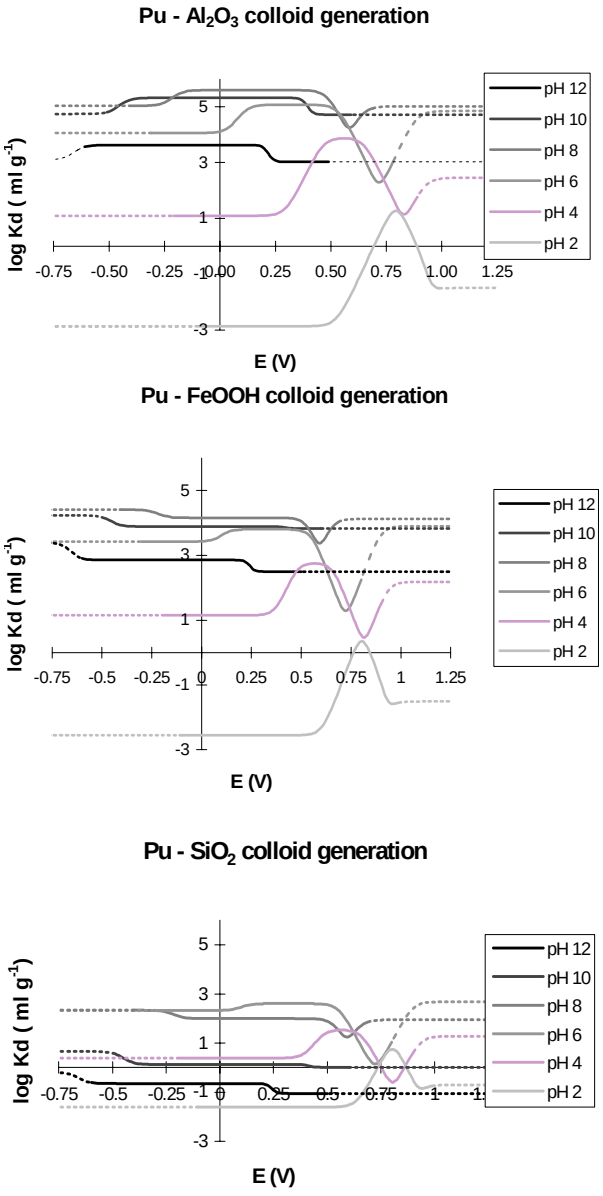

Fig. 6.3: *K_d values as a function of redox potential at different pH values for the sorption of plutonium onto 200 nm Al_2O_3, FeOOH and SiO_2 colloids without carbonates in solution.*

6.4 Future work

The participation in the Colloid and Radionuclide Retardation program at Grimsel has been fruitful. This program was completed at the end of 2003. We now participate in the project: Colloid Formation and Migration (CFM). This project aims at understanding the generation of colloids at a bentonic bloc/groundwater flow interface with a quasi-stagnant water.

Analytical tests on single colloids by ICP-MS will continue (in collaboration with University of Geneva) with tests on uranium colloids as oxides and sorbed on clay particles as well as on standard gold colloids. The redox work is soon completed, however, calculations are now dealing with polymerisation on model colloids as generation mode.

At PSI, interest is placed on using the large facilities (SLS). We plan candidate studies for the micro-EXAFS beam line.

6.5 References

MOERI A., ALEXANDER W.R., GECKEIS H., HAUSER W., SCHÄFER T., EIKENBERG J., FIERZ TH., DEGUELDRE C., MISSANA T. (2003)
The colloid and radionuclide retardation experiment at the Grimsel test site, influence of bentonite colloids on the radionuclide migration in a granitic fracture. Colloids and Surfaces A 217, 33-47

DEGUELDRE C., FAVARGER P.-Y. (2003)
Colloid analysis by single particle inductively coupled plasma – mass spectroscopy: a feasibility study. Colloids and Surfaces A 217 137-142

6.6 Publications

6.6.1 Peer reviewed journals and reports

DEGUELDRE C., FAVARGER P.-Y.[1], BITEA C.[2] (2004)
Zirconia colloid Analysis by Single Particle Inductively Coupled Plasma - Mass Spectroscopy, Anal. Chim. 518 137-142
[1] University of Geneva, Switzerland
[2] INE, Forschungszentrum Karlsruhe, Karlsruhe, Germany

DEGUELDRE C., FAVARGER P.-Y.[1] (2004)
Thorium Colloid Analysis by Single Particle Inductively Coupled Plasma - Mass Spectrometry. Talanta 62 1051-1054
[1] University of Geneva, Switzerland

DEGUELDRE C., REED D.[1], KROPF A.J.[1], MERTZ C.[1] (2004)
XAFS study of americium sorbed on groundwater colloids. J. Synchrotron Rad. 11 198-203
[1] CMT, Argonne National Laboratory, Argonne, Il, USA

6.6.2 Conferences/Workshops/Presentations

DEGUELDRE C., BOLEK M.[1] (2004)
Modelling colloid generation with plutonium: the effect of pH and redox potential: Poster @ nrc6, Aachen, 31 August - 3 September 2004 and Publication in proceedings
[1] University of Geneva, Switzerland

6.6.3 Internal reports

DEGUELDRE C., BOLEK M.[1] (2003)
Modelling colloid generation with plutonium: the effect of pH and redox potential: PSI Technical Report TM-44-03-06
[1] University of Geneva, Switzerland

7 DIFFUSION PROCESSES

L.R. Van Loon, M.A. Glaus, F. González, W. Müller R. Rossé

7.1 General

The main effort of the group "Diffusion Processes" was involved in diffusion experiments on Opalinus clay samples and on compacted clay minerals:

- Diffusion coefficients and rock capacity factors for $^{85}Sr^{2+}$ parallel and perpendicular to the bedding were measured by through- and out-diffusion. Experiments on $^{134}Cs^{+}$ have been started.
- Diffusion of $^{85}Sr^{2+}$ in compacted Na-montmorillonite was investigated as a function of sample thickness and ionic strength.
- An abrasive peeling method was developed for measuring diffusion profiles of strongly sorbing tracers in dense argillaceous rocks. First tests with $^{134}Cs^{+}$ and $^{22}Na^{+}$ have been performed.
- Time-of-flight neutron scattering measure-ments were performed on compacted Na- and Ca-montmorillonite, Na- and Ca-illite and kaolinite.
- Diffusion of HTO in compacted Na-montmorillonite was investigated as a function of temperature.

The activities in the field of organic ligands focused on the reactivity of α-isosaccharinic acid under alkaline conditions in presence and absence of solid phases such as portlandite and cement.

A Ph.D Student (Fatima González) joined the group in January 2004. She is studying the dynamics and structure of confined water in compacted clay systems using mainly time-of-flight neutron scattering (TOF-NS) techniques.

The NF-PRO project (6th EU framework) was started in January 2004. PSI is work package leader of the subtask "Diffusion and retention in the near field". A coordination meeting was organised at PSI at the beginning of April 2004. So far, bentonite samples have been prepared, resaturated and diffusion of $^{36}Cl^{-}$ has been started.

The diffusion experiment in Mont Terri (DI-A) is continuing in the 9th phase of the Mont Terri Project. The diffusion of non-sorbing (HTO, I^{-}, Br^{-}), weakly sorbing (Cs^{+}) and strongly sorbing tracers ($^{60}Co^{2+}$, Eu^{3+}) has been started. PSI is involved in the preparation of the artificial pore water and the tracer cocktail, and in the analysis of I^{-}, Br^{-}, Cs^{+}, Eu^{3+}, HTO, $^{85}Sr^{2+}$ and Co^{2+}.

7.2 Diffusion in Opalinus Clay

The diffusion experiments in Opalinus Clay (VAN LOON & SOLER 2004) were continued, and the diffusion of $^{85}Sr^{2+}$ perpendicular and parallel to the bedding was studied. In the case of the diffusion parallel to the bedding, the concentration of the tracer in the source reservoir decreased during the experiment. To model the on-going data, the computer code has to be modified to take this time-dependent boundary condition into account (see also section 3).

The diffusion of $^{134}Cs^{+}$ perpendicular to the bedding could be started. The total concentration of Cs^{+} was 10^{-3} M. At this concentration, the sorption distribution coefficient, R_d, is ca. 10^{-2} m^3 kg^{-1} (LAUBER et al. 2000). Hence, the through-diffusion can be studied in a time-window of 1-2 years. At lower concentration of Cs^{+}, the sorption is too high (up to 1 m^3 kg^{-1}) so that the through-diffusion technique can not be used any longer because of the very long break-through time.

In general, diffusion of strongly sorbing tracers cannot be studied using the through-diffusion technique. In-diffusion combined with high-resolution analytical techniques is the method of choice to tackle this problem. An abrasive peeling method was developed to analyse the diffusion profiles of strongly sorbing tracers. The principle behind the abrasive peeling technique is the removing of thin layers of material by abrasive grinding of the material on a silicon carbide paper. After grinding of the material, the radionuclide associated with the material can be measured directly with γ-spectrometry (γ-emitters), or with liquid scintillation counting (LSC) or α-spectroscopy (α-, β-emitters) after dissolution of the material. From the activity measured in the grinding swarf, the diffusion profile can be determined and the diffusion parameters be calculated. Fig. 7.1 shows the results obtained for the in-diffusion of $^{134}Cs^{+}$ and $^{22}Na^{+}$ in an OPA sample from Mont Terri. The total concentration of Cs and Na was 10^{-8} M and $3 \cdot 10^{-1}$ M, respectively. The values of the effective diffusion coefficient and R_d values derived from the diffusion profiles are summarised in Table 7.1. In the case of $^{22}Na^{+}$ there was an excellent agreement with the values derived from through-diffusion experiments ($D_e = 1.4 \times 10^{-11}$ m^2 s^{-1}; $R_d = 1.0 \times 10^{-4}$ m^3 kg^{-1}).

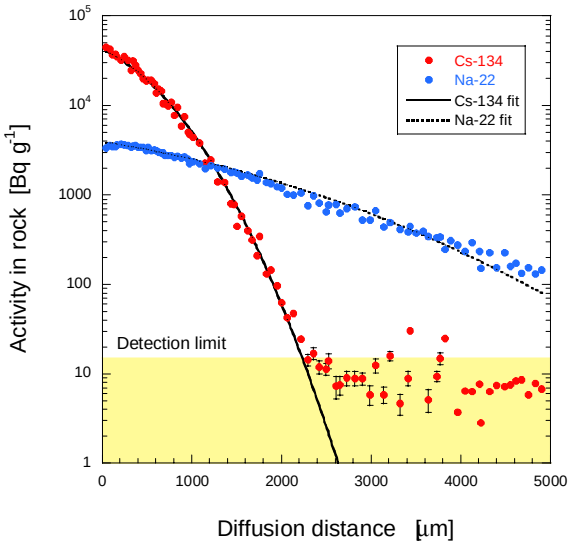

Fig. 7.1: *Diffusion profiles for $^{134}Cs^{+}$ and $^{22}Na^{+}$ measured by in-diffusion combined with abrasive peeling. The solid lines are fitted curves using a single reservoir method with decreasing source concentration for a semi-infinite case (SHACKELFORD 1991).*

Table 7.1: *Summary of the diffusion parameters derived from the in-diffusion measurements.*

	D_e [m^2 s^{-1}]	K_d [m^3 kg^{-1}]
$^{22}Na^{+}$	$1.6x10^{-11}$	$1.1x10^{-4}$
$^{134}Cs^{+}$	$3.4x10^{-11}$	0.297

7.3 Diffusion in compacted montmorillonite

The long-term aim of these experiments is a better understanding of the transport behaviour of sorbing and non-sorbing cations and anions in the buffer material of a repository for HLW. Diffusion processes dominate the dispersion of these ions – similarly to the situation in Opalinus clay. As a first step in the direction of studying the through-diffusion of moderately sorbing tracers, experiments are carried out using highly compacted (bulk density of ~1900 $kg{\cdot}m^{-3}$) montmorillonite (Na^{+}-form) for studying the diffusion of ^{85}Sr. The main objective of these experiments is to test the recently constructed diffusion cells, in which the sample thickness can be varied between 1 and 10 mm. These experiments will reveal to what extent it will be necessary to consider the diffusive properties of the filter plates made from sintered stainless steel that confine the compressed material when deriving the diffusion parameters of interest. In a second instance the influence of the ionic strength in the external solution on the diffusive properties of ^{85}Sr is tested in this experiment. First results for the 5 mm cells are shown in Fig. 7.2. For the purpose of a preliminary assessment of the transport parameters involved, the data are modelled assuming constant boundaries on the high-concentration reservoirs and no influence of the filter plates on diffusion. The results of this modelling exercise are shown in Table 7.2 and as the solid lines in Fig. 7.2.

Table 7.2: *Preliminary estimates of effective diffusion coefficients (D_e) and rock capacity factors (α) for the diffusion of ^{85}Sr through compacted montmorillonite in the Na^{+}-form (5 mm sample thickness).*

Bulk density ($kg{\cdot}m^{-3}$)	Ionic strength (M)	D_e ($\cdot10^{11}$) ($m^2{\cdot}s^{-1}$)	α	D_e/α ($\cdot10^{11}$) ($m^2{\cdot}s^{-1}$)
1970	0.5	2.1±0.15	12.5±0.13	0.17±0.02
1920	0.7	1.4±0.10	6.5±0.07	0.22±0.03
1970	1.0	0.94±0.07	5±0.05	0.19±0.02

The results given in Table 7.2 and Fig. 7.2 open a series of questions: (i) What is the reason for the observed dependence of D_e on the external ionic strength, and (ii) why is there no effect of ionic strength on the initial phase of the diffusion experiments?

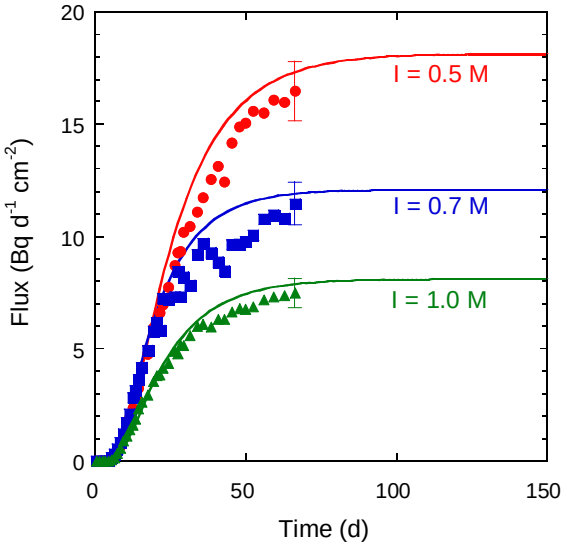

Fig. 7.2: *Diffusion of ^{85}Sr in montmorillonite in the Na^{+}-form compacted to a dry bulk density of ~1950 $kg{\cdot}dm^{-3}$ at the ionic strengths indicated ($NaClO_4$). The model curves were evaluated for constant boundary conditions at the high-concentration reservoir, which was not the case in the experiment. For this reason the model curves slightly overestimate the flux observed in the experiments.*

It may be too early for any conclusions to be drawn from these observations. However, the results indicate that both the diffusion and sorption properties of ^{85}Sr are affected by changes in ionic strength. The D_e/α values shown in Table 7.2, which represent apparent diffusion coefficients, suggest that these effects may compensate each other.

Owing to the preliminary character of the modelled diffusion parameters (cf. section 3) and to the fact that the steady-state phase has not been reached in the experiments shown in Fig. 7.2, no attempt has been made yet to compare the results obtained from experiments carried out with clay samples of different thickness.

7.4 The use of ultra thin clay membranes in diffusion studies

In order to study the diffusion of strongly sorbing radionuclides with through-diffusion techniques, thin clay samples have to be used. A new 2-years project will be started in October 2004. Aim of the project is to study the feasibility of the use of supported clay membranes in through-diffusion studies and to evaluate whether electrochemical measurements on clay membranes can be used to characterize the membranes and to extract relevant information for the diffusive transport in compacted clay systems. A specialist in electrochemical phenomena in membranes (A. Yaroshchuck) could be contracted for this purpose.

7.5 Dynamics of confined water in compacted argillaceous systems

Since the beginning of 2004, a PhD student is working on the properties (dynamics) of confined water in compacted argillaceous systems. It was recently found that water in contact with a SiO_2 surface forms a high-density liquid phase with a density 1.17 $g \cdot cm^{-3}$ (ENGEMANN ET AL. 2004).

Quasi-elastic neutron scattering measurements on different confined systems are on-going (Na-montmorillonite, Ca-montmorillonite, Na-illite, Ca-illite, kaolinite). First results on Na-montmorillonite show that the microscopic diffusion coefficient in this confinement is smaller than that in bulk water. A temperature scan between 333 and 200 ^oK indicated that the freezing point of confined water was shifted towards –13 ^oC. This is in good agreement with the study of ENGEMANN et al. (2004) who found a shift of the freezing point of water in contact with SiO_2 towards –17 ^oC.

First measurements of the activation energy of the diffusion of HTO in Na-montmorillonite (ρ=1900 kg m^{-3}) were performed and resulted in E_a = 25 kJ mol^{-1}. This value is significantly larger than that of free water (18 kJ mol^{-1}).

7.6 Organic ligands

Experiments addressing the reactivity of α-isosaccharinic acid (α-ISA) in systems containing artificial cement pore water and either $Ca(OH)_2$ or crushed hardened cement paste as a solid phase were carried out. The purpose of the experiments was to optimise the experimental conditions, at which chemical transformation of α-ISA can be studied, and to draw first conclusions on the driving forces involved in these reactions. Such reactions were observed during experiments at elevated temperature, in which cellulose has been degraded under alkaline conditions (GLAUS & VAN LOON, 2004). The experiments carried out in the last year have unambiguously shown that chemical transformation of α-ISA to acetate, formiate, glycolate and lactate as the main products occurs in the presence of $Ca(OH)_2$ under anaerobic conditions at elevated temperatures (86 °C in the experiments), i.e. the decrease in α-ISA concentration as a function of time cannot be solely explained by uptake on the solid. At ambient temperature some conflicting results have been obtained; however there are strong indications that transformation of α-ISA can be observed on timescales of months. Similar conclusions can also be drawn for the experiments where crushed hardened cement paste was the solid phase. Whereas the decrease of α-ISA concentration as a function of time was difficult to show owing to the experimental uncertainties involved, there are clear indications for the formation of the same transformation products as in the case of the reactions studied in the presence of $Ca(OH)_2$. For the second project phase, which will be finished by summer of 2005, some refinements in the experiments carried out so far are planned, in order to make possible that semi-quantitative kinetic information may be derived from the experimental data. These refinements basically comprise of experiments in the presence of $Ca(OH)_2$ using lower concentrations of α-ISA and experiments with hardened cement paste carried out at elevated temperature. Further the influence of solutions containing native products of chemical transformation of α-ISA on radionuclide sorption will be studied.

7.7 Analytical

A radioanalytical ion-chromatography technique was developed to assess the speciation of iodine in diffusion experiments. Importance was attached on testing, whether or not, the chemical equilibrium between iodide and iodate was shifted in the course of their separation. No such artefacts could be observed,

when injecting mixtures of known amounts of radiolabelled iodate and iodide to the separation system. It was further shown that a complete recovery of iodide was only obtained after pre-purification of the iodide tracer solution used. This suggests that other radioisotopes, interfering with the measurement of I-125, were present in the tracer solution.

As a side activity, concentrations of bromide and iodide in samples from DI-A experiment (phase #9) were measured by ion chromatography.

7.8 References

ENGEMANN S., REICHERT H., DOSCH H., BILGRAM J., HONKIMÄKI V., SNIGIREV A. (2004)
Interfacial Melting of Ice in Contact with SiO_2. Phys. Rev. Lett. 92, 205701-1 - 205701-4

GLAUS M.A., VAN LOON L.R. (2004)
Cellulose degradation at alkaline conditions: long-term experiments at elevated temperatures. PSI-Bericht Nr. 04-01, Nagra NTB 03-08

LAUBER M., BAEYENS B., BRADBURY M.H. (2000)
"Physico-chemical characterisation and sorption measurements of Cs, Sr, Ni, Eu, Th, Sn and Se on Opalinus Clay from Mont Terri". PSI Bericht Nr. 00-10, Nagra NTB 00-11

SHACKELFORD C.D. (1991)
Laboratory Diffusion Testing for Waste Disposal – a Review. J. Contam. Hydrol. 7, 177-217

VAN LOON L.R., SOLER J.M. (2004)
Diffusion in Opalinus Clay: Effect of confining pressure, sample orientation, sample depth and temperature. PSI Bericht Nr 04-03, Nagra NTB 03-07

7.9 Publications

7.9.1 Peer reviewed journals and reports

GLAUS M.A., VAN LOON L.R. (2004)
A generic procedure for the assessment of the effect of concrete admixtures on the retention behaviour of cement for radionuclides: concept and case studies. PSI-Bericht Nr. 04-02, Nagra NTB 03-09

GLAUS M.A., LAUBE A., VAN LOON L.R. (2004)
A Generic Procedure for the Assessment of the Effect of Concrete Admixtures on the Sorption of Radionuclides on Cement : Concept and Selected Results. Mat. Res. Soc. Symp. Proc. 807, 365-370

GAUTSCHI A.[1], MARSCHALL P.[1], SCHWYN B.[1], BAEYENS B., BRADBURY M.H., GIMMI TH., MAZUREK M.[2], VAN LOON L.R., WABER N.[2], WERSIN P.[1] (2004)
Geoscientific Basis for Making the Safety Case for a SF/HLW/ILW Repository in Opalinus Clay in NE Switzerland (Project Entsorgungsnachweis) – II: The Geosphere as a Transport Barrier : Hydraulic, Diffusion and Sorption Properties. NEA/RWM/IGSC 8, 63-70
[1] Nagra, Wettingen, Switzerland
[2] Rock-Water Interaction (RWI), University of Bern, Switzerland

RAI D.[1], HESS N.J.[1], XIA Y.[1], RAO L.[2], CHO H.M.[2], MOORE R. C.[3], VAN LOON L.R. (2003)
Comprehensive Thermodynamic Model Applicable to Highly Acidic to Basic Conditions for Isosaccharinate Reactions with Ca(II) and Np(IV). J. Sol. Chem. 32, 665-689
[1] Pacific Northwest National Laboratory, Richland, WA, USA
[2] Lawrence Berkeley National Laboratory, Berkeley, CA, USA.
[3] Sandia National Laboratories, Albuquerque, New Mexico, USA.

RORIF, F.[1], VALCKE, E.[1], GLAUS M.A. (2004). The effect of cellulose degradation products on the solubility and sorption of Pu and Am in alkaline-plume-affected and in unaffected Boom Clay. Mat. Res. Soc. Symp. Proc. 807, 633-638
[1] SCK•CEN, Mol, Belgium

VAN LOON L.R., SOLER J.M.[1] (2004)
Diffusion in Opalinus Clay: Effect of confining pressure, sample orientation, sample depth and temperature. PSI Bericht Nr 04-03, Nagra NTB 03-07
[1] CSIC-IJA, Barcelona, Spain

WERSIN P.[1], VAN LOON L.R., SOLER J.[2], YLLERA A.[3], EIKENBERG J., GIMMI TH., HERNAN P.[4], BOISSON J.-Y.[5] (2004)
Long-term Diffusion Experiment at Mont Terri : First Results from Field and Laboratory Data. Appl. Clay Science 26, 123-135.
[1] Nagra, Wettingen, Switzerland
[2] CSIC-IJA, Barcelona, Spain
[3] CIEMAT, Madrid, Spain
[4] ENRESA, Madrid, Spain
[5] IRSN, Fontenay-aux-Roses, France

7.9.2 Conferences/Workshops/Presentations

GONZÁLEZ F., JURANYI F.[1,2], GIMMI TH., VAN LOON L.R. (2004). Dynamics of Confined Water in Compacted Clay Systems. The 7th International Conference on Quasi-Elastic Neutron Scattering, 1- 4 September, Arcachon, France.
[1] Physical Chemistry, Saarland University, Saarbrücken, Germany
[2] Laboratory for Neutron Scattering, PSI, Villigen, Switzerland

8 THE MICRO-XAS BEAMLINE PROJECT: STATUS AND MICROXAS RESULTS

D. Grolimund, A.M. Scheidegger, M. Harfouche, B. Meyer, M. Willimann

8.1 Overview

The core assignments of the microXAS beamline project are to design, build, and finally operate a synchrotron-based X-ray microprobe facility dedicated to X-ray absorption spectroscopy (XAS) and X-ray fluorescence (XRF) techniques (GROLIMUND et al., 2002a,b; SCHEIDEGGER, PRINS, 2000). Further, the beamline project team is expected to develop an active microXAS research program covering both aspects, fundamental and applied research as well as analytical instrumentation development.

Over the past years, mainly due to considerable instrumental and theoretical advances, synchrotron-based X-ray XAS and XRF have developed into key analytical techniques for a broad range of scientific disciplines including environmental sciences (waste management, geochemistry, atmospheric science, etc.), chemistry and catalysis, materials science, or life science. In the past, the application of 'classical' XAS and XRF using unfocused X-ray beams has frequently resulted in unique contributions towards an improved molecular-level understanding of material structure and chemical reactivity.

Further advancements have come with the small source size and low emittance of new 3rd generation synchrotron sources – such as the Swiss Light Source – in combination with recent innovations in the design and production of hard X-ray focusing optics which allows the construction of dedicated high-flux microprobe beamlines. Concurrently, the availability of micro-focused X-ray radiation is triggering the development and/or improvement of various analytical microprobe techniques, including analytical, imaging, and spectroscopic tools. Some of these tools are exclusive to synchrotron facilities, e.g., X-ray absorption spectroscopy. Consequently, synchrotron-based microprobes provide the ability to characterize complex samples in a non-destructive manner with **high spatial resolution** and sensitivity as well as chemical specificity – all being crucial prerequisites for investigations in most scientific disciplines.

Notably, in addition to the high resolution in the space domain, the microXAS beamline will also offer unique time resolution. This key feature is originating from to the associated *FEMTO* project which will allow investigations of time-dependent phenomena in the femtosecond time regime (INGOLD et al., 2002; SCHOENLEIN et al., 2000). The 'joint venture' microXAS/*FEMTO* is sharing the beamline optics and considerable parts of the experimental infrastructure. The *FEMTO* project will implement a slicing source allowing hard X-ray pulses of approximately 100 femto seconds to be produced. The slicing is based on the interaction of high intensity, femto-second laser pulses with the electron beam in the modulator, a second, wiggler-type insertion device to be installed with microXAS 5L straight section. As an ultimate goal, time-resolved studies with a resolution of ~100 femto seconds should be feasible at the microXAS beamline to study time-dependent phenomena in condensed matter relevant to physics, chemistry, biology, or environmental science (e.g., BRESSLER et al., 2002; BRESSLER et al., 2003).

Last but not least, measurements of closed active samples will be possible at the microXAS beamline. In combination with the PSI Hotlab, which is available for sample preparation and intermediate storage, a world-unique userlab for micro-beam X-ray investigations of active samples will be created.

In the following, a status report of the microXAS beamline project, as well as an illustrative example of microXAS research, is presented.

8.2 Project Status

Over the past months, extensive work packages could be completed and several milestones were accomplished. For each beamline section a summary is provided below.

8.2.1 Machine – Beamline Interface and Front end

The front-end represents the first section of the beamline which was completely installed. Compared to a standard SLS front-end, the microXAS version is characterized by a higher complexity. Rather exceptionally, two beams, (i) the 'undisturbed' microXAS beam and (ii) the sliced *FEMTO* beam, have to be guided though all front-end components. Accordingly, specialized components and/or special functional capabilities had to be designed and installed to comply with the 'beam duality'.

One of the – quite literally – most exciting milestones was the delivery and subsequent installation of our primary radiation source, the in vacuum mini-gap undulator U19. Shortly after installation, the magnetic gap could be closed for the first time and the first insertion device light could be produced. The increase

in luminous intensity with closing gap could be monitored and recorded with X-ray beam position monitors located in the front-end (Fig. 8.1).

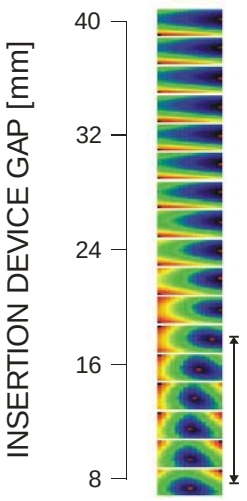

Fig. 8.1: *Closing of the insertion device gap: Rising luminous intensity with increasing reduction of the insertion device gap. Right-side arrow indicates the gap range with dominating undulator radiation.*

8.2.2 Beamline Optics

Recently, the installation of the beamline optics, with the two key pieces (i) torroidal mirror and (ii) monochromator, could be completed. The successful installation of the highly fragile, 1 meter long silicon single crystal mirror into the bender mechanism and into the mirror tank corresponded to another, quite relieving milestone for all involved parties. Fig. 8.2 shows the reflective surface of the installed, but unbent cylindrical mirror. While the sagital radius (~10 cm) is static in nature and is obtained by mechanical polishing, the tangential radius is obtained by dynamic bending. The optical radius of 4.5 km requires sub-micron precision of the bending system.

Both devices, the torroidal mirror and the monochromator, had to go through different cycles of mechanical tests in order to verify the engineering specifications. While we have generally obtained promising results, the ultimate tests of the performance, however, have to be conducted under realistic conditions – in particular vacuum pressure and maximal heat load – using X-rays beams. In the context of destructive heat load or power density effects, the installation of the cryogenic cooling circuit of the monochromator represents another important milestone.

Imposed by the *FEMTO* project and the proposed micro-focusing scheme, the beamline has to be operated windowless up to the experimental hutch (minimization of beam disturbance and flux reduction by windows). In order to guarantee the proposed vacuum conditions (in particular to protect the ring vacuum), a differential pumping unit and several control loop including fast-closing valves have been installed. For each vacuum section, stable pressure conditions within the specified tolerances have been achieved shortly after closing up the beamline tubing.

Awaiting the final approval by the radiation safety department, the beamline optics is ready to deliver X-rays into the experimental hutch.

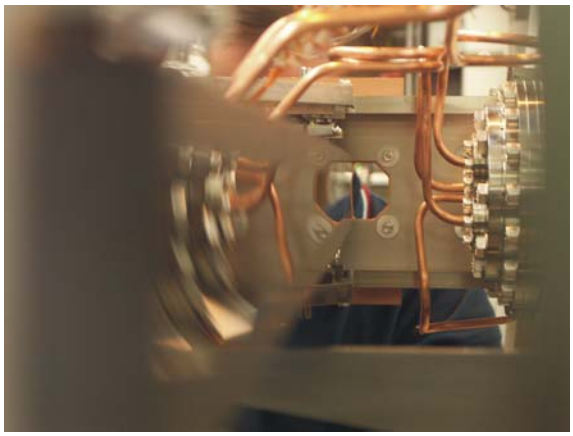

Fig. 8.2: *The reflective surface of the unbent cylindrical mirror installed in the dynamic bender.*

8.2.3 Experimental infrastructure and beamline controls

Considerable efforts have been undertaken over the past months to finalize the design and expedite both manufacturing and installation of the experimental infrastructure. Key units were (i) intermediate focus unit including beamline termination, (ii) experimental tables, (iii) sample stages, (iv) micro-focusing optics, and (v) detector systems.

The experimental tables and the beamline termination unit are already installed and are currently undergoing preliminary commissioning tests. A first sample stage unit has been assembled and was successfully integrated into the SLS control system.

Concerning detector systems, photodiodes and ion-chambers for transmission experiments as well as a Stern-Heald detector system for measurements in fluorescence and electron-yield mode, respectively, are ready for operation.

Orders for a multi-element Ge solid-state detector and a high resolution, wavelength dispersive X-ray detector system (WDX) have been placed. These devices are expected to be shipped to the SLS in the near future. A single element solid state detector is currently set up with the main goal of advancing the integration of solid state detector systems, together

with the newly developed, high throughput readout electronics, into the beamline control system.

Based on the anticipated needs of the user community, considerable resources (capital and labour) have to be invested in the experimental infrastructure. The most outstanding example is the detector portal system required to exchange and position the different detector system around the sample. As an illustration, Fig. 8.3 shows a 3D model of the portal with a typical setup to be used during the measurements of active samples (see Section 8.3). The portal development corresponds to a collaborative project of the microXAS project team and the LOG-AMI department of PSI (H.U. Walther; H. Baechli). The system is currently being manufactured and will be available for installation by the end of the year.

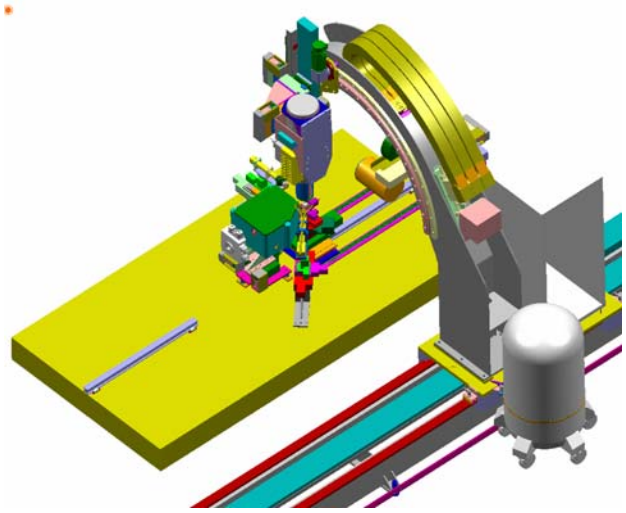

Fig. 8.3: *3D model of the detector portal showing the Ge-detector in vertical position for the measurements of active samples.*

In order to be able to ensure the requested beam stability and quality of the microbeam, a number of specialized diagnostic devices are under development. Most important are fast beam position monitors (BPM) and a high resolution X-ray eye. The later device corresponds to a key tool during the focusing of the X-ray beam. Based on the ESRF design a customized version was developed and is currently being manufactured at the machine shop of PSI. Central requirements were high spatial resolution, full compatibility with the control system, and cost effectiveness. Further, the instrument was conceptualized in view of its use within a proposed automated focusing routine.

The BPMs are an integral part of a feedback system required to stabilize the monochromatized beam. Deviations from the zero trajectory are recorded by two BPMs, located between the monochromator and the intermediate focus point, and are converted to piezo-driven corrections to be executed by the second monochromator crystal. Led by the PX-I project team, a new generation of beam position monitors is currently under development (joint project by PX-I, LUCIA, microXAS, and PSI-LMN). First prototypes are in operation at the PX-I beamline and installed at the microXAS beamline.

Regarding micro-focusing optics, a Kirkpatrick-Baez (KB) first mirror system– optimized for sub-micron focusing – is currently being tested at the optics laboratory of the Advanced Light Source (ALS) for its optical quality. For a second KB system the call for tender is still pending. This second KB unit will be specially tailored towards the needs of pump-probe applications (*FEMTO* project).

In addition to the above listed hardware components software dominated fields (i) beamline controls, (ii) data acquisition, and (iii) user interfaces evolved to extremely demanding work packages and a high work load. In these areas of beamline development an even further increasing workload is anticipated over the forthcoming months.

8.3 Measurements of Active Samples

Within 2004 substantial progress has been made by the working group for the measurements of active samples at the microXAS beamline *(working group: A. Scheidegger, R. Dähn (LES); M. Nicolet, D. Gavillet, R. Restani, P. Heimgartner (LWV), H.U. Walther (LOG-AMI)).* After the safety department at PSI approved the proposed concept (RESTANI et al., 2003), the concept was presented to the 'Bundesamt für Gesundheit' (BAG, regulatory agency for SLS). BAG confirmed that there is no principal show-stopper for the proposed concept and advised us to go ahead with outlining the technical details.

As next steps, the design of the specimen containment was initiated together with the construction department at PSI. Due to the very limited space available around the sample the entire set-up needs to be kept as small as possible. A schematic outline of the specimen containment is given in Fig. 8.4. The *specimen holder* consists of an air tight container holding up to three specimens with one layer of Kapton windows. The *specimen holder* is encapsulated in a *safety case,* again air tight, with a single or double layer of Kapton windows (for an overall double or triple encapsulation) to insure a contamination free analysis of the specimens on the beamline. The Kapton windows allow good transmission of the X-Ray beam and insures the containment of the specimens. The *specimen holder* also contains a reference substrate (fluorescence screen) that is used for beam alignment by an optical microscope. The surface of the active samples must be

mounted within a few hundreds of microns with respect to the surface of the reference substrate in order to avoid that beam size on the sample (normally a few μm^2) significantly increases due to the divergence of the micro beam (3 mrad).

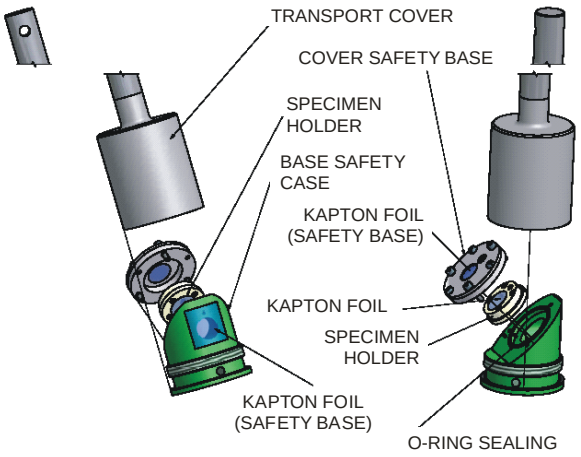

Fig. 8.4: *Outline of the active specimen containment system consisting of a specimen holder, its safety case with a massive base and a safety base cover, and a steel cover used for transport.*

The safety case containing the specimen holder will be covered by a protective steel cover for transportation (*transport cover*, Fig. 8.4). The specimens will be entirely encapsulated in the above outlined containment system in the Hotlab. Once brought to the beamline with a certified type A transport container, the containment system is mounted on a dedicated sample manipulator designed for measurements of active samples. In cases where the activity is so high that shielding is required, Pb shielding will be placed as close as possible horizontally around the sample. The detectors required for the experiments (e.g. 30-element Ge-detector for fluorescence and CCD for X-ray diffraction) will then be placed in the vertical position. A dedicated detector portal has been designed for this purpose (Fig. 8.3, Section 8.2.3).

Currently the details of the specimen holder and the containment system are outlined and the procedure on how to load the samples in the 'Hotlab' are finalized. Furthermore, decontamination issues, the transport procedure, and the measurement protocol at the beamline are outlined. The detailed information will then be discussed once again with the safety department at PSI and the BAG.

A 3-step procedure is proposed for initiating the measurements of active samples at the microXAS beamline:

(i) Commissioning of the specimen holder and sample manipulator dedicated for active samples using inactive samples. This phase will also be used for testing the entire experimental procedure, including transport and sample manipulation

(ii) First experiments with weakly active samples (starting Spring 2005)

(iii) Step-wise extension of the measurements towards experiments with hot samples.

8.4 Time scale for realization

In 2003/2004 the work focused on the construction and installation of the beamline components. Major milestones were the installation of the frontend (December 2003), the mirror (March 2003), and the insertion device (April 2004). The delivery of the monochromator was strongly delayed and technical problems during its installation (March and May 2004) caused a further delay. In August 2004 the construction of beamline including beamline infrastructure (cooling and electric media, air-condition, network) shall be completed and the first synchrotron light in the experimental hutch is expected in September 2004. The remaining part of 2004 and the first half of 2005 will be dedicated to the beamline commissioning. The commissioning includes

- thorough tests of all optical and diagnostic components
- integration of the 30-element solid-state Ge detector, the wavelength dispersive X-ray (WDX) spectrometer for fluorescence measurements and the charged coupled device (CCD) area detector for diffraction
- set-up of the micro-focusing system with the Kirkpatrick-Baez (KB) mirror system, the sample manipulator, and the microscope.

Critical issues will be the development of a fast data acquisition system for XRF mapping and the set-up of the control system and the user interface. During the commissioning phase pilot experiments with expert users will be initialized, first for macro-, and then for microbeam experiments. We currently anticipate that the beamline will be opening for users within the second half of 2005.

8.5 Personnel

The personnel situation within the microXAS beamline team did not change in 2003/2004 except that M. Harfouche joint LES as a Postdoc (September 2003) and now supports the beamline project. Clearly, for the upcoming beamline commissioning phase additional man-power personnel is mandatory. It is foreseen that R. Dähn will be partly involved in the

commissioning. Furthermore, we anticipate at least some man-power support (G. Kuri) from the side of LWV at PSI for the commissioning. Nevertheless, for the long-term operation of the beamline the situation with respect to man-power remains critical or will even worsen when M. Harfouche leaves the microXAS team (contract ends August 2005). The criticality of the man-power situation has been pointed out independently by both the LES Program Committee and the LES Audit team.

8.6 MicroXAS research

Besides our obligations for the microXAS beamline, the beamline project team has developed an active microXAS research program over the course of the last few years. While our involvement in microXAS activities with respect to waste repository systems (in particular clays and cement) are outlined in sections 4 and 5, we present a microXAS case study on "*Cs migration in complex geological media: New insights through micro-imaging and micro-spectroscopy*"[#].

8.6.1 Introduction

The concern about the log-term fate of radionuclides (and other hazardous chemicals) in the subsurface environment has resulted in the development of numerous theoretical models incorporating an ever increasing number of reactive transport processes. While the (hypothetical) complexity of the theoretical models increased steadily, the corresponding growth in quantity and quality of experimental investigations did not keep pace, by far. However, reliable experimental data are most crucial regarding model validation and calibration. In particular field-scale data of highly reactive radionuclides with large retardation are extremely scarce. The lacking of such field data can mainly be attributed to experimental and analytical difficulties. First of all, for strongly retarded radionuclides the spreading pattern is spatially highly restricted due to transport velocities of a few micrometers to millimeters per year. As a consequence, conducting breakthrough experiments on the field-scale is not feasible within reasonable time scales. Secondly, the ubiquitous spatial micro-variability (physical and chemical heterogeneity) of geological materials represents another serious obstacle. Notably, however, even large field-scale reactive transport phenomena have been recognized to be triggered by micron-scale processes.

Accordingly, any practical analytical technique must comprise high spatial resolution (micron scale) and high chemical specificity. Recent advancement in micro-analytical techniques, in particular *synchrotron based X-ray microprobe techniques* as well as *laser ablation coupled to ICP-MS* detection open new opportunities in probing the multi-dimensional spreading of strongly retarded radionuclides under realistic field conditions.

Within the present study, such microprobe techniques were employed to analyze the field-scale migration of Cs as investigated at the Mont Terri Underground Rock Laboratory (DI-A experiment). The diffusion pattern from a Cs source into the bulk rock (Opalinus clay rock) was studied by complementary techniques including bulk digestion and solution ICP-AES, as well as *laser ablation-ICP-MS* and *synchrotron-based microXRF and EXAFS.*

8.6.2 Materials and Methods

The investigated Opalinus rock samples are originating from the overcore BDI-A1, which was excavated after completion of the log term diffusion (DI-A) experiment at the Mont Terri rock laboratory, Switzerland. After extraction, drillcore $P9_{1,2}$ was embedded in epoxy resin and further sectioned by diamond wheel cutting. A typical fragment used for the different microprobe investigations is depicted in Fig. 8.5. The interface between the quartz-filled injection borehole (left) and the rock matrix is clearly visible.

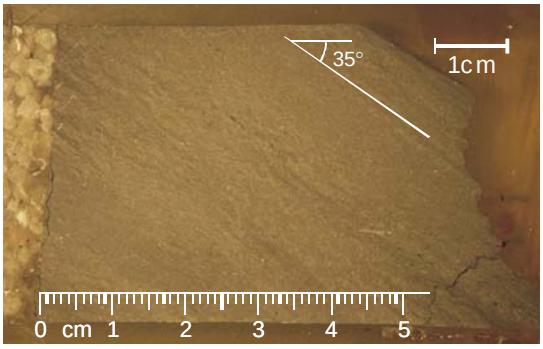

Fig. 8.5: *Opalinus clay rock fragment investigated by micro LA-ICP-MS and microXRF.*

The LA-ICP-MS analysis was carried out at the Laboratory of Inorganic Chemistry, Section Elemental and Trace Analysis, ETH Zurich. A 266 nm Nd:YAG laser ablation system (LSX 500, SD Acquisitions/ CETAC) was coupled to a Perkin Elmer Elan 6000 ICP-MS. Ablation crater were measured to be approximately 40 µm in diameter.

[#] Collaborative work by Daniel Grolimund[1], Detlef Günther[2], Andre M. Scheidegger[1], Beat Aeschlimann[2], Paul Wersin[3], Steve M. Heald[4].

1: Paul Scherrer Institute, Waste Management Laboratory and Swiss Light Source, Villigen PSI, Switzerland
2: Swiss Federal Institute of Technology, Laboratory for Inorganic Chemistry, Zürich, Switzerland
3: NAGRA, Wettingen, Switzerland
4: Advanced Photon Source, PNC-CAT, Argonne, IL, USA

All synchrotron-based microXAS investigations reported here were conducted at Sector 20 (PNC-CAT) of the Advanced Photon Source (APS), Argonne, USA. Operation conditions of the APS were 7 GeV and 100 mA current (top-up mode).

The microprobe beamline 20-ID is an insertion device line dedicated to X-ray microbeam applications in materials and environmental sciences (HEALD et al., 2001; HEAD et al., 1999). The X-ray microbeam is obtained by directly imaging the source by means of two elliptical mirrors aligned in a classical Kirkpatrick-Baez arrangement (HOWELLS et al., 2000; KIRKPATRICK & BAEZ, 1948; YANG et al, 1995). Typical focual spot size during the measurements was 4x3 μm^2. The X-ray beam was monochromatized by means of a fixed-exit double crystal monochromator using either a pair of Si(111) or Si(311) crystals. Energy calibrations were carried out using standard metal foils measured in transmission.

Two-dimensional X-ray fluorescence maps were collected using a fully motorized x-y scanning stage. Fluorescence emission was monitored by simultaneous use of two detector systems: (i) an energy dispersive 13-element Ge solid-state detector (Canberra) and (ii) a Microspec WDX wavelength dispersive spectrometer. While the energy resolution of the Ge solid state detector is typically around 130 – 150 eV, the WDX equipment has an energy resolution as narrow as a few eV. For the investigation of Cs migration in Opalinus clay rock, such a superior resolving power is mandatory to discriminate the fluorescence emission of the trace concentrations of Cs (L_α line, 4.29 keV) against the deluging fluorescence emission arising from the macro concentrations of Ca and Ti present in the clay material (K_β line, 4.01keV and K_α 4.51 keV, respectively). Fig. 8.6 depicts a comparison of the energy resolution of the Ge solid state detector and the WDX spectrometer. The fuorescence originates from an Opalinus clay rock sample illuminated with 7.1 keV radiation.

After determining the location of the Cs diffusion front by microXRF maps, Cs K-edge EXAFS spectra were collected to determine the chemical speciation of the interfacial Cs species responsible for the retardation of Cs within the Opalinus clay rock material.

As alternative analytical techniques to investigate selected samples of different drillcores, wet chemical extraction and laboratory source based macro X-ray fluorescence (macroXRF) analysis were employed prior to the microprobe analysis. Both techniques yield total elemental contents of macro and trace elements. However, the spatial resolution of both techniques is limited to the corresponding sampling volume. As the wet chemical extraction procedure is based on cation exchange reaction involving Cs and K, the extraction data have to be corrected for the incomplete replacement of (specific) sorbed Cs by solution K. Using calibrated XRF measurements, the extraction yield was determined to be approx. 0.5.

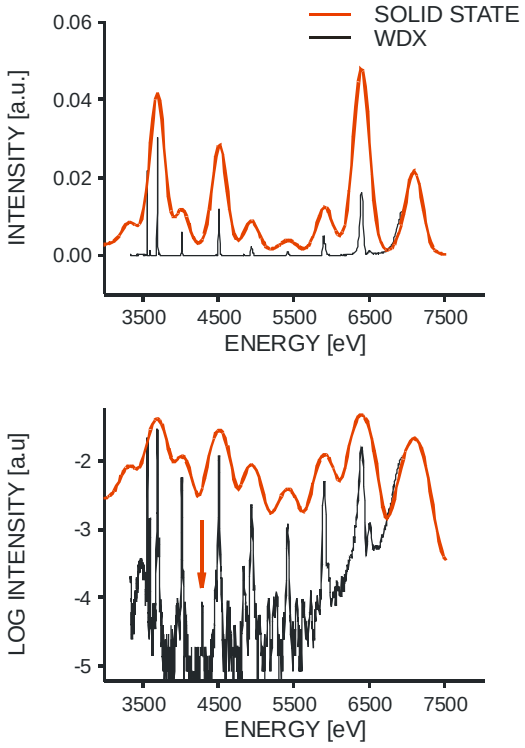

Fig. 8.6: *Comparison of the energy resolution of a Ge solid state detector and a WDX spectrometer based on the fluoresence emission from a Cs containing Opalinus clay rock sample (~150ppm Cs). The arrow indicates the fluorescence L_α line of Cs that is completely hidden by Ca K_β and Ti K_α emission lines in case of the solid state detector.*

8.6.3 Selected results

Bulk analysis revealed averaged information regarding the decrease of the Cs concentrations as a function of migration distance. Results obtained by the four different independent techniques (macroXRF and wet chemical extraction as well as LA-ICP-MS and microXRF) show a good agreement as illustrated in Fig. 8.7. A distinct Cs diffusion front can be established. However, this illustration demonstrates clearly, that the micron scale spatial resolution of microprobe techniques is mandatory to represent the Cs diffusion profile. Due to the experimentally limited spatial resolution, the macroscopic measurements yield only two groups of data points over the whole

range of Cs migration (one group at ~12mm, another at ~25mm, see bottom illustration in Fig. 8.7). Obviously, solely based on only two data points, the reconstruction of an entire diffusion profile corresponds to a highly ill-posed problem.

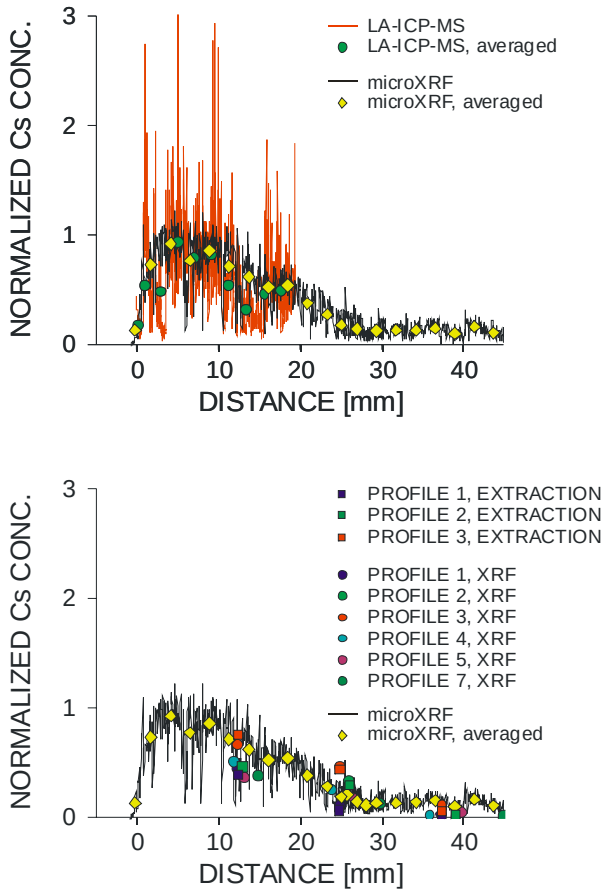

Fig. 8.7: *Cs diffusion profiles. (top) Line-scans extending from the quartz-filled injection borehole into the Opalinus clay rock material recorded by two different microprobe techniques are shown. (bottom) For comparison, the microscopic data are overlaid by data points obtained by macroscopic measurements (macroXRF and wet chemical extraction).*

The data plotted in Fig. 8.7 were obtained by investigating separate profiles (1 to 7) from different drillcores that were spatially separated by up to one meter. Thus, the variation in Cs concentration indicates the presence of spatial heterogeneity in the sampling area of the migration experiment. This conclusion can be made based on the fact that the variation in Cs concentration measured by both, macroXRF and chemical extraction, is significantly larger than the *analytical error* of the corresponding measurements.

Compared to the Cs profiles presented here, corresponding migration pattern of inert tracers show a considerably reduced variation (MOERI et al., 2003; data not shown). Consequently, the variation in Cs concentration established by macroXRF and chemical extraction can be mainly contributed to the *chemical* heterogeneity in OPA material.

This finding is supported by the LA-ICP-MS and microXAS measurements. The apparent 'noise' in the LA-ICP-MS and microXRF data is fully reproducible from an analytical point of view and thus, the variability in Cs concentration reflects the spatial heterogeneity of the Opalinus clay rock. This conclusion is further supported by Fig. 8.8, depicting the concentration profiles for calcium, titanium and cesium within the first 15 mm from the injection borehole boundary. The logarithmic representation clearly shows that within a few microns the concentration of macro elements are changing by more than one order of magnitude. As will be discussed below in detail, the sorbed Cs concentration at a given location is strongly related to the prevailing macro element distribution and related mineral composition.

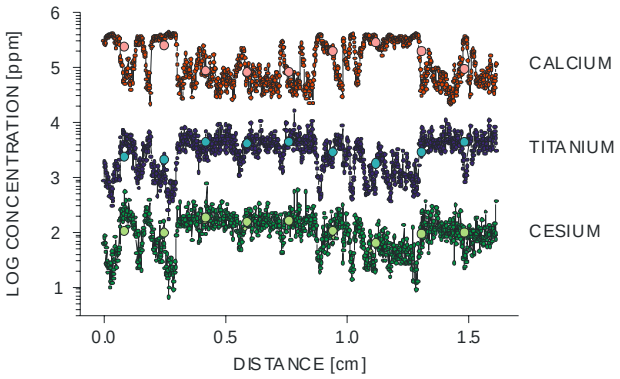

Fig. 8.8: *Concentration profiles for calcium, titanium and caesium within the first 15 mm from the injection borehole boundary. Data were obtained by LA-ICP-MS.*

Spatially refined analysis using micro-analytical techniques allowed for process oriented investigations. Various two-dimensional element mappings (with spatial resolutions of 3 to 50 microns) show a heterogeneous distribution of the matrix elements. Fig. 8.9 illustrates two-dimensional elemental distributions maps recorded at the forefront of the Cs diffusion profile.

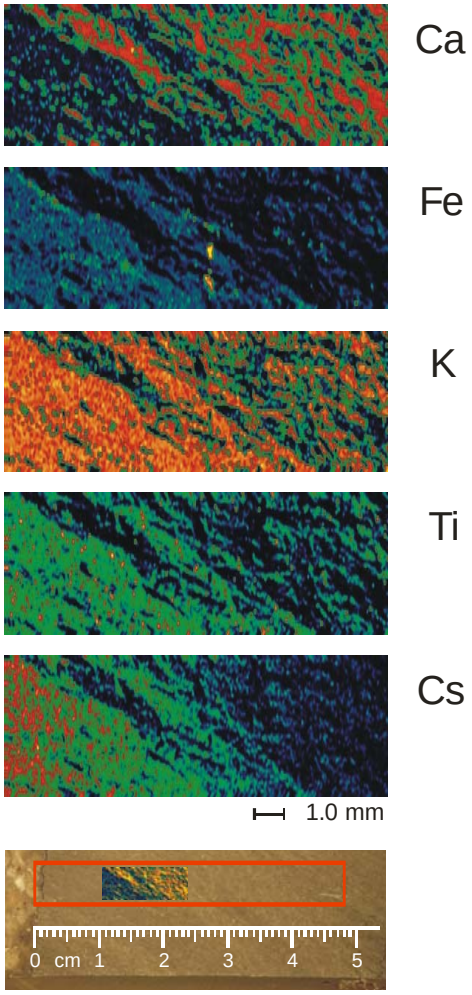

Fig. 8.9: *Two-dimensional elemental distributions maps recorded at the forefront of the Cs diffusion profile. The location of the high-resolution maps relative to the injection borehole boundary is illustrated in the bottom panel.*

Distinct distribution pattern are observed. The spatial features exhibit a characteristic length scale of approximately 300µm. Based on the characteristics of the elemental distributions maps one can further conclude that the host rock material corresponds to a complex mineral composite with an interlinked 3D network structure.

The distribution maps show pronounced elemental correlations or autocorrelations and thus contain important information towards the identification of the reactive solid phase(s). For example, it is readily apparent from Fig. 8.9 that the Ca-rich patches seem not responsible for Cs retardation (areas dominated by Ca are basically free of Cs). On the other hand, the Cs distribution pattern is almost indistinguishable from those of Ti or K.

The strength of the synchrotron-based analytical approach is that both, micro-scale elemental distribution and molecular-level information about the interfacial Cs speciation present in the rock material can be obtained.

In the present study we have recorded Cs K-edge EXAFS spectra in order to gain information about next-near neighboring atoms of Cs in OPA. Although the data analysis is not yet finalized, first preliminary results are illustrated in Fig. 8.10. Due to the chemical complexity of the sample and the fact that Cs concentration in the sample is rather dilute, advanced data analysis tools such as wavelet analysis were used (MUNOZ et al., 2003; ADDISON & ADDISON, 2002). Both, the Fourier and the Wavelet transform clearly show the presence of *two* next-near neighboring atomics shells (Cs-O backscattering pairs). The split of the Cs-O coordination sphere indicates that Cs is specifically bound to geochemical minerals present OPA.

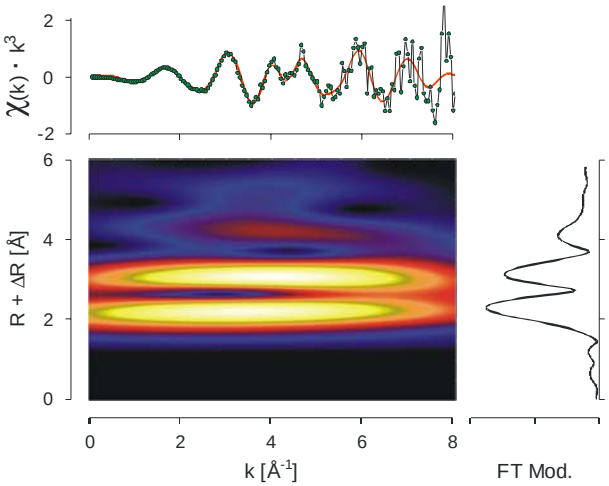

Fig. 8.10: *Cs K-edge EXFAS and corresponding Fourier and Wavelet transform.*

The study clearly shows that based on the use of a multitude of complementary analytical techniques, new detailed insights into the diffusion process of highly reactive chemicals in complex natural porous media can be elaborated. The microXAS facility at the Swiss Light Source can be expected to make valuable contribution to improve our understanding of the field-scale transport of strongly sorbing radionuclides and other pollutants in geological materials related to waste management.

8.7 References

ADDISON P.S., ADDISON N. (2002)
The Illustrated Wavelet Transform Handbook, Institute of Physics Publishing

BRESSLER CH., SAES M., CHERGUI M., GROLIMUND D., ABELA R., PATTISON PH. (2002)
Towards Structural Dynamics in Condensed Chemical Systems Exploiting Ultrafast Time-Resolved X-Ray Absorption Spectroscopy, J. Chem. Phys., 116, 2955

BRESSLER CH., SAES M., ABELA R., GROLIMUND D., JOHNSON S.L., HEIMANN P.A., CHERGUI M. (2003)
Observing Transient Chemical Changes by Ultrafast X-ray Absorption Spectroscopy, Physical Review Letters, 90, 047403

GROLIMUND D., SCHEIDEGGER A.M., VAN DER VEEN J.F., ABELA R. (2002)
Layout of the microXAS beamline at SLS. PSI Scientific Report 2001, IV, 139-148

GROLIMUND D., SCHEIDEGGER A.M., VAN DER VEEN J.F., ABELA R. (2002)
Layout of the microXAS beamline: Design Study. PSI Scientific Report 2001, VII, 56-57

HEALD S.M., BREWE D.L., STERN E.A., KIM K.H., BROWN F.C., JIANG D.T., CROZIER E.D., GORDON R.A. (1999)
XAFS and micro-XAFS at the PNC-CAT beamlines, Journal of Synchrotron Radiation, 6, 347-349 Part 3, May 1, 1999

HEALD S.M., STERN E.A., BREWE D.L., GORDON R.A., CROZIER E.D., JIANG D.T., CROSS J. (2001)
XAFS at the Pacific Northwest Consortium-Collaborative Access Team undulator beamline, Journal of Synchrotron Radiation, 8, 342-344

HOWELLS M.R., CAMBIE D., DUARTE R.M., IRICK S., MACDOWELL A.A., PADMORE H.A., RENNER T.R., RAH S., SANDLER R. (2000)
Theory and practice of elliptically bent X-ray mirrors, Optical Engineering, 39 (10), 2748-2762

INGOLD G., STREUN A., SINGH B., ABELA R., BEAUD P., GROLIMUND D., KNOPP G., RIVKIN L., SCHLOTT V., SCHMIDT T., SIGG H., VAN DER VEEN J.F., WRULIN A., KHAN S. (2002)
Conceptual Design: Sub-Picosecond Hard X-Ray Source, PSI Scientific Report 2001, VII, Paul Scherrer Institute, Villigen PSI, Switzerland

INGOLD G., ABELA R., BEAUD P., GROLIMUND D., JOHNSON J., MUNOZ M., RIVKIN L., SCHLOTT V., SCHMIDT T., SCHULZ L., STREUN A., VAN DER VEEN J.F., CHUBAR O., KHAN S., TARNOVSKY A. (2003)
Status: Undulator X-ray Source for Time-resolved ps- and sub-ps Pump/Probe Experiments in the Range 5-18 keV, PSI Scientific Report 2002, VII, Paul Scherrer Institute, Villigen PSI, Switzerland

KIRKPATRICK P., BAEZ A.V. (1948)
Formation of Optical Images by X-Rays, Journal of the Optical Society of America, 38, 766-774

MUNOZ M., ARGOUL P., FARGES F. (2003)
Continuous Cauchy wavelet transform analyses of EXAFS spectra: a qualitative approach. American Mineralogist, 88, 694-700

RESTANI R., GAVILLET D., MEYER B., SCHEIDEGGER A.M. (2003)
Konzeptvorschlag für ein Aktivproben-Containment an der micro-XAS Beamline. AN-43-02-12, Rev.1, Paul Scherrer Institute, Villigen PSI

SCHEIDEGGER A.M., GROLIMUND D., MEYER B., ABLEA R., VAN DER VEEN J.F. (2003)
Status of the microXAS Beamline Project, PSI Scientific Report 2002, VII, Paul Scherrer Institute, Villigen PSI, Switzerland

SCHEIDEGGER A.M., PRINS R. (2000)
Joint Proposal by the Swiss XAS User Community for an EXAFS Beamline for Heterogeneous and Dilute Systems at the Swiss Light Source (SLS), Paul Scherrer Institute, Villigen PSI

SCHMIDT T., INGOLD G., IMHOF A., PATTERSON B.D., PATTHEY L., QUITMANN C., SCHULZE-BRIESE C., ABELA R. (2001)
Insertion devices at the Swiss Light Source (phase I), Nuclear Instruments & Methods A, 467, 126-129

SCHOENLEIN R.W., CHATTOPADHYAY S., CHONG H.H.W., GLOVER T.E., HEIMANN P.A., SHANK C.V., ZHOLENTS A., ZOLOTOREV M. (2000)
Generation of femtosecond pulses of synchrotron radiation, Science, 287, 2237

YANG B.X., RIVERS M., SCHILDKAMP W., ENG P.J. (1995)
Geocars microfocusing Kirkpatrick-Baez mirror bender development, Review of Scientific Instruments, 66 (2), 2278-2280

8.8 Publications

8.8.1 Peer reviewed journals and reports

BRESSLER CH.[1], SAES M.[1], ABELA R., GROLIMUND D., JOHNSON S.L., HEIMANN P.A.[2], CHERGUI M.[1] (2003)
Observing Transient Chemical Changes by Ultrafast X-ray Absorption Spectroscopy, Physical Review Letters, 90, 047403
[1] University of Lausanne, Switzerland
[2] Advanced Light Source, Berkeley, CA, USA

DÄHN R., SCHEIDEGGER A.M., MANCEAU A.[1], SCHLEGEL M.[1], BAEYENS, B., BRADBURY, M.H., MORALES M.[2] (2003)
Structural evidence for the sorption of metal ion on the edges of montmorillonite layers: A polarized EXAFS study. Geochim. Cosmochim. Acta. **67(1)** 1-15
[1] LGIT, University Joseph Fourier, Grenoble, France
[2] CEA-Saclay, Gif-sur-Yvette, Cedex, France

GAWELDA W.[1], BRESSLER CH.[1], SAES M.[1], KAISER M.[1], TARNOVSKY A.[1], JOHNSON S.L., GROLIMUND D., ABELA R., CHERGUI M.[1] (2003)
Picosecond Time-Resolved X-Ray Absorption Spectroscopy of Solvated Organometallic Complexes, Synchrotron Radiation News (invited), 16, 12, (2003)
[1] University of Lausanne, Switzerland

GAWELDA W.[1], SAES M.[1], KAISER M.[1], TARNOVSKY A.[1], JOHNSON S.L., GROLIMUND D., ABELA R., CHERGUI M.[1], BRESSLER CH.[1] (2004)
Structural dynamics and electronic structure changes probed with lasers and X-rays, p. 353ff, in "Femtochemistry and Femtobiology: Ultrafast Events in Molecular Science" edited by M.M. Martin and J.T. Hynes, Elsevier
[1] University of Lausanne, Switzerland

GROLIMUND D., SENN M.[1], JANOUSCH M., BONHOURE I., SCHEIDEGGER A.M., MARCUS M.[2] (2004)
Shedding new light on history using micro-focused synchrotron radiation. Spectrochimica Acta B, in press
[1] EMPA, Dübendorf, Switzerland
[2] Advanced Light Source, Berkeley, CA, USA

SAES M.[1], GAWELDA W.[1], KAISER M.[1], TARNOVSKY A.[1], BRESSLER CH.[1], CHERGUI M.[1], JOHNSON S.L., GROLIMUND D., ABELA R. (2004)
Ultrafast Time-Resolved X-Ray Absorption Spectroscopy of Chemical Systems, Physica Scripta, in press (2004)
[1] University of Lausanne, Switzerland

SAES M.[1], BRESSLER CH.[1], VAN MOURRIK F.[1], GAWELDA W.[1], KAISER A.[1], CHERGUI M.[1], GROLIMUND, D., ABELA, R., GLOVER E.[2], HEIMANN P.A.[2], SCHOENLEIN R.W.[2], JOHNSON S.L., LINDENBERG A.M.[2], FALCONE R.W.[2] (2004)
A Setup for Ultrafast Time-Resolved X-Ray Absorption Spectroscopy, Review of Scientific Instruments, 75, 24-30
[1] University of Lausanne, Switzerland
[2] Advanced Light Source, Berkeley, CA, USA

SCHEIDEGGER A.M., GROLIMUND D., CUI D.[1], DEVOY J.[1], SPAHIU K.[2], WERSIN P.[3], BONHOURE I. JANOUSCH M. (2003)
Reduction of selenite on iron surfaces: A micro-spectroscopic study. J. de physique IV, 104:417-420
[1] Studsvik Nuclear AB, Nyköping, Sweden
[2] SKB, Stockholm, Sweden
[3] Nagra, Wettingen, Switzerland

STRUIS R.P.W.J., LUDWIG C., LUTZ H., SCHEIDEGGER A.M. (2004)
Speciation of zinc in MSWI-fly ash after heat treatment: A Zn K-Edge EXAFS Study. Environ. Sci. Technol., 38, 3760-3767

8.8.2 Conferences/Workshops/Presentations

DÄHN R., SCHEIDEGGER A.M., MANCEAU A.[1], BAEYENS B., BRADBURY M.H. (2004)
Uptake mechanisms of Ni(II) on montmorillonite as determined by X-ray absorption spectroscopy. Geochim. Cosmochim. Acta. 68(11), A164 Suppl. 1
[1] LGIT, University Joseph Fourier, Grenoble, France

GAWELDA W.[1], SAES M.[1], KAISER M.[1], TARNOVSKY A.[1], JOHNSON S.L., GROLIMUND D., ABELA R., CHERGUI M.[1], BRESSLER CH.[1] (2003)
A Setup for Ultrafast Time-Resolved X-Ray Absorption Spectroscopy, poster presentation, 4th SLS User Meeting, Paul Scherrer Institute, Villigen PSI, Switzerland, October, 2003
[1] University of Lausanne, Switzerland

GAWELDA W.[1], SAES M.[1], JOHNSON S.L., GROLIMUND D., ABELA R., TARNOVSKY A.[1], CHERGUI M.[1], BRESSLER CH.[1] (2003)
Time-Resolved X-Ray Absorption Spectroscopy at Synchrotrons with Picosecond Temporal Resolution, oral presentation, 12th International Conference on X-ray Absorption Fine Structure (XAFS 12), Lund/Malmö, Sweden, June, 2003
[1] University of Lausanne, Switzerland

GAWELDA W.[1], SAES M.[1], KAISER S.[1], JOHNSON S.L., GROLIMUND D., ABELA R., TARNOVSKY A.[1], CHERGUI M.[1], BRESSLER CH.[1] (2003)
Time-Resolved X-Ray Absorption Spectroscopy at Synchrotrons with Picosecond Temporal Resolution, poster presentation, International Workshop on "Ultrafast Science with X-Rays and Electrons", Montreux, Switzerland, April, 2003
[1] University of Lausanne, Switzerland

GROLIMUND D. (2003)
Status and Potential of the microXAS Beamline, oral presentation, LES program committee meeting, Paul Scherrer Institute, Villigen PSI, Switzerland, October, 2003

GROLIMUND D., SCHEIDEGGER A.M., JANOUSCH M., MEYER B., ABELA R., VAN DER VEEN J.F., FLANK A.-M.[1], LAGARDE P.[1], CAUCHON G.[1], BAC S.[1], DUBUISSON J.M.[2] (2003)
MicroXAS and LUCIA: Two X-ray Microprobe Beamline Projects at the Swiss Light Source (SLS), poster presentation, 12th International Conference on X-ray Absorption Fine Structure (XAFS 12), Lund/Malmö, Sweden, June, 2003
[1] LURE, Université Paris-Sud, France
[2] SOLEIL, Gif sur Yvette, France

GROLIMUND D., SCHEIDEGGER A.M., SIMIONOVICI A.[1], BOHIC S.[1], WORMS I.[1], KOLA H.[2], SIMON D.[2], WILKINSON K.[2] (2003)
Enlightening the Functionality of Single Cell Biosensors by micro-XRF and micro-XANES, accepted as poster presentation, 17th International Congress on X-Ray Optics and Microanalysis (ICXOM 17), Chamonix, France, September, 2003
[1] ESRF, Grenoble, France
[2] University of Geneva, Switzerland

GROLIMUND D., SCHEIDEGGER A.M., SIMIONOVICI A.[1], BOHIC S.[1], WORMS I.[2], KOLA H.[2], SIMON D.[2], WILKINSON K.[2] (2003)
Inner Life of a Biosensor: New Insights by X-ray Microprobes, oral presentation, 12th International Conference on X-ray Absorption Fine Structure (XAFS 12), Lund/Malmö, Sweden, June, 2003
[1] ESRF, Grenoble, France
[2] University of Geneva, Switzerland

GROLIMUND D., SENN M.[1], JANOUSCH M., BONHOURE I., SCHEIDEGGER A.M., MARCUS M.[2] (2003)
Shedding new Light on History using Micro-focused Synchrotron Radiation, oral presentation, 17th International Congress on X-Ray Optics and Microanalysis (ICXOM 17), Chamonix, France, September, 2003
[1] EMPA, Dübendorf, Switzerland
[2] Advanced Light Source, Berkeley, CA, USA

INGOLD G., ABELA R., BEAUD P., GROLIMUND D., JOHNSON S.L., MUNOZ M., RIVKIN L., SCHLOTT V., SCHMIDT T., SCHULZ L., STREUN A., VAN DER VEEN J.F., CHUBAR O.[1], KHAN S.[2], TARNOVSKY A.[3]
Sub-picosecond Hard X-ray Source at the Swiss Light Source (SLS), poster presentation, 12´th International Conference on X-ray Absorption Fine Structure (XAFS 12), Lund/Malmö, Sweden, June, 2003.
[1] SOLEIL, Gif surYvette, France
[2] BESSY, Berlin, Germany
[3] University of Lausanne, Switzerland

INGOLD G., ABELA R., BEAUD P., GROLIMUND D., JOHNSON S.L., RIVKIN L., SCHLOTT V., SCHMIDT T., SCHULZ L., STREUN A., VAN DER VEEN J.F., CHUBAR O.[1], KHAN S.[2], TARNOVSKY A.[3] (2003)
Status: undulator X-Ray Source for Time-Resolved ps and sub-ps Pump/Probe Experiments in the Range 5-18 keV, poster presentation, International Workshop on "Ultrafast Science with X-Rays and Electrons", Montreux, Switzerland, April, 2003
[1] SOLEIL, Gif surYvette, France
[2] BESSY, Berlin, Germany
[3] University of Lausanne, Switzerland

JANOUSCH M., FLANK A.-M.[1], LAGARDE P.[1], CAUCHON G.[1], BAC S.[1], DUBUISSON J.M.[1], SCHMIDT TH., WETTER R., GROLIMUND D., SCHEIDEGGER A.M. (2004)
LUCIA - a new 1-7 keV μ-XAS Beamline, AIP Conference Proceedings, 705, 312-315
[1] LURE, Université Paris-Sud, France

NACHTEGAAL M.[1], SCHEIDEGGER A.M., DÄHN R., FURRER G.[1] (2004)
Ni immobilisation by Al-modified montmorillonite: A novel uptake mechanism deduced by P-EXAFS. Geochim. Cosmochim. Acta. 68(11), A163 Suppl. 1
[1] ETH Zürich, Switzerland

SAES M.[1], GAWELDA W.[1], KAISER M.[1], TARNOVSKY A.[1], JOHNSON S.L., GROLIMUND D., ABELA R., BRESSLER CH.[1], CHERGUI M.[1] (2003)
Picosecond Time-Resolved X-Ray Absorption Spectroscopy of Solvated Organnometallics, poster presentation, 4th SLS User Meeting, Paul Scherrer Institute, Villigen PSI, Switzerland, October, 2003
[1] University of Lausanne, Switzerland

SAES M.[1], GAWELDA W.[1], TARNOVSKY A.[1], JOHNSON S.L., GROLIMUND D., ABELA R., CHERGUI M.[1], BRESSLER CH.[1] (2003)
Picosecond Time-Resolved X-Ray Absorption Spectroscopy of Laser-Excited Aqueous $[Ru(bpy)_3]^{2+}$, poster presentation, 12th International Conference on X-ray Absorption Fine Structure (XAFS 12), Lund/Malmö, Sweden, June, 2003
[1] University of Lausanne, Switzerland

SAES M.[1], GAWELDA W.[1], KAISER M.[1], TARNOVSKY A.[1], JOHNSON S.L., GROLIMUND D., ABELA R., CHERGUI M.[1], BRESSLER CH.[1], (2003)
Picosecond Time-Resolved X-Ray Absorption Spectroscopy of Laser-Excited Aqueous $[Ru(bpy)_3]^{2+}$, poster presentation, International Workshop on "Ultrafast Science with X-Rays and Electrons", Montreux, Switzerland, April, 2003
[1] University of Lausanne, Switzerland

SCHEIDEGGER A.M. (2003)
X-ray absorption spectroscopy (XAS). Invited lecture at the annual meeting of the 'Schweiz. Arbeitsgemeinschaft für Spektrometrie und Elementanalytik', Paul Scherrer Institut, Villigen, Switzerland, April 2003

SCHEIDEGGER A.M., GROLIMUND D., DÄHN R., BONHOURE I., WIELAND E., CUI D.[1] (2003)
The use of XAFS in Nuclear Waste Management, Invited talk at the International XAFS XII Conference, Malmö, Sweden
[1] Studsvik Nuclear AB,Sweden

SCHEIDEGGER A.M., GROLIMUND D., DÄHN R., BONHOURE I., CUI D.[1] (2003)
Use of X-ray absorption spectroscopy (XAS) to study radionuclide uptake on nuclear waste repository materials. Invited talk at the 225th American Chemical Society Meeting, New Orleans, USA, March 2003
[1] Studsvik Nuclear AB, Sweden

SCHEIDEGGER A.M., GROLIMUND D., VESPA M., WIELAND E., DAEHN R., CUI D.[1], MARCUS M.[2] (2003)
Metal Speciation in Waste Repository Materials using microXRF and microXAFS, oral presentation, 17th International Congress on X-Ray Optics and Microanalysis (ICXOM 17), Chamonix, France, September, 2003
[1] Studsvik Nuclear AB, Sweden
[2] Advanced Light Source, Berkeley, CA, USA

SCHEIDEGGER A.M., GROLIMUND D., VESPA M., HARFOUCHE M., WIELAND E., DÄHN R., CUI[1] D. (2004)
Metal speciation in heterogeneous waste repository materials using micro-XRF and micro-XAS. Geochim. Cosmochim. Acta. 68(11), A363 Suppl. 1
[1] Studsvik Nuclear AB, Sweden

SCHEIDEGGER A.M., GROLIMUND VESPA M., HARFOUCHE M., WIELAND E., DÄHN R., CUI D.[1] (2004)
Metal speciation in heterogeneous waste repository materials using micro-XRF and micro-XAS, Invited talk at the 13th Annual V.M. Goldschmidt Conference, Copenhagen, Denmark, June 2004
[1] Studsvik Nuclear AB, Sweden

VESPA M., WIELAND E., DÄHN R., GROLIMUND D., SCHEIDEGGER A.M. (2004)
EXAFS study of Ni uptake by hardened cement paste. Geochim. Cosmochim. Acta. 68(11), A166 Suppl. 1

8.8.3 Internal reports

GROLIMUND D., SENN M.[1], JANOUSCH M., BONHOURE I., SCHEIDEGGER A.M., MARCUS M.[2] (2004)
Shedding new light on historical artifacts using micro-focused synchrotron radiation. PSI Scientific Report 2003, **7**, 60, Paul Scherrer Institute, Villigen PSI, Switzerland
[1] EMPA, Dübendorf, Switzerland
[2] Advanced Light Source, Berkeley, CA, USA

INGOLD G., ABELA R., BEAUD P., GROLIMUND D., JOHNSON J.L., RIVKIN L., ROHNER M., SCHLOTT V., SCHMIDT T., SCHULZ L., STREUN A., VAN DER VEEN J.F., CHUBAR[1], TARNOVSKY A.[2] (2004)
Femto Project: Status of the FEMTO Insertion, PSI Scientific Report 2003, VII, Paul Scherrer Institute, Villigen PSI, Switzerland
[1] SOLEIL, Gif surYvette, France
[2] University of Lausanne, Switzerland

INGOLD G., ABELA R., BEAUD P., GROLIMUND D., JOHNSON J.L., MUNOZ M., RIVKIN L., SCHLOTT V., SCHMIDT T., SCHULZ L., STREUN A., VAN DER VEEN J.F., CHUBAR O.[1], KHAN S.[2], TARNOVSKY A.[3] (2003)
Status: Undulator X-ray Source for Time-resolved ps- and sub-ps Pump/Probe Experiments in the Range 5-18 keV, PSI Scientific Report 2002, VII, Paul Scherrer Institute, Villigen PSI, Switzerland
[1] SOLEIL, Gif sur Yvette, France
[2] BESSY, Berlin, Germany
[3] University of Lausanne, Switzerland

SAES M.[1], GAWELDA W.[1], BRESSLER CH.[1], TARNOVSKY A.[1], CHERGUI M.[1], ABELA R., GROLIMUND D., FALCONE R.W.[2], JOHNSON S.L., LINDENBERG A.M.[2], HEIMANN P.A.[3], SCHOENLEIN R.W.[2] (2003)
Time-Resolved X-ray Absoprtion Spectroscopy (XAS), PSI Scientific Report 2002, VII, Paul Scherrer Institute, Villigen PSI, Switzerland
[1] University of Lausanne, Switzerland
[2] University of California Berkeley, Berkeley, CA, USA
[3] Advanced Light Source, Berkeley, CA, USA

SCHEIDEGGER A.M., JANOUSCH M., GROLIMUND D., CUI D.[1] (2004)
Reduction of selenite on iron surfaces: A micro-XRF/XAS study. PSI Scientific Report 2003, **7**, 59, Paul Scherrer Institute, Villigen PSI, Switzerland
[1] Studsvik Nuclear AB, Sweden

8.9 Others, Teaching

LÜTZENKIRCHEN J., STUMPF T., BRENDLER V., BAEYENS B., GROLIMUND D., (eds.) (2004)
Int. Workshop on sorption processes at oxide and carbonate mineral water interfaces, Karlsruhe, March 25-26, 2004, Book of extended abstracts, Wiss. Berichte, FZKA 6986, Forschungszentrum Karlsruhe, Karlsruhe

GROLIMUND D.
PhD committee member, Aalborg University, Faculty of Engineering and Science, DK

SCHEIDEGGER A.M. (2003)
X-ray absorption spectroscopy (XAS) an der SLS. Invited lecture at the 'Labor für Radio- und Umweltchemie der Universität Bern und des PSI', Paul Scherrer Institut, Villigen, Switzerland, May 2003

SCHEIDEGGER A.M., GROLIMUND D. (2004)
The micro-XAS beamline at the Swiss Light Source (SLS): A new analytical facility dedicated to micro-beam applications. Invited lecture at the 'General Energy' (ENE) Department, Paul Scherrer Institut, Villigen, Switzerland, September 2004